ISSN 0915-9916

Readout

HORIBA Technical Reports

June 2026
English Edition No. 61

Analysis and Measurement Technologies Contributing to Next-Generation Healthcare

2025 Masao Horiba Awards

HORIBA

Readout
HORIBA Technical Reports
June 2026 No.61

Analysis and Measurement Technologies Contributing to Next-Generation Healthcare
2025 Masao Horiba Awards

In the post–COVID-19 era, the importance of developing technologies has been increasing—not only for safety assessment of genetically modified cells and analysis of immune functions, but also for diagnostic techniques that are user-friendly, rapid, and highly accurate, as well as for ensuring the quality of biopharmaceuticals. In this issue, we present an overview of the Masao Horiba Award focusing on "analytical and measurement technologies that contribute to next-generation medicine," together with HORIBA's technologies and initiatives that support medical diagnosis and research.

Seeking fresh greenery and blooming flowers, I ventured deep into the mountains of Shikoku. When I spotted a bumblebee approaching the blossoms of a flowering crabapple (hanakaidō), I pressed the shutter release, feeling the vibrant pulse of life all around me.
-Photographer Hideo Matsui-
(Member of Nikakai Association of Photographers)

Name of this Journal

This Journal is named "Readout" in the hope that "the products and technology we have created and developed will be read out and so become widely known".

Foreword

The Spectroscopic-Data Science Revolution: Transforming Next-Generation Clinical Testing and Biopharmaceutical Manufacturing

Jun Ivan Nishimura Tanikawa

General Manager
Bio & Healthcare Technology Division
HORIBA, Ltd.

As we stand on the threshold of a new era in precision medicine—where treatments are tailored to individual patients based on their unique molecular profiles—the convergence of spectroscopy and artificial intelligence (AI) promises to transform the landscape of clinical laboratory testing, drug development, and biologics manufacturing. At the heart of this transformation are minimally invasive tests that analyze biomarkers present at very low concentrations in blood or other body fluids, enabling early detection of diseases like cancer, monitoring of progression, and guidance of personalized therapies—without relying on more invasive and less specific traditional methods. These technologies also extend to the production of biologics—complex therapeutic proteins, and cell/gene therapies—where real-time spectroscopic monitoring ensures consistency and quality, directly supporting the delivery of tailored treatments central to precision medicine. Once confined to specialized research domains, these technologies are now poised to deliver unprecedented precision, speed, and accessibility in next-generation diagnostics and therapeutics.

Spectroscopy techniques such as fluorescence, Raman, and mass spectrometry—has long provided a molecular fingerprint of biological samples, capturing subtle biochemical changes and global phenotypic responses that are often invisible to targeted assays. Traditional in vitro diagnostics (IVD) often require labeled reagents with specific targets and sample preparation, while also risking artifacts from labeling. The advantages of spectroscopy can compensate for certain limitations of traditional IVD, including its non-destructive nature, minimal sample preparation, and multiplexed detection of endogenous biomolecules in complex body fluids—making it ideally suited for revolutionary concepts like liquid biopsies[*1]. Spectroscopy in IVD is not yet widely accessible to clinical laboratories, largely because of limited automation, lack of standardized databases, operational complexity, high capital cost of the instrumentation, and insufficient clinical-trial evidence. Looking ahead, the integration of AI with spectroscopy is expected to transform the way we handle complex, overlapping spectra in which subtle disease signatures are often buried in noise. At the same time, spectral data are highly sensitive to variations in sample preparation, instrument calibration, environmental conditions (e.g., temperature, fluorescence background in Raman), and patient demographics. Without standardized collection and calibration protocols, AI models risk learning spurious correlations instead of true biological signals, resulting in bias and poor generalizability. Ensuring high data quality, improving model interpretability and explainability, and complying with medical device regulations will be essential to unlock the full potential of this next generation of spectroscopic diagnostic testing.

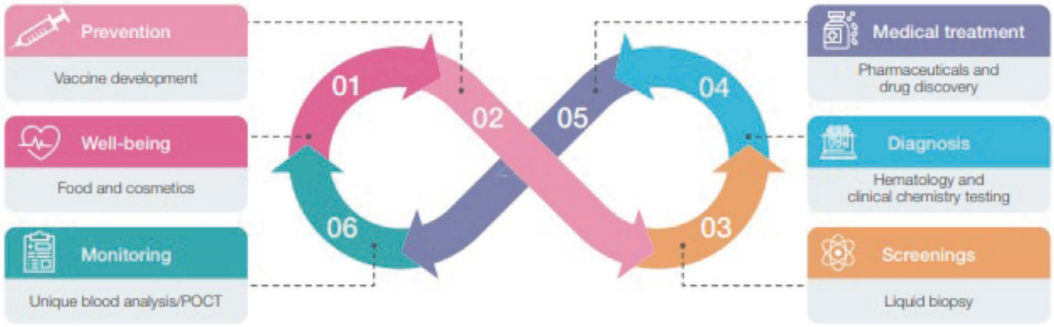

Figure 1 Areas in the healthcare journey where HORIBA aims to provide unique solutions.

Equally transformative is the role of these technologies in drug discovery and manufacturing. Spectroscopy serves as a cornerstone for process analytical technology (PAT)[*2], enabling real-time monitoring of chemical reactions, polymorph identification, and quality control in continuous manufacturing flows. The global biologics market already accounts for more than 30% of total pharmaceutical sales and is growing faster than small-molecule drugs. At the same time, major regulators (FDA, EMA, PMDA) explicitly promote PAT and Quality by Design (QbD)[*3], and their guidance and inspection reports increasingly highlight the importance of real-time analytics. As the industry moves from offline HPLC and traditional biochemistry assays toward in-line and on-line monitoring in both upstream and downstream processes, continuous, model-based control powered by spectroscopy and multivariate analysis is emerging as one of the most exciting growth areas in modern biomanufacturing.

HORIBA Medical's story began in the 1980s, when we started incorporating the technologies and expertise that have allowed us to remain one of the world's established hematology analyzer companies. Since 2015, HORIBA has also launched a bio–life science initiative focused on developing solutions that support the drug development and production processes of new drugs. These two strategic directions share a common goal: to transform the healthcare journey[*4]—from next-generation diagnostics to innovative approaches that improve the manufacturing of biopharmaceutical products. By strengthening synergies across our internal teams, we aim to foster collaborations with leaders in cutting-edge fields such as liquid biopsy and advanced bio-pharma processes, creating new value for the future of healthcare.

HORIBA is one of the few companies worldwide that is both an active player in the IVD market and possesses the optical spectroscopy building blocks needed to help transform the future of medicine—delivering deeper insights into complex biological samples and enabling real-time applications that will be essential to meet next-generation of treatment manufacturing demands.

Inspired by the vision of our founder, Dr. Masao Horiba who aimed to contribute to the fields of medicine and healthcare through innovative analysis and measurement technologies, the theme for 2025 Masao Horiba Awards was "Analysis and Measurement Technologies Contributing to Next-Generation Healthcare." This award honors researchers outside the company and aims to advance the field by broadly sharing achievements in analysis and measurement.

This volume of Readout reminds us that the true power of science lies in its ability to translate discovery into tangible solutions—bringing hope for a better world by advancing one of humanity's most important priorities: healthcare.

*1 Liquid Biopsy: Testing blood or other body fluids for tumor-derived components.
*2 Process Analytical Technology (PAT): A method for measuring and analyzing manufacturing processes in real time (or near real time) to control quality.
*3 Quality by Design (QbD): A systematic approach that designs manufacturing processes on the basis of scientific evidence and proactively ensures quality at the design stage.
*4 Healthcare Journey: A series of medical experiences and processes, from prevention, testing, diagnosis, and treatment to prognostic management, viewed from the perspective of patients or users.

* Editorial note: This content is based on HORIBA's investigations in the year of publication, unless otherwise stated.

2025 Masao Horiba Awards Award Details

* This article is an English translation of the original Japanese version published in Readout No. 61.

About Masao Horiba Awards

The Masao Horiba Award's is an encouragement and recognition given to researchers and engineers who are making remarkable achievements in the field of science and technology related to analysis, measurement, and their applications at universities or public research institutions both domestically and internationally.

Eligible fields

Analysis and Measurement Technologies Contributing to Next-Generation Healthcare

Comments

Chairperson, 2025 Masao Horiba Awards Screening Committee
Director,
Central Institute for Experimental Medicine and Life Science
Professor Emeritus, Keio University
Makoto Suematsu

I would like to extend my sincere and heartfelt congratulations to all of you who have received the Masao Horiba Awards. I also wish to express, once again, my sincere gratitude for the opportunity to hold such a wonderful occasion at Kyoto University.

Before commenting on the selection process for this award and the key points discussed, I would like to note that this year witnessed a major event in the academic community. As you are all aware, Professor Shimon Sakaguchi and Professor Susumu Kitagawa were awarded the Nobel Prize. Their research was long regarded as belonging to fields in which "such a thing cannot be possible", yet through steady and sustained effort they ultimately achieved remarkable results. I would like to convey my deepest respect and congratulations for this outstanding achievement.

The Masao Horiba Awards was established in 2003 by Dr. Masao Horiba. I understand that, beginning with his time as a student at Kyoto University, Dr. Horiba pursued research on the pH meter and, after overcoming many difficulties, succeeded in developing it into a commercial product—what would today be described as a student venture. This background is reflected in the Masao Horiba Awards emphasis on the originality, future potential, and innovativeness of research. Moreover, rather than incremental development, the award's basic policy is to recognize research that demonstrates a leap forward—what is often referred to as a "quantum leap".

This year, a total of 44 applications were received, including 34 from Japan and 10 from overseas, and the Screening Committee conducted a careful review. Each research project had its own distinctive strengths. Among them, Professor Kaji's label-free and non-destructive technology is becoming an important keyword for future medical research. In addition, Professor Nishihara's work was highly evaluated not only for identifying a new function of the coronavirus spike protein, but also for its detection technology, its potential for expansion into other fields, and its degree of advancement. Furthermore, leveraging nanowire technology, Professor Yasui developed a technique that enables diverse vesicles to be identified and sorted in liquid biopsy. Because liquid biopsy addresses a wide range of targets—from plants and bacteria to human organs and viral particles—effectively separating and analyzing these entities is a critical challenge.

Finally, we selected Professor Lin Huang for the Honorable Mention. Centered on cancer research, Professor Huang has been advancing drug development, and the work has also indicated potential applicability to Alzheimer's disease; accordingly, further expansion into applications is anticipated.

In closing, I sincerely hope that the research conducted by the Masao Horiba Awards recipients will be translated into applications not only in cancer but also across a wide range of medical fields. With my best wishes for the awardees' continued success, I conclude these remarks.

Development of non-labeled, non-destructive single stem cell analysis technology for cell therapy

Noritada Kaji

In regenerative medicine and cancer diagnosis, the development of technologies capable of non-invasively evaluating cell states is imperative. This study developed an analytical technique capable of high-throughput measurement of mechanical properties at the single-cell level, specifically "cell deformability", without the need for labeling or destruction. The integration of microfluidic device technology with a concurrent electrical and optical measurement system has enabled the development of a device capable of accurately quantifying cell deformability. This method facilitates the millisecond-scale measurement of the deformation response of individual cells. Furthermore, the implementation of this technology enabled the successful detection of cytoskeletal changes induced by drugs, the evaluation of stem cell pluripotency, and the highly sensitive detection of limited number of circulating tumor cells (CTCs) in whole blood.

Keywords
microfluidic device, cell deformability, single-cell level, pluripotency

Introduction

Cell deformability (softness and hardness) is one of the “phenotypes” closely related to cellular functional states such as carcinogenesis, differentiation, and aging. Quantification of this property is extremely useful as an indicator of cellular health and undifferentiated state. Numerous studies have reported the evaluation of mechanical properties such as cell deformability at the single cell level using various methods, including direct force measurement techniques such as atomic force microscopy (AFM)[1], optical tweezers[2], and micropipettes[3], as well as indirect methods that infer deformability from cellular behavior in microfluidic systems[4]. However, as shown in Figure 1, all of these methods have a significant trade-off between measurement accuracy and throughput, and no definitive method that satisfies both has yet been developed. Despite the fact that cell deformability measurement is still in its methodological infancy, new insights into cell biology are being gained using a cell deformability flow cytometer based on microfluidic devices. For example, it has been reported that when mouse neurons are reprogrammed into iPS cells and then differentiated back into neurons, the deformability of the cells decreases (becomes stiffer) during reprogramming into iPS cells and increases (becomes softer) during differentiation into neurons[5] (Figure 2). In that study, it was reported that stem cells such as ES cells and iPS cells have lower cell deformability than differentiated cells, and normal cells have lower cell deformability than cancer cells. Such a “non-labeled, non-destructive method for continuous monitoring of cellular mechanical properties by measuring cell deformability” provides information about intact cells that has been difficult to obtain using chemical or biochemical methods that inevitably cause some damage to the cells. This method has potential as a new methodological approach in cell biology, such as a pre-transplantation cell diagnostic method in regenerative medicine, and is expected to contribute broadly to academic research and industrial applications.

In this study, we focused on cell deformability, one of the “phenotypes” of cells, and developed a non-labeling, non-destructive, high-throughput cell analysis method that can be described as “cell palpation” (Figure 3). While conventional cell sorters (FACS) require molecular markers and mechanical measurement methods such as AFM have throughput limitations, this technology may become the only approach capable of rapidly evaluating living cells based on their mechanical properties without labeling or destruction.

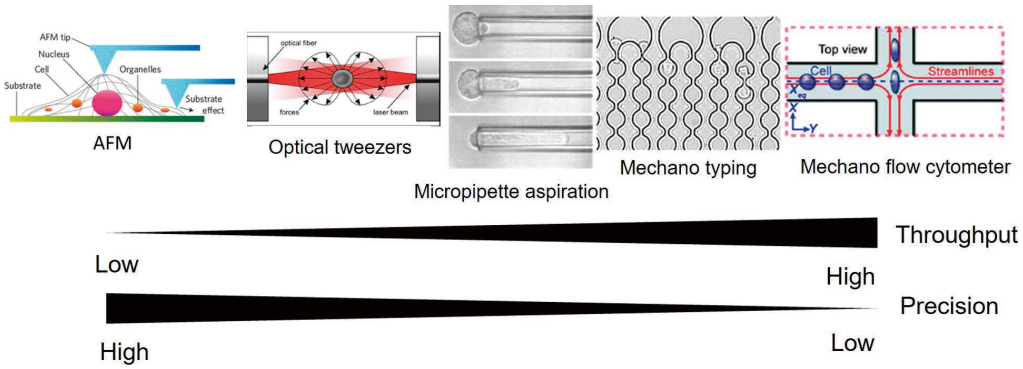

Figure 1 Single cell analysis method focusing on the mechanical properties of cells. There is a trade-off between accuracy and throughput.

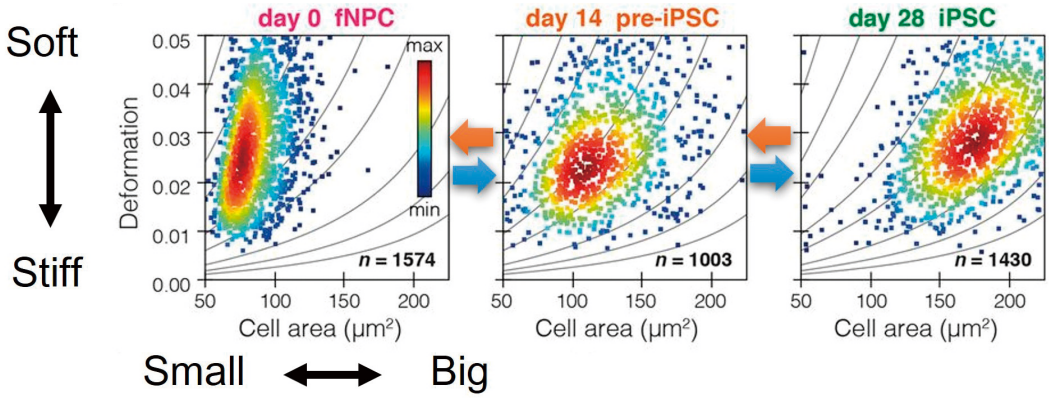

Figure 2 As dedifferentiation into iPS cells progresses, cells become larger and harder, and as differentiation into nerve cells progresses, cells become smaller and softer. Cited from Reference 5.

Integration of microfluidic device with a concurrent electrical and optical measurement system

In this study, we developed a method to examine cells one by one by "palpating" them using microfluidic devices. Since cells have a diameter of about 10-20 μm, we designed a device by sequentially arranging a first-stage microchannel slightly larger than the cell size (about 20-25 μm) and a second-stage microchannel slightly smaller than the cell size (about 5-10 μm). This design allows us to measure cell size and then determine cell deformability by analyzing the rate at which cells pass through the constriction. This design allows for a measurement system that can compensate for variations in cell size, ensuring that such variations do not affect measurements of cell deformability, thereby enabling the construction of a device that can "palpate" individual cells while they are alive.

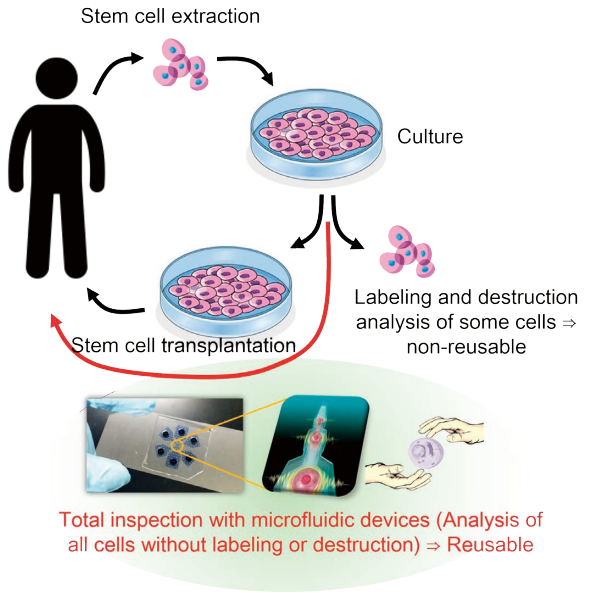

Figure 3 In previous stem cell transplants, after extracting stem cells, only a portion of the cultured cells were analyzed, and the remaining cells were transplanted, which did not eliminate the risk of cancerization. Using the method developed in this study, it is possible to inspect all cells, enabling the provision of safer and more reliable cell therapy.

First, the microfluidic channel geometry of the current and optical simultaneous measurement section was modified from a simple straight type to one with a narrow-constricted channel whose width is such that cells must deform to pass through. We constructed a measurement system that evaluates cell deformability based on changes in current values (reduction in current values caused by the interruption of ion currents) and their duration as cells pass through the narrowed flow channels. We comprehensively optimized the shape and size of the flow channels, the current measurement system, and the optical observation system, and established the basic performance of the microdevice for cell sensing (Figure 4). We then used

model cells (HeLa cells) treated with drugs that affect the formation of the cytoskeleton, which plays a crucial role in cellular mechanical properties (e.g., Latrunculin A and Paclitaxel), to verify how the detected current values and their duration change in response to cellular deformability. The results showed that Latrunculin A, which inhibits actin polymerization, shortened the time it took for cells to pass through the narrow flow channel, whereas Paclitaxel, which inhibits microtubule depolymerization, prolonged the passage time. This result suggests that the mechanism underlying the observed changes is that inhibition of actin polymerization leads to a weakened cytoskeleton, whereas inhibition of microtubule depolymerization leads to microtubule elongation, which strengthens the cytoskeleton and causes cells to become "stiffer". We have successfully detected such changes in cellular mechanical strength non-invasively and non-destructively within tens of milliseconds (Figure 5)[6].

Cell deformability measurements of cancer stem cells

To further validate the performance of this device, we focused on stem cells used in cell therapy. In cell therapy, it is essential to use "quality assured" cells that have been tested prior to transplantation to ensure that the somatic stem cells to be transplanted are undifferentiated and non-cancerous. However, to study the differentiation state of stem cells, external gene introduction such as fluorescent staining or gene expression systems is essential, making it impossible to transplant the tested cells as they are. If there is a correlation between the differentiation

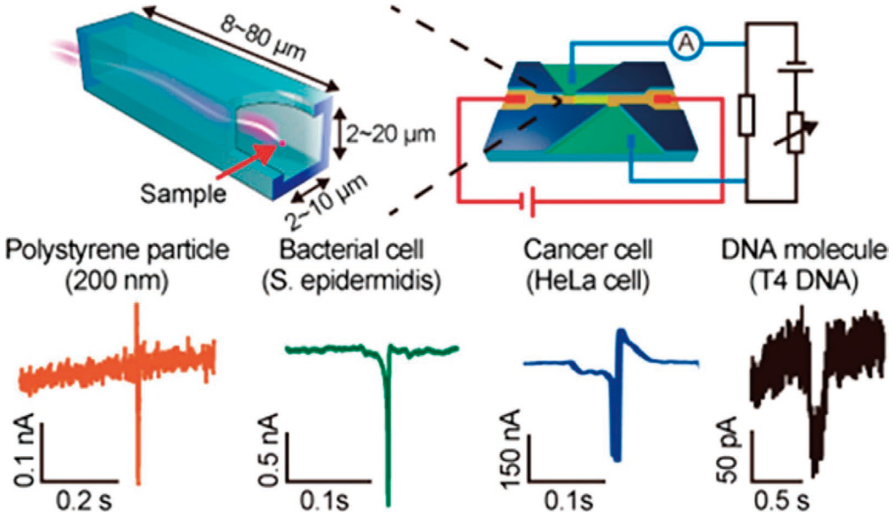

Figure 4 Initial study of the current and optical simultaneous measurement section and examples of measurement results for various samples. The electrical circuit was optimized for measuring cell deformation by introducing a bypass circuit to reduce current noise and improve the signal-to-noise ratio.

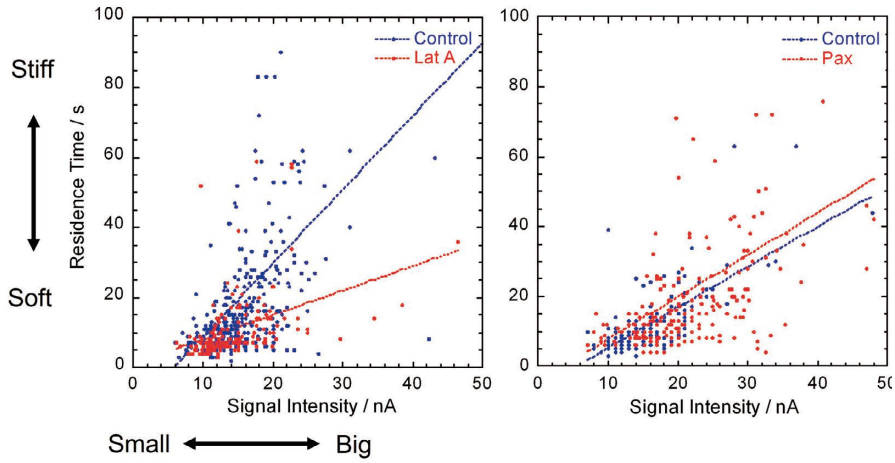

Figure 5 Differences in cell deformation ability based on the different mechanisms of action of Latrunculin A (Left) and Paclitaxel (Right) were detected using this device.

state of cells and their mechanical properties, this device could be used to inspect cells, collect them again, and apply them to cell therapy, making it very useful. Therefore, we focused on HT29 cells, which are intestinal epithelial cells with high pluripotency that can differentiate into various cell types, and investigated how their mechanical properties change depending on their differentiation state. Intestinal cells differentiate and mature by proliferating in the crypt region and migrating to the apical region of the microvillus. During this differentiation process, mechanical properties change and if these changes can be detected with this device, a non-labeled, non-destructive analysis can be achieved. HT29 cells are derived from colon adenocarcinoma and therefore contain a heterogeneous population of cells, including many cells with high pluripotency, characteristic of intestinal epithelial cells, as well as cells without such characteristics. Previous biochemical studies have shown that the highly pluripotent cell population exhibits high aldehyde dehydrogenase (ALDH) activity and increased cell surface expression of the cell membrane protein CD44v9. Therefore, we first used a cell sorter (FACS) to separate high activity/high expression cells from low activity/low expression cells based on these biomarkers, and then investigated the mechanical properties of each cell population. The results showed that cell populations with high ALDH activity and high CD44v9 expression had a broader distribution of cell deformability and contained a higher proportion of "stiff" cells compared to those with low activity/low expression[7]. These results are consistent with similar experiments using iPS cells for dedifferentiation and differentiation experiments[5] (i.e., cells with higher pluripotency tend to be "stiffer" and become "softer" upon differentiation) and represent the first study in the world to directly correlate mechanical properties of HT29 cells with pluripotency (Figure 6)[5]. Such cell analysis was achieved at the single cell level with a throughput of tens of milliseconds per cell. Furthermore, since these cell analyses were performed on a microfluidic device, the integration of a downstream sorting mechanism could lead to the development of a new unlabeled, non-destructive single-cell analysis technique as an alternative to traditional fluorescence-based FACS.

Circulating tumor cells (CTCs) detection in whole blood based on cell mechanics

Based on these proof-of-concept studies, we also attempted applied research on the detection of circulating tumor cells (CTCs) in blood. CTCs are cancer cells that have leaked from the primary tumor into the bloodstream and contain information about the primary tumor. Capturing and analyzing these cells can provide insight into tumor metastasis, malignancy diagnosis, treatment progression and prognosis. However, because blood cells make up the majority of blood (approximately 5 billion red blood cells and 5 million white blood cells per 1 mL of whole blood) and CTCs are present in only a few to a few dozen cells, their detection and capture is extremely challenging. In this study, we attempted to detect CTCs using the newly developed current-optical simultaneous measurement system. We found that the current signal from CTCs was more than 10 times larger than that from blood cells as they passed through the detection region, demonstrating that this method can be applied to quantify CTCs in whole blood (Figure 7)[8],[9].

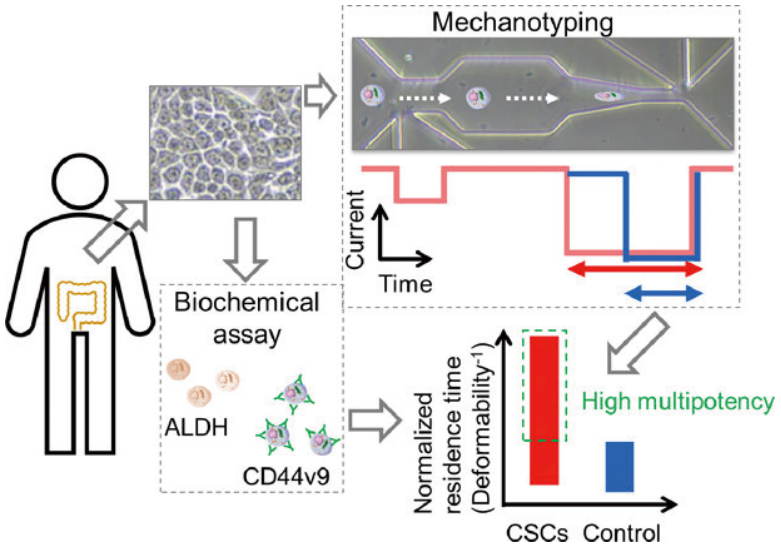

Figure 6 Multipotent cells were classified based on their mechanical properties without labeling or destruction.

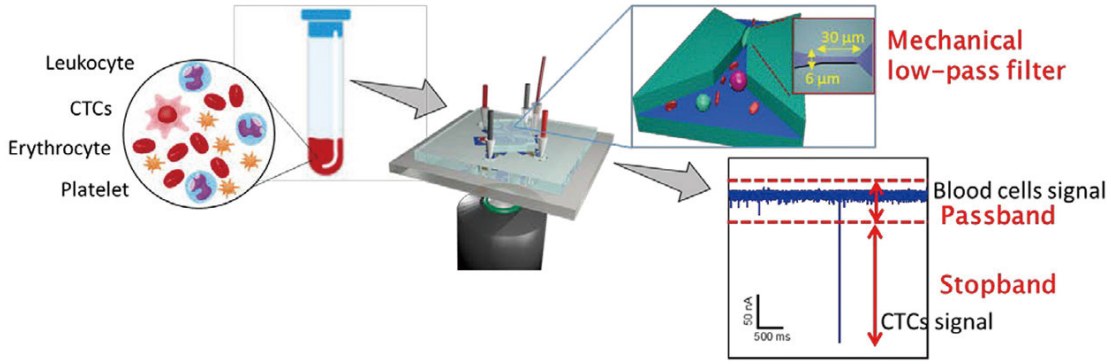

Figure 7 CTCs were detected from whole blood samples rapidly and specifically in milliseconds.

Conclusions

The mechanical properties of cells reflect various factors, including the position and molecular concentration of organelles in the cytoskeleton and cytoplasm, as well as the state of the nucleus. Therefore, treating cells as viscoelastic bodies and studying elastic and viscous terms alone is not sufficient to fully describe them. Furthermore, chemical interactions between the cell membrane surface and the contact substrate cannot be ignored in contact-based analysis methods. In this study, to minimize chemical interactions with the microchannel constriction surface, the surface was treated with a hydrophilic polymer or BSA (bovine serum albumin) prior to use. However, we believe that the chemical interactions between the cell membrane and the microfluidic channel surface can be used to detect cell type-specific interactions. We are currently developing a method to detect interactions by immobilizing antibodies specific for cell surface antigens on the microfluidic channel surface and have successfully detected both the mechanical properties of cells and their surface molecules simultaneously (manuscript in preparation). In this study, which was conducted against the background of previous research that primarily focused on investigating the properties of cells by treating them as viscoelastic bodies, the significant contribution lies in establishing a method to perform analyses that were previously impossible without fluorescent labeling or cell destruction followed by PCR amplification of genes, such as the analysis of cell pluripotency, in an unlabeled, non-destructive manner at the single cell level.

References

[1] B. Hartmann, et al., Profiling native pulmonary basement membrane stiffness using atomic force microscopy, *Nature Protocols*, 19(5) 1498-528 (2024)
[2] L. Shen, et al., Joint subarray acoustic tweezers enable controllable cell translation, rotation, and deformation, *Nat Commun*, 15(1) 9059 (2024)
[3] H. Li, et al., Biomechanics of phagocytosis of red blood cells by macrophages in the human spleen, *Proc Natl Acad Sci U S A*, 121(44) e2414437121 (2024)
[4] C. Petchakup, et al., Microfluidic Impedance-Deformability Cytometry for Label-Free Single Neutrophil Mechanophenotyping, *Small*, 18(18) 2104822 (2022)
[5] M. Urbanska, et al., De novo identification of universal cell mechanics gene signatures. *eLife*, 12:RP87930 (2024)
[6] M. Sano, N. Kaji, A. C. Rowat, H. Yasaki, L. Shao, H. Odaka, T. Yasui, T. Higashiyama, Y. Baba. Microfluidic Mechanotyping of a Single Cell with Two Consecutive Constrictions of Different Sizes and an Electrical Detection System, *Analytical Chemistry*, 91(20) 12890-9 (2019)
[7] M. Terada, S. Ide, T. Naito, N. Kimura, M. Matsusaki, N. Kaji. Label-Free Cancer Stem-like Cell Assay Conducted at a Single Cell Level Using Microfluidic Mechanotyping Devices, *Analytical Chemistry*, 93(43) 14409-16 (2021)
[8] T. Suzuki, N. Kaji, H. Yasaki, T. Yasui, Y. Baba. Mechanical Low-Pass Filtering of Cells for Detection of Circulating Tumor Cells in Whole Blood, *Analytical Chemistry*, 92(3) 2483-91 (2020)
[9] H. Suzuki, K. Fujiyoshi, N. Kaji, M. Tokeshi, Y. Baba. Observation of Ethanol-Induced Condensation and Decondensation Processes at a Single-DNA Molecular Level in Microfluidic Devices Equipped with a Rapid Solution Exchange System, *Analytical Chemistry*, 92(13) 9132-7 (2020)

Dr. Noritada Kaji
Department of Applied Chemistry
Faculty of Engineering
Kyushu University
Professor

Protein Analysis Technique Based on Latent Luciferase Activity

Ryo Nishihara

Bioluminescence is the emission of light resulting from the oxidation of luciferin*1 by the catalytic action of the enzyme luciferase. During the development of bioluminescence imaging*2 techniques, the author observed that luciferin can emit light even in the absence of luciferase. Building on this finding, the author discovered that proteins other than luciferase possess pseudo-luciferase activity, that is, they catalyze the luminescent reaction of specific luciferins. This study exploits the intrinsic pseudo-luciferase activity of proteins to develop a luminescent assay for quantifying their abundance and structural changes by mixing luciferin with the sample. This article outlines the principles and applications of this technique and discusses its potential use in rapid diagnostics and quality control of biopharmaceuticals.

*1 Luciferin: a class of substrates for enzyme luciferases that emit light upon oxidation.

*2 Bioluminescence imaging: a technique based on the addition of luciferin to cells or organisms engineered to express luciferase, enabling visualization, for example, of cancer cells *in vivo*.

Keywords
chemiluminescence, bioluminescence, luciferin, proteins, enzymatic reactions

Introduction

Bioluminescence is a phenomenon in which luciferin, a substrate derived from luminous organisms, is oxidized by the enzyme luciferase, also originating from luminous organisms, and the resulting chemical energy is released as light (Figure 1A)[1]. Unlike fluorescence, bioluminescence does not require an external excitation light source and is therefore free of issues such as autofluorescence and phototoxicity. Consequently, bioluminescence has become a highly sensitive optical analytical technique widely used across diverse fields, including cancer cell detection and food hygiene inspection, and plays an important role in the life sciences. However, conventional bioluminescence techniques require prior labeling of the target biomolecule (e.g., cells or proteins) with luciferase via genetic engineering or chemical conjugation. This labeling step hinders the implementation of bioluminescence as a rapid and simple analytical technique.

During the development of bioluminescence imaging techniques, the author discovered that administering a native luciferin from a marine luminous organism to animals without luciferase labeling produced luminescence within the organism[2]. This observation suggested that luciferin can undergo luminescent reactions with biomolecules other than its native enzyme, luciferase, prompting an investigation into whether proteins other than luciferase might possess latent luciferase-like catalytic capacity—hereafter referred to as pseudo-luciferase activity.

In the marine ostracod *Cypridina hilgendorfii, Cypridina* luciferin is oxidized by *Cypridina* luciferase to emit light (Figure 1A). The imidazopyrazinone ring*3 within this luciferin—a common scaffold in many marine bioluminescent organisms—is an essential structural motif for light emission (Figure 1A)[1].

*3 Imidazopyrazinone ring: Core luminescent scaffold found in many marine bioluminescent organisms.

A comparative analysis of luciferin structures among these organisms indicates that, over the course of evolution, side chains[*4] attached to the C2–C6 positions of the imidazopyrazinone ring became diversified and optimized for the luciferase-mediated oxidation reaction of each organism. The luminescence observed by the author in animal bodies was likewise derived from a luciferin containing the imidazopyrazinone ring. Because luciferins with this ring structure undergo luminescence via a relatively simple mechanism that requires no cofactors other than oxygen (in contrast to firefly luciferin, which requires ATP), the reaction most likely occurs nonspecifically with endogenous molecules[*5] that can interact with the side chains. Furthermore, artificial modification of the side chains does not abolish the luminescent capability of the imidazopyrazinone ring[3]. Based on these properties, the author hypothesized that designing the side chains of luciferin to bind specifically to a protein of interest (POI) would enable the development of a system in which luminescence occurs only upon luciferin binding to the POI (Figure 1B).

This article describes a novel luminescent assay that enables both quantitative and qualitative evaluation of proteins simply by mixing the sample with luciferin. This method exploits the pseudo-luciferase activity, which involves the luminescence reaction of luciferin catalyzed by the POI itself, thereby eliminating the need for conventional reagents such as luciferase, antibodies, or enzymes.

*4 Side chain: Here, substituents attached to the central imidazopyrazinone ring.

*5 Endogenous molecules: Molecules naturally present within living organisms.

Quantitative Luminescent Analysis of Viral Proteins

The global COVID-19 pandemic, which emerged in 2019 and was caused by SARS-CoV-2, led to the rapid development of therapeutic and diagnostic technologies targeting viral RNA and antigens. Among viral components, the spike (S) protein, located on the viral surface, has received particular attention because it mediates viral entry into host cells and is therefore a key target for diagnostic and therapeutic development. Some structural analyses have revealed that the S protein contains multiple hydrophobic pockets that can bind a variety of ligands, including linoleic acid[4]. Considering that the luminescent reaction of luciferins containing an imidazopyrazinone ring requires a hydrophobic pocket as the site of oxidation, the pseudo-luciferase activity of the S protein was explored in the present study by selecting luciferins whose side chains fit the hydrophobic pockets of the S protein[5].

Because luciferins possessing an imidazopyrazinone ring do not require any cofactors other than oxygen, luminescence generation can be evaluated simply by mixing the S protein with the luciferin substrate. Therefore, 36 luciferins, including coelenterazine (CTZ)[*6], *Cypridina* luciferin, and their synthetic derivatives with artificially modified side chains, were tested for luminescence in the presence of the S protein (Figure 2A). Among these luciferins,

*6 Coelenterazine: A natural luciferin found in many bioluminescent organisms such as Aequorea victoria and sea pansy *Renillareniformis*.

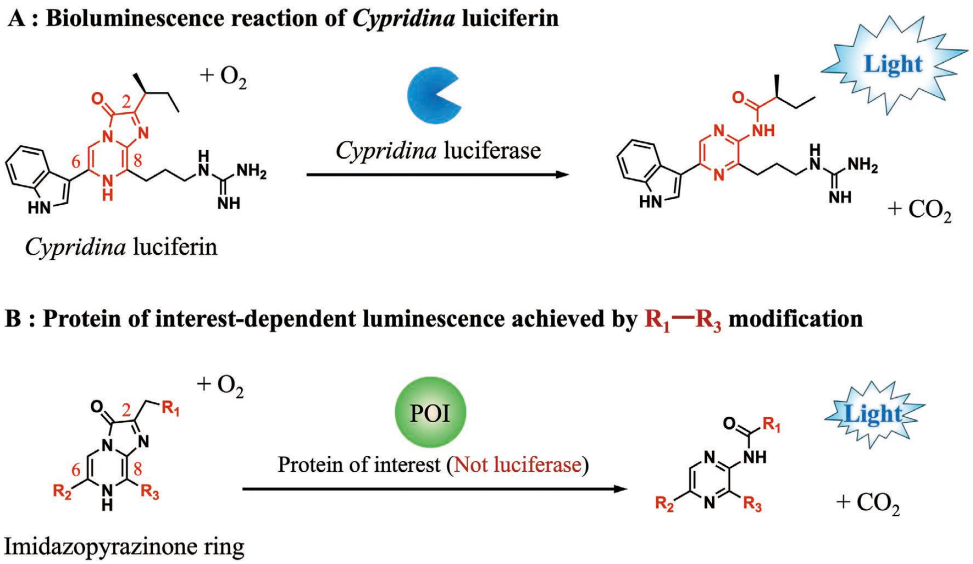

Figure 1 (A) Bioluminescence scheme of *Cypridina hilgendorfii*, a luminous marine organism: *Cypridina* luciferin is oxidized in the presence of *Cypridina* luciferase, producing light. The red region represents the imidazopyrazinone ring. (B) Concept of this study: Modification of the C-2, C-6, and C-8 side chains (R_1–R_3) of the imidazopyrazinone ring to develop luciferins that are oxidized and emit light in the presence of target proteins, enabling their application to protein analysis.

only *Cypridina* luciferin exhibited luminescence (Figure 2A), demonstrating that the SARS-CoV-2 S protein possesses pseudo-luciferase activity that specifically catalyzes the luminescent reaction of *Cypridina* luciferin. Like native *Cypridina* luciferase, the S protein induced blue luminescence using *Cypridina* luciferin. Interestingly, *Cypridina* luciferin did not emit light in the presence of proteins found in human saliva, such as α-amylase or mucin. By exploiting this high reaction specificity, the quantitative detection of S protein in untreated human saliva was achieved with an accuracy comparable to that of the enzyme-linked immunosorbent assay (ELISA)[*7]. The developed assay requires only the addition of *Cypridina* luciferin to saliva, followed by measurement of the spontaneously generated blue luminescence using a commercial luminometer (Figure 2B).

For the diagnosis of SARS-CoV-2 infection, two major approaches are used: PCR testing, which involves amplification and detection of virus-specific genes, and antigen testing, which consists of the detection of viral protein antigens. PCR is highly sensitive and reliable for definitive diagnosis; however, it requires approximately two hours to obtain results, making it unsuitable for the rapid processing of a large number of samples. In contrast, the luminescent assay developed here requires no sample pretreatment and enables quantitative analysis in just one minute, offering unprecedented rapidity and simplicity compared with conventional methods.

*7 Enzyme-linked immunosorbent assay (ELISA): An antibody-based method for quantitative detection of target molecules.

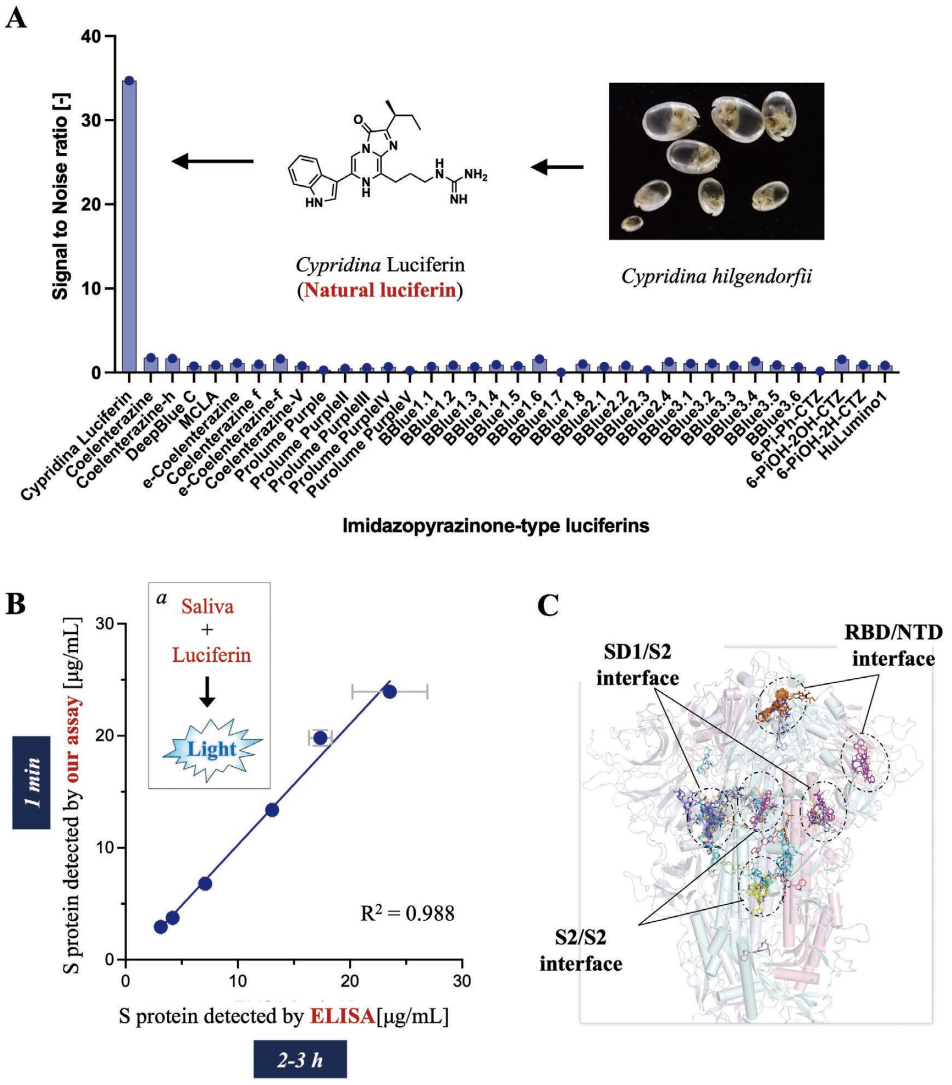

Figure 2 (A) Luminescence response from SARS-CoV-2 spike (S) protein treated with imidazopyrazinone-type luciferins. The signal-to-noise ratio indicates the ratio of the total luminescence of the luciferin/S protein pair relative to that of luciferin only. (B) Correlation between the measured concentrations of SARS-CoV-2 S protein using our developed luminescence assay and ELISA. The inset *a* depicts the luminescence assay scheme. (C) Docking simulation of luciferin with S protein.

Cypridina luciferin did not react with the S protein of another coronavirus, MERS-CoV, because this luciferin emits efficiently within the characteristic hydrophobic pocket located at the interface of the SARS-CoV-2 S protein domain[*8], suggesting potential utility for distinguishing between viral species. As shown in Figure 2C, the binding poses of *Cypridina* luciferin in the S protein of SARS-CoV-2 were predicted by docking simulations[*9]. Because these domain interfaces are present in all SARS-CoV-2 variants, this method enables luminescence-based detection not only of the original Wuhan strain but also of variants such as Omicron.

These findings demonstrate that this protein analysis method, which exploits the pseudo-luciferase activity intrinsic to viral proteins, enables rapid and straightforward quantification of viral proteins, outperforming existing technologies. This approach represents an innovative platform with strong potential for future viral diagnostics.

*8 Protein domain: A structural unit typically composed of 100–200 amino acids.
*9 Docking simulation: A computational method used to predict the stable binding configuration between a protein and another molecule.

Application to Other Protein Analyses via Development of Artificial Luciferins

By modifying the chemical structure of native luciferin, this technique can be extended beyond viral proteins to the analysis of human-derived proteins. In marine bioluminescent organisms, the side chains of the imidazopyrazinone ring have been evolutionarily tuned to fit the luciferase specific of each species[1]. For example, although the luciferins of luminous organisms such as the sea pansy *Renillareniformis*, the firefly squid *Watasenia scintillans*, and the marine ostracod *Cypridina hilgendorfii* possess the imidazopyrazinone ring, their side-chain structures differ markedly (Figure 3A). Thus, the diversity of bioluminescent systems found in nature primarily arises from variations in the side chains conjugated to the imidazopyrazinone ring, thereby enabling species-specific luminescent reactions without cross-reactivity.

Herein, based on the principle of molecular evolution in nature, artificial luciferins were designed and synthesized by introducing side chains optimized for the target protein into the imidazopyrazinone ring. This strategy enabled us to expand the applicability of the luminescent assay principle to a wide range of proteins. Indeed, artificial luciferins that emit light in response to human serum albumin (HSA)[6] and immunoglobulin G (IgG)[7] — representative human proteins—were successfully developed (Figure 3B). As with the SARS-CoV-2 S protein, simple mixing of these artificial luciferins with the target proteins was sufficient to enable their detection. The next section describes specific examples of protein analysis technologies implemented using artificial luciferins.

Quantitative Luminescent Analysis of Human-Derived Proteins

HSA maintains blood osmotic pressure, buffers pH, and binds and transports exogenous substances such as drugs.

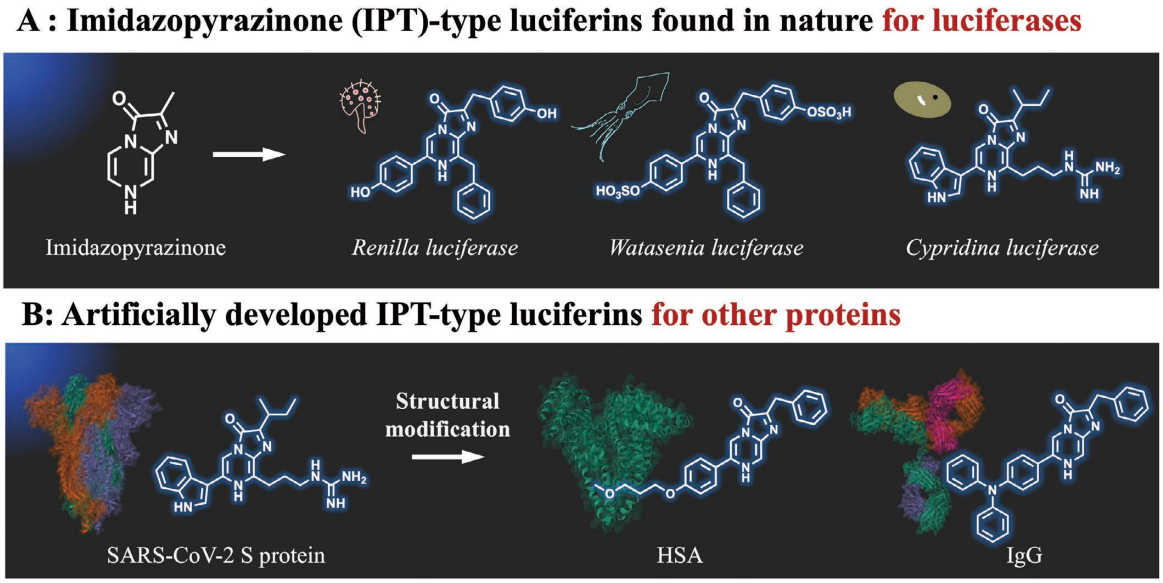

Figure 3 Molecular design of luciferins found in nature (A) and those tailored for protein analysis (B).

This drug-binding capability arises from the hydrophobic pockets within HSA. By exploiting this property, a luciferin that emits light upon binding to the hydrophobic pockets of HSA[6] was developed to quantify HSA in serum as an important indicator of kidney function and liver-related diseases. A total of 18 luciferins, including the natural luciferin CTZ and artificial luciferins with modified side chains, were evaluated for their luminescence properties in the presence of HSA. Only the artificial luciferin was found to produce luminescence (Figure 4A), indicating that the appropriate tuning of the imidazopyrazinone side chain enables the development of luciferins that emit light in the presence of specific human-derived proteins.

Cocrystal structural analyses with various drugs*10 previously revealed that HSA has two major drug-binding sites (site 1 and site 2)[8]. Thus, competitive inhibition assays*11 were performed using drugs that specifically bind to each site, i.e., warfarin to site 1 and ibuprofen to site 2 (Figure 4B). As a result, ibuprofen strongly inhibited the luminescence generated by the artificial luciferin and HSA, whereas warfarin showed no inhibitory effect, suggesting that the artificial luciferin binds to site 2. This result was supported by docking simulations (Figure 4C). Given that site 2 is a hydrophobic pocket, these results demonstrate that the artificial luciferin requires a hydrophobic environment to produce luminescence. Artificial luciferins that emitted light in the presence of HSA did not luminesce with more than 10 other human-derived proteins (Figure 4A). Surprisingly, no luminescence occurred even with bovine serum albumin (BSA), despite its high sequence similarity to HSA (75%) and drug-binding site similar to site 2 of HSA. Therefore, the artificial luciferin could detect subtle structural differences between the site 2 pockets of the two proteins, emitting light only when HSA was present.

Next, HSA in serum was quantified using the artificial luciferin. HSA levels in serum below 35 mg/mL can indicate conditions such as liver cirrhosis and chronic hepatitis; therefore, rapid and accurate quantification is essential. In contrast with the conventional bromocresol green colorimetric method, which suffers from low specificity, and ELISA, which requires two–three hours for a complete measurement, the artificial luciferin developed here reacts specifically with HSA and emits light immediately upon mixing, enabling rapid and accurate

*10 Cocrystal structural analysis: Analysis of the crystal structure formed by a protein and its bound molecules using techniques such as X-ray crystallography.

*11 Competitive inhibition assay: An experimental method that evaluates whether the molecule inhibits the reaction between an enzyme (or protein) and its substrate/binding partner.

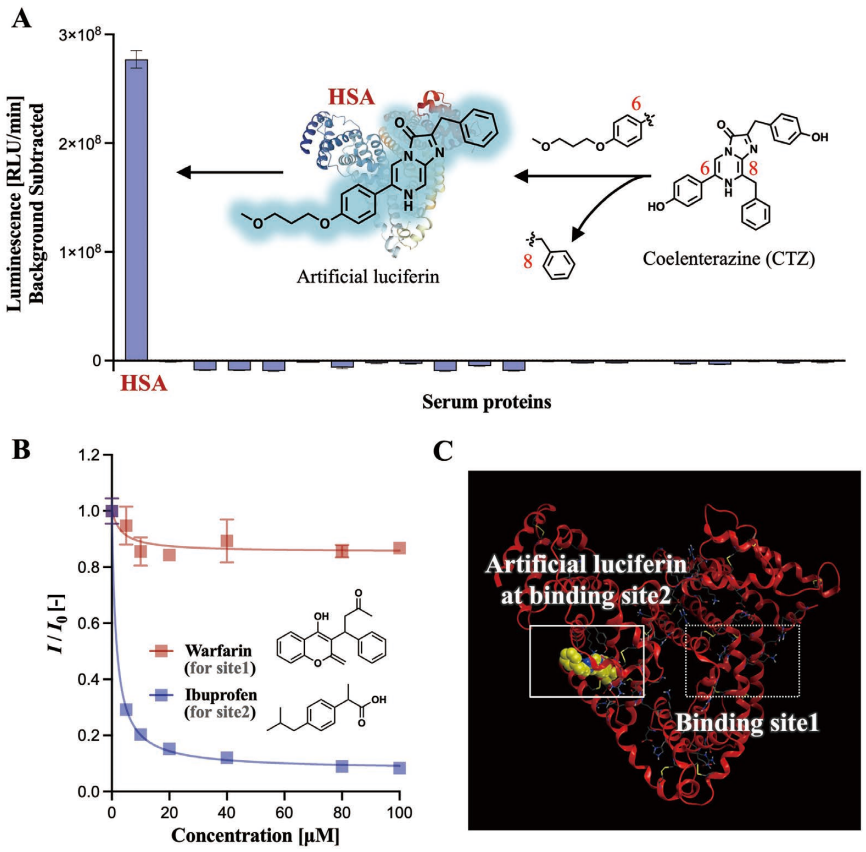

Figure 4 (A) Human serum albumin (HSA)–selective luminescence of artificial luciferin created by modifying the side chains of the natural luciferin CTZ. (B) Luminescence response with (I) and without the binding drug (I_0) (C) Docking simulation of artificial luciferin with HSA.

quantification. The luminescence intensity of the artificial luciferin correlated with the HSA concentration, and HSA levels calculated from the luminescence intensity measured within one minute without any pretreatment of serum samples showed strong agreement with ELISA results. Thus, serum HSA can be rapidly quantified by simply mixing the luciferin with the sample. More recently, this technique has been further applied to quantify trace urinary albumin (a marker of diabetic nephropathy)[9] and free copper ions in serum (biomarkers of Wilson and Menkes diseases)[10], demonstrating its potential for the rapid diagnosis of various diseases.

Owing to its simplicity and rapidity, this method is also suitable for on-site analysis and diagnostics. For instance, applying the artificial luciferin that reacts with HSA onto a portable 15 mm × 15 mm test strip enables the quantification of HSA in serum by simply adding a single drop of serum to the test strip[11]. Because HSA levels in serum differ markedly between patients with liver cancer and healthy individuals, this test strip successfully distinguished these groups by quantifying HSA in serum. This technique requires no antibodies or enzymes and relies solely on low-cost, low-molecular-weight artificial luciferins, providing a reagent-free protein detection approach. In addition, the test strips exhibit excellent storage stability even at room temperature. Combining this technique with commercially available portable handheld luminescence detectors is expected to enable on-site analyses for routine monitoring of health status.

Qualitative Luminescent Analysis of Human-Derived Proteins

Antibodies such as IgG play essential roles in recognizing and eliminating viruses and bacteria and are widely used as diagnostic and therapeutic reagents. However, antibodies are sensitive to environmental stress during manufacturing, storage, and use and may lose their native function upon denaturation*12. Currently, antibody denaturation is commonly evaluated using size-exclusion chromatography (SEC) and dynamic light scattering (DLS), but these methods require specialized expertise and advanced operational skills.

To address these limitations, artificial luciferins were designed to change their emission wavelength (color of emitted light) in response to the structural state of IgG, thereby enabling simple detection of protein structural changes (Figure 5A)[7]. Specifically, an artificial luciferin was

*12 Denaturation: Loss or alteration of a protein's native structural conformation.

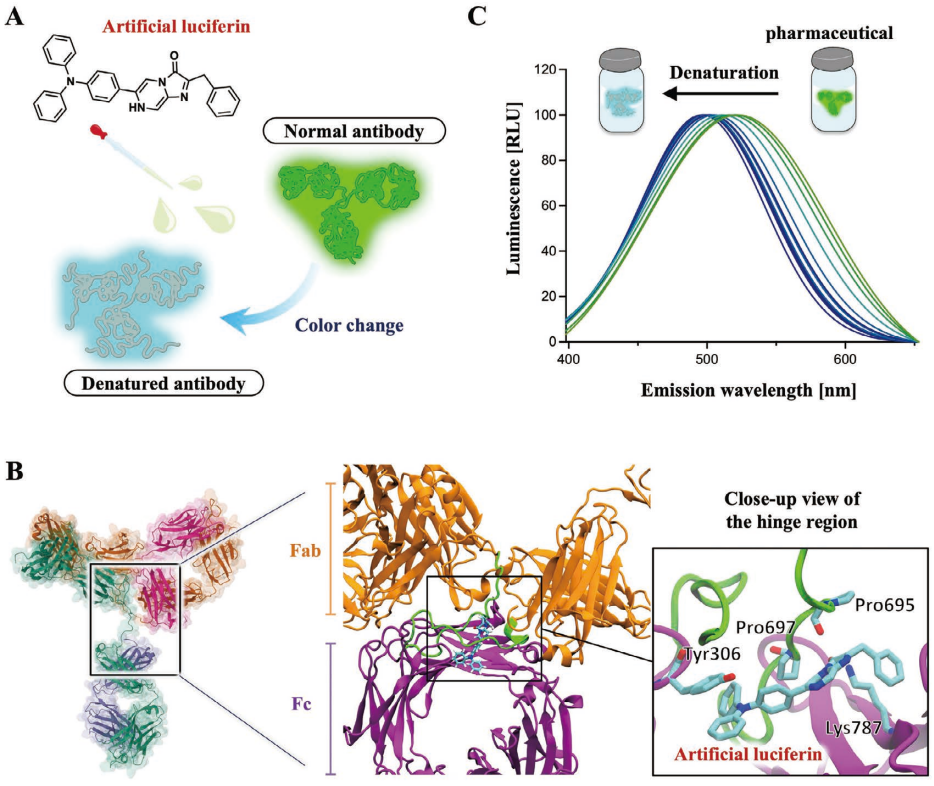

Figure 5 (A) Changes in the luminescence color of artificial luciferin depending on the structural states of IgG. (B) Binding pose of artificial luciferin at the hinge region of IgG obtained from MD simulations. (C) Spectral shift of the emission associated with denaturation of a therapeutic antibody.

designed and synthesized by introducing a triphenylamine (TPA) group as a side chain at the C-6 position of the imidazopyrazinone ring (Figure 5A). The TPA moiety undergoes intramolecular rotation in response to external stimuli such as physical stress or solvent conditions, altering the HOMO–LUMO bandgap[*13]. Accordingly, it was hypothesized that structural changes in IgG would be transmitted through the TPA group, thereby shifting the emission wavelength of the artificial luciferin.

As expected, the developed artificial luciferin exhibited luminescence upon reaction with IgG, generating green emission for native IgG and blue emission for heat-denatured IgG (Figure 5A). Thus, an artificial luciferin that enables qualitative evaluation of the IgG structure based on emission color was successfully developed. Furthermore, molecular dynamics (MD) simulations[*14] predicted that the luciferin binds, via the TPA group, to a hydrophobic pocket located within the hinge region[*15] of IgG (Figure 5B). Considering that this hinge region is also present in several antibody therapeutics[*16], the quality of antibody therapeutics could be evaluated using the artificial luciferin.

Antibody therapeutics, which are used to treat various diseases such as cancer and osteoporosis, are primarily developed based on IgG, particularly IgG1, IgG2, and IgG4 among the four IgG subclasses (IgG1, IgG2, IgG3, and IgG4). To evaluate the applicability of the artificial luciferin, its luminescence properties were measured using antibody therapeutics developed based on these subclasses. Luminescence was observed for all tested therapeutics; however, a marked shift in emission wavelength between the native and denatured states was observed only for the IgG2-based therapeutic. The hinge region of IgG differs among subclasses in characteristics such as length and the number of disulfide bonds[*17]. Therefore, the changes in the emission wavelength of the artificial luciferin can be mainly attributed to structural changes specific to the hinge region of IgG2. As the amount of heat-denatured IgG2 increases, the emission wavelength of the artificial luciferin shifts from green to blue, enabling the quantitative evaluation of IgG2 denaturation based on the magnitude of this wavelength shift (Figure 5C).

Fluorescence-based analytical methods using fluorescent dyes are also used for quantifying denatured antibodies. However, because such methods measure fluorescence intensity, they are susceptible to background signals arising from the excitation light source. In contrast, the newly developed luminescence method relies on changes in the emission wavelength of the luciferin rather than on intensity, enabling more reliable quantification. Furthermore, measurements are completed within three minutes after mixing the artificial luciferin with IgG. Compared with SEC and DLS, this method is far simpler and faster, making it a promising tool for the quality evaluation of IgG-based antibody therapeutics and diagnostic antibodies. In addition, by modifying the chemical structure of the luciferin, this approach could be extended to the evaluation of IgG1- and IgG4-based therapeutics and diagnostic reagents.

*13 HOMO–LUMO bandgap: Energy difference between the ground state and the excited state of electrons in the molecular orbital theory.

*14 Molecular dynamics (MD) simulation: A method that analyzes the dynamic properties and structural changes of substances by numerically solving Newton's equations of motion in classical mechanics to simulate the motion of atoms and molecules.

*15 Hinge region: A flexible region connecting the Fab and Fc domains of IgG.

*16 Antibody therapeutics: Drugs composed of antibodies designed to bind to specific disease-related molecules.

*17 Disulfide bond: A covalent bond formed between cysteine residues, contributing to protein structure and function.

Conclusion

This article describes the discovery of previously unrecognized pseudo-luciferase activity inherent in target proteins and demonstrates that, by leveraging this property, both the quantity and quality of proteins can be analyzed via simple mixing of luciferin with the sample. Because the luciferins used in this method selectively recognize and bind to specific proteins and emit light upon reaction, the use of antibodies or enzymes is unnecessary, and measurements can be completed within a few minutes. This high level of simplicity and rapidity clearly distinguishes the technique from conventional protein analytical methods such as ELISA, which typically requires several hours (Figure 6).

During the COVID-19 pandemic, immunochromatographic tests contributed substantially to society by enabling rapid diagnosis; however, their reliance on antibodies makes it challenging to address continuously emerging viral variants. In contrast, Cypridina luciferin emits light at a structurally conserved region of the SARS-CoV-2 S protein, suggesting applicability not only to the original Wuhan strain but also to multiple variants. Moreover, like immunochromatographic tests, this novel method can be adapted for on-site testing using luciferin-coated test strips, which are stable at room temperature. Thus, this technology holds promise as a complementary tool to existing diagnostic methods in future pandemics.

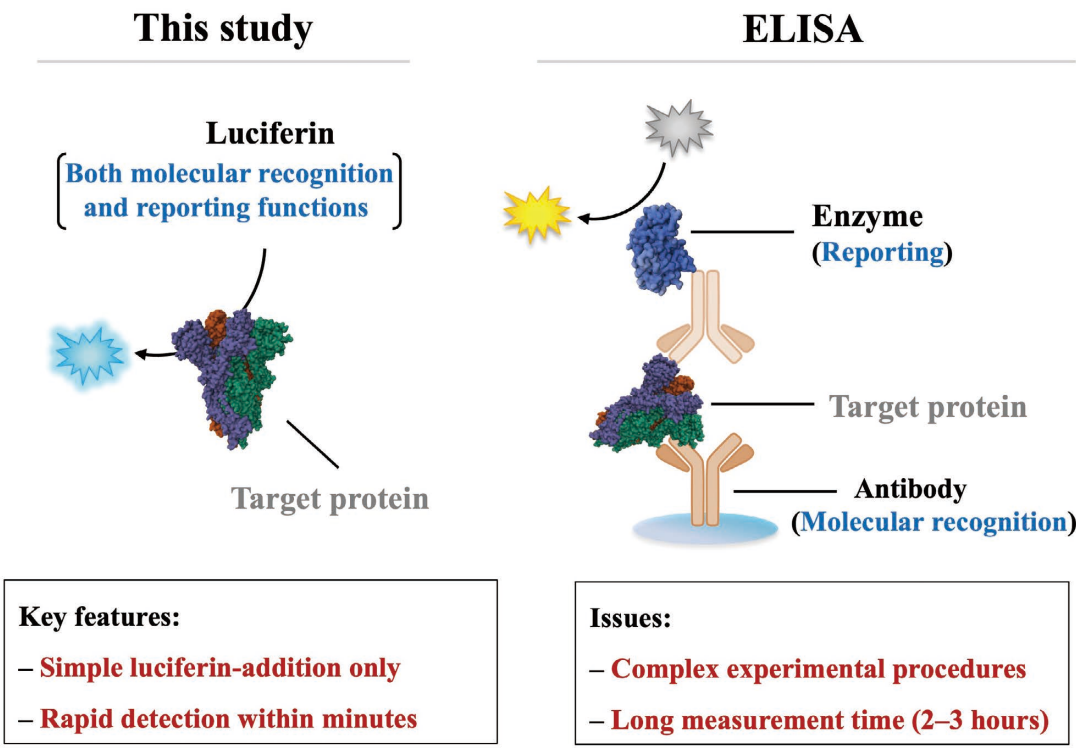

Figure 6 Comparison of the present technique with the conventional protein analytical method ELISA.

This study also demonstrates that the development of artificial luciferins enables the detection of structural changes in proteins for which obtaining antibodies is challenging. Antibodies used as therapeutics and diagnostics are highly sensitive to environmental stress during manufacturing and storage; denaturation not only compromises their native function but also reduces production efficiency. Because artificial luciferins emit light upon binding to structural regions commonly found in IgG, they are expected to serve as a useful quality-control tool for IgG-based antibody therapeutics and diagnostics.

Overall, this technique represents a next-generation analytical and measurement platform that can contribute to the development and manufacturing of biopharmaceuticals with the rapid detection of infectious diseases and quality assessment. By adopting an innovative approach that does not rely on conventional measurement principles, this method allows targeting proteins that are otherwise difficult to analyze. Future work will focus on further validating the effectiveness and reproducibility of this technique as a rapid-testing tool.

References

[1] Shimomura, O. Bioluminescence: Chemical Principles and Methods. *Bioluminescence: Chemical Principles and Methods* 2006, 1–471. DOI: 10.1142/9789812773647_0001

[2] Nishihara, R.; Paulmurugan, R.; Nakajima, T.; Yamamoto, E.; Natarajan, A.; Afjei, R.; Hiruta, Y.; Iwasawa, N.; Nishiyama, S.; Citterio, D. Highly bright and stable NIR-BRET with blue-shifted coelenterazine derivatives for deep-tissue imaging of molecular events in vivo. *Theranostics* 2019, 9, 2646–2661. DOI: 10.7150/thno.32219

[3] Nishihara, R.; Suzuki, H.; Hoshino, E.; Suganuma, S.; Sato, M.; Saitoh, T.; Nishiyama, S.; Iwasawa, N.; Citterio, D.; Suzuki, K. Bioluminescent coelenterazine derivatives with imidazopyrazinone C-6 extended substitution. *Chem. Commun.* 2015, 51, 391–394. DOI: 10.1039/C4CC06886F

[4] Toelzer, C.; Gupta, K.; Yadav, S. K. N.; Borucu, U.; Davidson, A. D.; Kavanagh Williamson, M.; Shoemark, D. K.; Garzoni, F.; Staufer, O.; Milligan, R.; Capin, J.; Mulholland, A. J.; Spatz, J.; Fitzgerald, D.; Berger, I.; Schaffitzel, C. Free fatty acid binding pocket in the locked structure of SARS-CoV-2 spike protein. *Science* 2020, 370, 725–730. DOI: 10.1126/science.abd3255

[5] Nishihara, R.; Dokainish, H.; Kihara, Y.; Ashiba, H.; Sugita, Y.; Kurita, R. Pseudo-Luciferase Activity of the SARS-CoV-2 Spike Protein for Cypridina Luciferin. *ACS Cent. Sci.* 2024, 10, 283–290. DOI: 10.1021/acscentsci.3c00887

[6] Nishihara, R.; Niwa, K.; Tomita, T.; Kurita, R. Coelenterazine Analogue with Human Serum Albumin-Specific Bioluminescence. *Bioconjugate Chem.* 2020, 31, 2679 -2684. DOI: 10.1021/acs.bioconjchem.0c00536

[7] Nishihara, R.; Niwa, K.; Tomita, T.; Yamamoto, E.; Kurita, R. Discovery of Pseudo-Luciferase Activity in Immunoglobulin G (IgG) and Its Application to the Detection of IgG Denaturation. *Anal. Chem.* 2025, 97, 9935–9943. DOI: 10.1021/acs.analchem.5c00646

[8] Ghuman, J., Zunszain, P., Petitpas, I., Bhattacharya, A., Otagiri, M., and Curry, S. Structural basis of the drug-binding specificity of human serum albumin. *J. Mol. Biol.* 2005, 353, 38–52. DOI: 10.1016/j.jmb.2005.07.075

[9] Kihara, Y.; Kurita, R.; Nishihara, R. Caged luciferin for the detection of albuminuria based on the pseudo-esterase/luciferase activities of albumin. *Bull. Chem. Soc. Jpn.* 2025, 98, uoaf074. DOI: 10.1093/bulcsj/uoaf074

[10] Nishihara, R.; Kurita, R. Mix-and-read bioluminescent copper detection platform using a caged coelenterazine analogue. *Analyst* 2021, 146, 6139 -6144. DOI: 10.1039/D1AN01292D

[11] Kurita, R.; Nishihara, R. Dry chemistry utilizing artificial luciferin for human serum albumin quantification. *Sensors and Actuators B: Chemical* 2025, 423, 136700. DOI: 10.1016/j.snb.2024.136700

Dr. Ryo Nishihara

Senior Researcher
Health and Medical Research Institute
National Institute of Advanced Industrial Science and Technology (AIST)

Innovation in Liquid Biopsy with Nanowires and Its Clinical Translation to Next-Generation Healthcare

Takao Yasui

Liquid biopsy, which enables early disease detection and prognostic evaluation using only body fluids such as urine or blood, has emerged as a key technology for next-generation healthcare. This article introduces a comprehensive capture technology for extracellular vesicles (EVs) based on engineered oxide nanowires, along with highly sensitive analytical methods for microRNAs and membrane proteins derived from these vesicles. By integrating materials engineering with mechanistic insights into biomolecular interactions, this platform opens new avenues for cancer diagnosis, prognostic assessment, and elucidation of metastatic mechanisms. Clinical implementation of the technology is also underway.

Keywords
liquid biopsy, urine, extracellular vesicles (EVs), nanowires, early cancer detection

Introduction

Cancer remains the leading cause of death in Japan, with both incidence and mortality continuing to rise. Against the backdrop of population aging and increasingly diverse lifestyles, early detection and appropriate treatment of cancer represent critical medical and societal challenges. In recent years, rapid advances in biotechnology and nanotechnology have accelerated expectations for non-invasive diagnostic approaches, particularly liquid biopsy.

Liquid biopsy enables the detection and monitoring of diseases by analyzing biomolecules contained in body fluids such as blood, urine, and saliva. This approach allows not only early diagnosis but also disease progression assessment and treatment response evaluation in a minimally invasive manner. Among the most promising targets are extracellular vesicles (EVs), nanoscale membrane-bound particles secreted by virtually all cells in the body. EVs contain microRNAs that regulate gene expression and membrane proteins that determine cellular uptake specificity. Because these molecular cargos reflect the physiological and pathological states of their cells of origin, EVs can be considered “sealed messages” from cancer cells.

However, due to their extremely small size (40–200 nm), comprehensive and efficient capture of EVs has been technically challenging. To address this limitation, we developed an innovative EV capture platform based on engineered oxide nanowires by integrating materials science and analytical chemistry. This article presents a series of studies ranging from the development of high-efficiency EV capture technology to its applications in cancer detection, prognosis prediction, elucidation of metastatic mechanisms, and real-world clinical translation.

A new perspective on liquid biopsy through *in vivo* tracking of EVs in body fluids[1]

Tumor-derived EVs are known to circulate through body fluids, including blood, urine, and saliva, and contribute to the formation of pre-metastatic niches and modulation of immune responses. However, the precise mechanisms by which tumor-derived EVs are released, transported, and ultimately appear in urine have remained unclear. To address this question, we established a hybrid reporter system enabling *in vivo* tracking of tumor-derived EVs. By engineering EVs labeled with a CD63-conjugated dCas9/gRNA system, we successfully visualized and quantitatively analyzed the process by which tumor-derived EVs are taken up by glomerular cells in the kidney and subsequently excreted into urine. Using tumor-bearing mouse models and kidney organoids, we demonstrated that renal transcytosis and glomerular

endothelial transport play essential roles in this process. Furthermore, by employing a GeNL-based reporter system combining NanoLuc bioluminescence and superfolder GFP fluorescence, we revealed that tumor-derived EVs are more abundantly detectable in urine than in blood. These findings provide a scientific and engineering foundation for urine-based EV diagnostics and shift the focus from simple molecular capture to understanding the trafficking pathways of disease-related vesicles *in vivo*.

Development of a comprehensive EV capture platform using oxide nanowires

Following confirmation of tumor-derived EVs in urine, the next challenge was to develop a technology capable of capturing them comprehensively and efficiently. From a materials engineering perspective, we designed oxide nanowires with precisely controlled structural and surface properties. By combining microfabrication with self-assembly techniques, we established a reproducible method for fabricating nanowires with defined spatial positioning, material composition, surface characteristics, alignment, and dimensionality. We then developed a capture strategy based on the physicochemical properties of EVs. In particular, we leveraged Coulombic (electrostatic) interactions and hydrogen bonding between EV membranes and nanowire surfaces[2],[3]. By precisely tuning the isoelectric point of oxide nanowires, we achieved selective electrostatic attraction between nanowires and negatively charged EVs. Infrared spectroscopy and molecular dynamics simulations further revealed that surface-bound water molecules on zinc oxide nanowires form multipoint hydrogen bonds with EV membranes, generating strong interaction forces that surpass those of conventional methods[4]. Using this platform, we achieved greater than 99% recovery of EVs from just 1 mL of urine[5],[6], substantially outperforming ultracentrifugation and immunoaffinity methods, which typically achieve recovery rates of around 30%.

Application to early cancer detection using urinary microRNAs

Early detection is crucial for improving cancer prognosis, particularly at Stage I or II. However, conventional screening methods are often invasive or unsuitable for frequent testing. By applying our nanowire-based EV capture technology, we established a method for highly sensitive and comprehensive detection of microRNAs from just 1 mL of urine. We successfully identified more than 1,300 distinct microRNAs from urinary EVs for the first time worldwide[5]. Compared to conventional ultracentrifugation-based approaches, which typically detect only a few hundred microRNAs, this represented a significant breakthrough in liquid biopsy research. Using these high-dimensional urinary microRNA datasets, we developed machine learning–based diagnostic algorithms capable of distinguishing cancer patients from healthy individuals with high accuracy. For brain tumors, we achieved 95% accuracy, 97% sensitivity, and 92% specificity[7]. For Stage I lung cancer, we achieved an AUROC of 0.987, with 96% sensitivity and 96% specificity[6]. Furthermore, we demonstrated that microRNA expression patterns differ among ten cancer types, enabling organ-specific cancer discrimination. This urine-based liquid biopsy platform offers a highly non-invasive yet high-precision diagnostic alternative with the potential to redefine early cancer detection standards.

Membrane protein analysis for cancer subtype identification and prognostic evaluation

Beyond microRNAs, membrane proteins on EV surfaces contain critical biological information reflecting the characteristics of their cells of origin. We extended our nanowire-based platform to analyze EV membrane proteins. In urine samples from patients with gliomas, we identified elevated levels of the endothelial marker CD31 on EVs and demonstrated that urinary EV-associated CD31 enables high-accuracy identification of glioblastoma[8]. This represents the first report of non-invasive glioblastoma subtype identification based on urinary EV membrane protein analysis. We further applied membrane protein profiling to prognostic evaluation. In ovarian cancer patients, we analyzed CD81 and TACSTD2 expression on EVs isolated from ascites[9]. High expression levels were associated with increased recurrence risk and poor prognosis, suggesting a novel non-invasive biomarker for post-treatment outcome prediction. The nanowire platform allows EV capture without structural damage, enabling direct downstream immunodetection. This versatility makes it uniquely suited for multidimensional EV analysis.

Elucidating metastatic mechanisms through spatial EV analysis using nanowire sheets

Metastasis from primary tumors to distant organs is a critical determinant of patient survival. EVs are increasingly recognized as mediators of pre-metastatic niche formation; however, their spatial distribution within organs has remained poorly understood. To address this, we developed a flexible nanowire sheet based on cellulose nanofibers (CNF) that can be directly applied to organ surfaces. This biocompatible platform enables spatial mapping of EV release sites across curved tissue surfaces[10]. Using this approach, we analyzed organ-specific EV distribution patterns and demonstrated its applicability beyond oncology. For example, in congenital diaphragmatic hernia, we successfully captured disease-associated EV-derived microRNAs from amniotic fluid using the nanowire sheet platform[11]. We also demonstrated rapid and stable recovery of salivary exosome-derived microRNAs, enabling longitudinal health monitoring using minimal sample volumes[12]. By enabling not only quantitative but also spatial EV analysis, the nanowire sheet technology provides a new perspective for understanding metastasis and early disease detection.

Conclusion

This article has presented a comprehensive EV capture platform based on engineered oxide nanowires and its translation into liquid biopsy applications. By integrating nanoscale materials design with mechanistic insights into biomolecular interactions, this technology offers innovative solutions for early cancer detection, prognostic evaluation, and understanding metastatic mechanisms. These achievements extend beyond academic research into real-world clinical implementation. I co-founded the university-based startup Craif Inc., which provides the non-invasive urinary microRNA cancer risk assessment service “miSignal” across medical institutions nationwide. The technology has entered practical deployment and continues expanding its societal impact. Moving forward, we aim to further advance technologies capable of non-invasively and accurately decoding health status and disease signals from body fluid–derived biomolecules. Through interdisciplinary collaboration across medicine, engineering, and data science, we will continue contributing to the realization of next-generation healthcare systems.

References

[1] S. Kawaguchi, T. Ajiri, R. Mitsuya, R. Tsuchiya, K. Kunitake, Y. Tanaka, T. Yokoyama, K. Sato, Y. Sato, Z. Zhu, K. Chattrairat, Y. Kobayashi, K. Inoue, K. Imaeda, K. Ueno, S. Ryuzaki, A. Kato, Y. Kimura, A. Natsume, R. Kojima and T. Yasui; Glomerular routing of tumor-derived extracellular vesicles substantiates urinary biopsy; *Sci. Adv., 12*, eaeb0555 (2026).

[2] T. Yasui, P. Paisrisarn, T. Yanagida, Y. Konakade, Y. Nakamura, K. Nagashima, M. Musa, I. A. Thiodorus, H. Takahashi, T. Naganawa, T. Shimada, N. Kaji, T. Ochiya, T. Kawai and Y. Baba; Molecular profiling of extracellular vesicles via charge-based capture using oxide nanowire microfluidics; *Biosens. Bioelectron., 194*, 113589 (2021).

[3] P. Paisrisarn, T. Yasui, Z. T. Zhu, A. Klamchuen, P. Kasamechonchung, T. Wutikhun, V. Yordsri and Y. Baba; Tailoring ZnO nanowire crystallinity and morphology for label-free capturing of extracellular vesicles; *Nanoscale, 14*, 4484 (2022).

[4] K. Chattrairat, A. Yokoi, M. Zhang, M. Iida, K. Yoshida, M. Kitagawa, A. Niwa, M. Maeki, T. Hasegawa, T. Yokoyama, Y. Tanaka, Y. Miyazaki, W. Shinoda, M. Tokeshi, K. Nagashima, T. Yanagida, H. Kajiyama, Y. Baba and T. Yasui; Discrimination of extracellular miRNA sources for the identification of tumor-related functions based on nanowire thermofluidics; *Device, 2*, 100363 (2024).

[5] T. Yasui, T. Yanagida, S. Ito, Y. Konakade, D. Takeshita, T. Naganawa, K. Nagashima, T. Shimada, N. Kaji, Y. Nakamura, I. A. Thiodorus, Y. He, S. Rahong, M. Kanai, H. Yukawa, T. Ochiya, T. Kawai and Y. Baba; Unveiling massive numbers of cancer-related urinary-microRNA candidates via nanowires; *Sci. Adv., 3*, e1701133 (2017).

[6] T. Yasui, A. Natsume, T. Yanagida, K. Nagashima, T. Washio, Y. Ichikawa, K. Chattrairat, T. Naganawa, M. Iida, Y. Kitano, K. Aoki, M. Mizunuma, T. Shimada, K. Takayama, T. Ochiya, T. Kawai and Y. Baba; Early cancer detection via multi-microRNA profiling of urinary exosomes captured by nanowires; *Anal. Chem., 96*, 17145 (2024).

[7] Y. Kitano, K. Aoki, F. Ohka, S. Yamazaki, K. Motomura, K. Tanahashi, M. Hirano, T. Naganawa, M. Iida, Y. Shiraki, T. Nishikawa, H. Shimizu, J. Yamaguchi, S. Maeda, H. Suzuki, T. Wakabayashi, Y. Baba, T. Yasui and A. Natsume; Urinary microRNA-based diagnostic model for central nervous system tumors using nanowire scaffolds; *ACS Appl. Mater. Interfaces, 13*, 17316 (2021).

[8] K. Chattrairat, T. Yasui, S. Suzuki, A. Natsume, K. Nagashima, M. Iida, M. Zhang, T. Shimada, A. Kato, K. Aoki, F. Ohka, S. Yamazaki, T. Yanagida and Y. Baba; All-in-one nanowire assay system for capture and analysis of extracellular vesicles from an ex vivo brain tumor model; *ACS Nano, 17*, 2235 (2023).

[9] A. Yokoi, M. Ukai, T. Yasui, Y. Inokuma, K. Hyeon-Deuk, J. Matsuzaki, K. Yoshida, M. Kitagawa, K. Chattrairat, M. Iida, T. Shimada, Y. Manabe, I. Y. Chang, E. Asano-Inami, Y. Koya, A. Nawa, K. Nakamura, T. Kiyono, T. Kato, A. Hirakawa, Y. Yoshioka, T. Ochiya, T. Hasegawa, Y. Baba, Y. Yamamoto and H. Kajiyama; Identifying high-grade serous ovarian carcinoma–specific extracellular vesicles by polyketone-coated nanowires; *Sci. Adv., 9*, eade6958 (2023).

[10] A. Yokoi, K. Yoshida, H. Koga, M. Kitagawa, Y. Nagao, M. Iida, S. Kawaguchi, M. Zhang, J. Nakayama, Y. Yamamoto, Y. Baba, H. Kajiyama and T. Yasui; Spatial exosome analysis using cellulose nanofiber sheets reveals the location heterogeneity of extracellular vesicles; *Nat. Commun., 14*, 6915 (2023).

[11] S. Matsuo, A. Yokoi, K. Yoshida, M. Kitagawa, E. Asano-Inami, M. Miura, T. Yasui, S. Tano, T. Ushida, K. Imai, H. Kajiyama and T. Kotani; Amniotic fluid-derived small extracellular vesicles for predicting postnatal severe outcome of congenital diaphragmatic hernia; *Journal of Extracellular Biology, 3*, e160 (2024).

[12] T. Ajiri, M. Zhang, N. Mizukami, M. Iida, S. Kawaguchi, Y. Sekihara, K. Chattrairat, Z. Zhu, Y. Baba, H. Koga and T. Yasui; Routine monitoring of microRNAs in salivary exosomes using a cellulose nanofiber sheet; *Biosens. Bioelectron.*, 299, 118436 (2026).

Dr. Takao Yasui

Professor
Graduate School of Engineering
Nagoya University

Pioneering Metabolomic Mass Spectrometry: From Nanomaterials to Clinical Diagnosis in Oncology

Lin Huang

Ultra-sensitive detection of metabolites at extreme trace levels within complex systems remains a major challenge in physiology and biomedicine. Ultra-sensitive mass spectrometry (MS) has become the preferred analytical tool in metabolomic research, among these platforms, matrix-assisted laser desorption/ionization (MALDI) MS offers high-speed (30 s/sample) and high-throughput (>300 samples/run) analysis. This study addresses limitations in MALDI-MS by developing a Fe-metal-organic framework heterojunction via gradient pyrolysis (350-500°C). The optimized Fe_3O_4@Fe-MOF material (FM-450) enhances LDI performance, achieving 1,000-fold signal amplification versus conventional matrices. Integrated with machine learning, it demonstrates superior diagnostic performance for thymic epithelial tumors (AUC=0.960) and risk stratification (AUC=0.856), outperforming current clinical methods. This work advances material design for LDI MS and establishes a transformative approach for precision oncology through metabolic-driven diagnostics.

Introduction

Metabolites represent the ultimate downstream products of cellular regulation, offering direct snapshots of physiological and pathological states. Comprehensive profiling of low-molecular-weight (LMW) metabolites is therefore essential for understanding biological mechanisms, dissecting metabolic pathways, decoding signaling networks, and discovering biomarkers for disease diagnosis and therapeutic monitoring[1]. Conventional platforms such as nuclear magnetic resonance (NMR) and liquid/gas chromatography mass spectrometry (LC/GC-MS) are capable of performing these analyses[2]. However, NMR suffers from signal overlap and inherently low sensitivity (μmol L^{-1} range) typically restrict confident identification to <100 metabolites in complex matrices[3]. LC-MS and GC-MS, although sensitive to the nmol L^{-1} level, require laborious and chemically specific pre-treatment workflows (e.g., protein precipitation, liquid extraction, and derivatization) that progressively accumulate processing time, reduce overall sample throughput and ultimately hinder the scalability required for large-scale, high-throughput metabolomics. Consequently, the development of a facile yet ultrasensitive approach for LMW metabolite

detection remains an urgent and enduring challenge[4].

Matrix-assisted laser desorption/ionization mass spectrometry (MALDI-MS) achieves high-throughput screening (~384 samples per run) and rapid data acquisition (~30 s per sample) with minimal or no sample pretreatment (Figure 1a)[5]. Theoretical considerations predict that selecting a high-performance matrix should afford ultrasensitive detection, because the matrix both absorbs laser energy and mediates soft desorption/ionization of analytes with negligible fragmentation. However, conventional organic matrices generate intense background noise in the low-m/z region and suffer from poor energy/electron-transfer efficiency, which collectively compromise sensitivity, shot-to-shot stability and metabolite coverage[6]. As a result, MALDI-MS still falls short of the low-level reproducibility required for demanding applications such as the discovery of low-abundance early-disease biomarkers[7].

Recent advances in nanoscale matrices address these limitations through engineered material interfaces (Figure 1b, c). Two-dimensional metal-organic framework nanosheets (2D MOF NSs)[8], for instance, exhibit self-decomposition under laser ablation, thereby reducing the generation of background interference peaks. In addition, carboxyl groups in aromatic acid ligands within MOFs further enhance cation adduction efficiency through proton transfer mediation. Nevertheless, pristine MOFs still face practical constraints from rapid electron-hole recombination and suboptimal energy dissipation during LDI process. Current strategies primarily aim to construct noble metal/metal oxide heterostructures through extrinsic metallophilic functional group modifications or conventional thermal agitation methods to establish synergistic host-guest interfaces. However, these approaches are constrained by either complex multi-step procedures or weak interfacial coupling, hindering the efficient design of robust heterojunction architectures with precise interfacial control. A particularly promising approach involves the controlled partial pyrolysis of MOFs to engineer interfacial heterojunctions and defects, a method that enhances photogenerated charge carrier separation and may significantly improve LDI performance for precision medical applications[9].

In this work, we developed a gradient pyrolysis protocol (350-500°C) to construct Fe MOF NSs (denoted as Fe-MOF) derived heterojunction. These heterostructures incorporate magnetite nanoparticles (Fe_3O_4 NPs) with high photothermal conversion efficiency, enhancing interfacial ionization performance. The optimized Fe_3O_4@Fe-MOF heterojunction demonstrated a maximum 1,000-fold signal amplification in metabolite detection, enabling direct acquisition of serum metabolic fingerprints (SMFs) with ultralow sample consumption (1 μL). Through

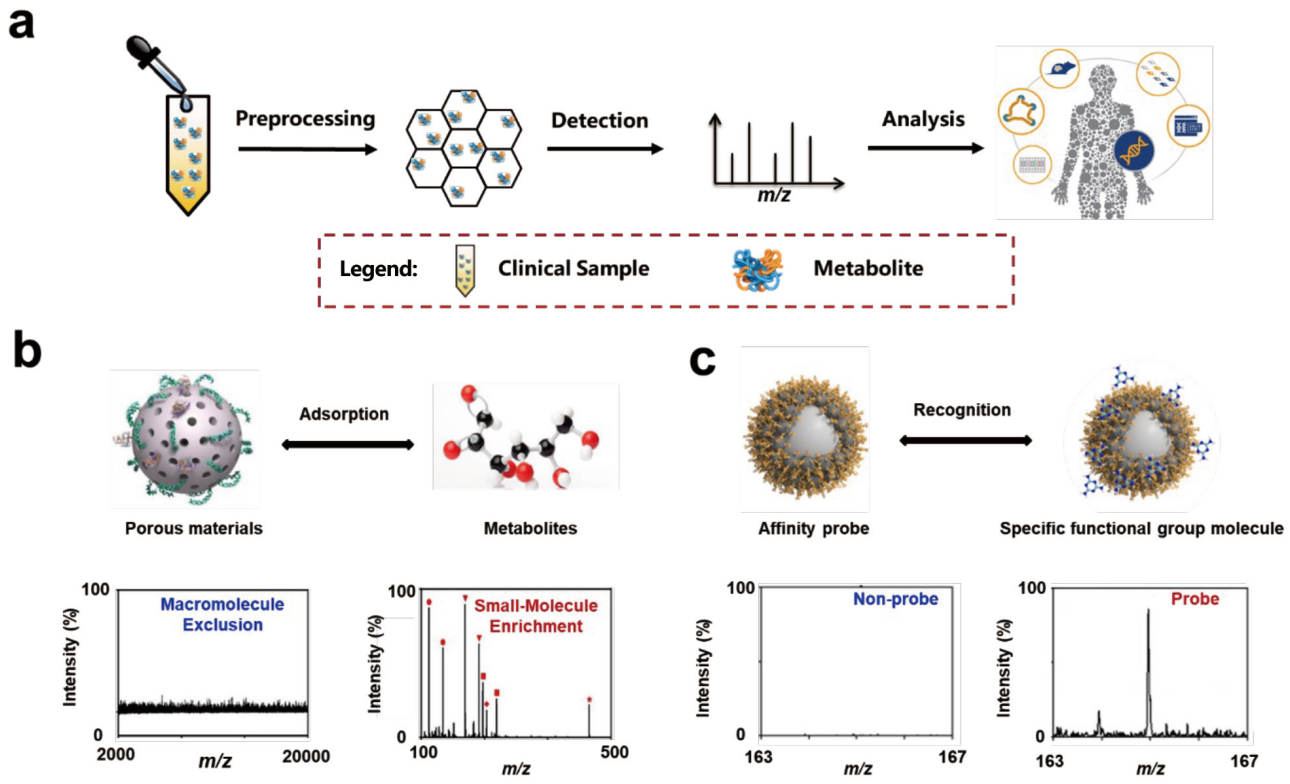

Figure 1 High-sensitivity metabolomics process and innovation of nanomaterials (a) Clinical sample acquisition and data processing procedure. (b) The adsorption of metabolites by porous materials enables molecular-specific detection. (c) Affinity probe materials enable the detection of target metabolites.

machine learning of SMF patterns, we constructed a robust diagnostic platform for distinguishing thymic epithelial tumors (TETs) from benign control (BC) with an area under the curve (AUC) of 0.960. Furthermore, a panel comprising 12 metabolites was identified for hierarchical risk stratification with AUC of 0.856. This work not only advances the rational design of advanced materials for LDI MS but also establishes a transformative platform for clinical metabolomics toward precision oncology.

Result

Design and Characterization of Materials

The strategic design of the Fe-MOF-derived heterojunction involved optimizing the pyrolysis conditions to create an ideal interface between the MOF framework and Fe_3O_4 nanoparticles (Figure 2a)[10]. Thermal analysis revealed that the MOF structure remained stable up to 350℃, with decomposition occurring between 350-500℃. At 450℃ (FM-450), the material achieved an optimal balance, with well-dispersed Fe_3O_4 nanoparticles (size 5-20 nm) embedded within a partially preserved MOF matrix[11]. This unique architecture created numerous heterointerfaces that enhanced light absorption and charge separation efficiency. The structural evolution during pyrolysis was characterized by multiple techniques. Firstly, the TEM images clearly showed the progressive formation of nanoparticles on the MOF surface, with FM-450 exhibiting uniform distribution without aggregation (Figure 2b). In addition, XRD patterns confirmed the coexistence of MOF and Fe_3O_4 crystal phases, while FTIR spectroscopy tracked the gradual decomposition of organic ligands. XPS analysis provided crucial insights into the chemical state changes, revealing an increase in oxygen vacancies and mixed valence states that contribute to the material's enhanced performance. Furthermore, the superiority of the heterojunction design over single-component materials was demonstrated through comparative studies with conventional MOFs (Fe-MIL-101, Fe-MOF-74). The FM-450 composite showed significantly improved photocurrent response and thermal conversion efficiency, attributed to the synergistic interaction between the components. This carefully engineered material architecture addresses fundamental limitations of previous matrices, providing a robust platform for metabolic analysis[12].

The FM-450 matrix demonstrated exceptional performance in LDI MS analysis, achieving up to 1,000-fold signal enhancement compared to conventional organic matrices (CHCA, DHB). This improvement was consistent

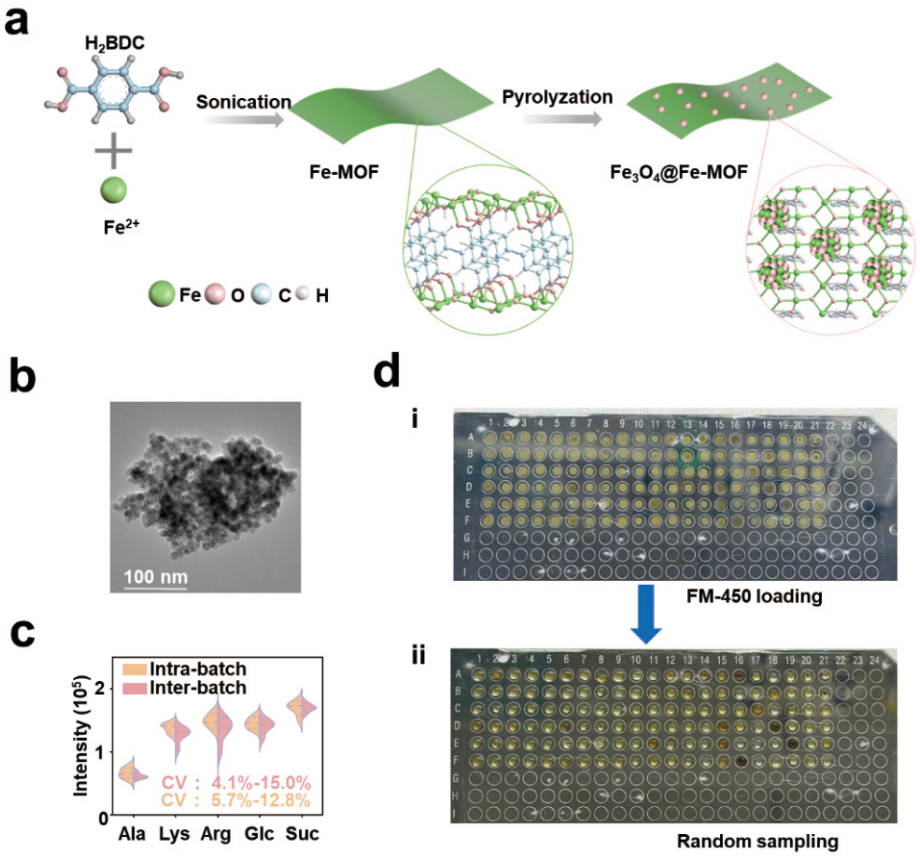

Figure 2 Preparation and characterization of MALDI-MS platform. (a) Schematic illustration of the preparation of Fe-MOF and its partial pyrolysis to form Fe_3O_4@Fe-MOF. (b) TEM of FM-450. (c) Intra-batch and inter-batch CVs of Na-adducted signals from five metabolites using FM-450 as the matrix. (d) FM-450 preload loading (i) and random sampling was performed in the inexperienced population (ii).

across multiple metabolite classes, including amino acids (alanine, lysine, arginine), sugars (glucose, sucrose), and organic acids, with detection limits reaching picomolar levels. The enhanced sensitivity enables detection of low-abundance metabolites that are often missed by conventional approaches, expanding the analytical coverage of the metabolome[13].

The matrix's performance was particularly notable in challenging analytical conditions. In high-salt environments (0.5 M NaCl) and protein-rich matrices (5 mg/mL BSA), FM-450 maintained excellent detection capability, whereas conventional matrices showed significant interference. This robustness stems from the material's mesoporous structure (pore size ≈2 nm), which selectively absorbs metabolites while excluding larger proteins and salts. The reproducibility of FM-450 was exceptional, with intra-batch and inter-batch coefficients of variation below 15%, compared to 30-97% for organic matrices (Figure 2c). This consistency is crucial for clinical applications where reliable quantitative data is essential for diagnostic decisions.

The practical advantages of the FM-450 platform extend beyond analytical performance (Figure 2d). The simplified sample preparation (no extraction or derivatization), minimal sample requirement (1 µL serum), and rapid analysis time (30 seconds per sample) make it suitable for high-throughput clinical screening. Additionally, the matrix's stability—maintaining performance for 6 months at room temperature and withstanding 10,000 laser irradiations—ensures operational reliability in routine laboratory use.

Mechanistic Insights into Enhanced Ionization

The exceptional performance of FM-450 originates from the synergistic combination of photothermal and photoelectric effects enhanced by the heterojunction structure. UV-vis spectroscopy confirmed strong absorption in the 300-400 nm range, matching the 355 nm laser wavelength used in LDI MS (Figure 3a). Photocurrent measurements demonstrated a twofold increase in charge carrier generation compared to pristine Fe-MOF, attributed to improved charge separation at the heterointerface (Figure 3b)[14].

Thermal imaging revealed rapid temperature increase under laser irradiation, with FM-450 showing the fastest heating rate among the tested materials. This efficient photothermal conversion facilitates analyte desorption, while the heterojunction structure promotes charge separation, increasing ionization efficiency. The material's band structure was characterized using Mott-Schottky analysis, revealing an S-scheme heterojunction that drives electrons from Fe_3O_4 to Fe-MOF, creating a built-in electric field that enhances charge separation (Figure 3c).

Scavenger experiments provided further mechanistic insights. The addition of juglone (electron scavenger) increased metabolite signals, while EDTA (hole scavenger)

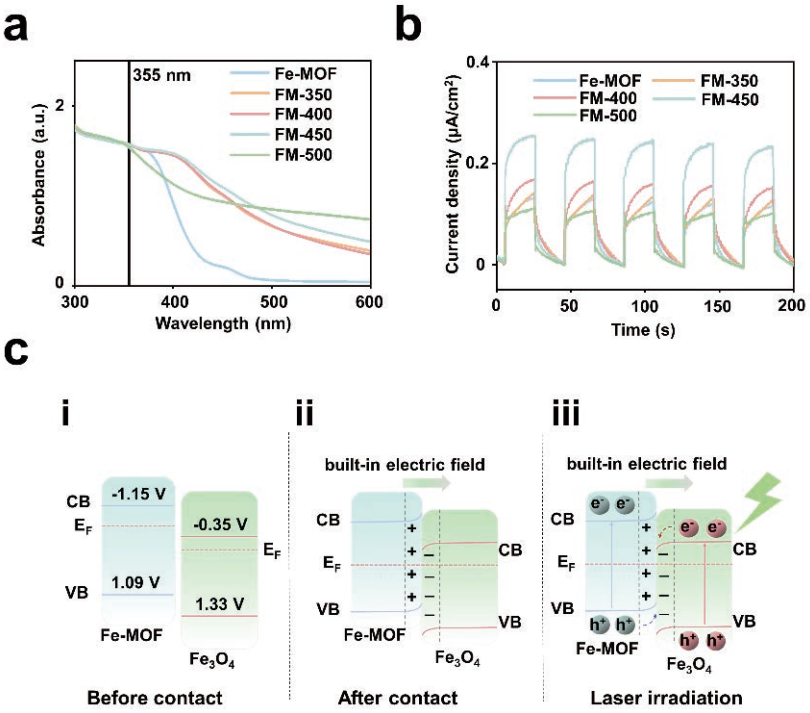

Figure 3 Mechanistic investigation of FM-450 in metabolite detection. (a) Ultraviolet-visible absorption spectra and (b) photocurrent-time curves of Fe-MOF and FM-X (X = 350, 400, 450, 500). (c) Schematic illustration of charge transfer route in FM-450 via the S-scheme heterojunction.

decreased signals, confirming that holes are the primary charge carriers in positive ion mode. This understanding of the fundamental mechanisms guides future material optimization and application to different analyte classes.

The heterojunction design represents a significant advancement over conventional matrices, addressing long-standing challenges in LDI MS. While organic matrices suffer from background interference and inorganic materials often show poor reproducibility, the FM-450 composite combines the advantages of both the excellent ionization efficiency from the heterojunction and consistent performance from the stable framework. This mechanistic understanding provides a foundation for rational design of next-generation matrices for metabolic analysis[15].

Clinical Application in TETs Diagnosis and Stratification

The clinical utility of the FM-450 platform was evaluated through a comprehensive study involving 243 participants. SMFs containing 698 features were acquired from each sample, covering mass range m/z 80-500[16]. Unsupervised analysis using principal component analysis (PCA) showed partial separation between benign controls and TETs patients, but significant overlap persisted, necessitating advanced machine learning approaches for accurate classification[17].

The LASSO regression algorithm demonstrated superior performance in distinguishing TETs from benign controls, achieving an AUC of 0.975 in the discovery cohort (n=172) and maintaining robust performance in the validation cohort (AUC=0.960, n=71; Figure 4a). A panel of 10 metabolites (Panel-10M) was identified through rigorous feature selection, showing consistent dysregulation in TETs patients (Figure 4b, c)[18]. These metabolites, involved in key pathways such as pyruvate metabolism, glycerolipid metabolism, and amino acid metabolism, provide biological insights into TETs pathophysiology[19].

For risk stratification, a more refined approach was necessary. The initial Panel-10M showed moderate performance in distinguishing LR from HR TETs (AUC=0.700), prompting the development of a specialized 12-metabolite panel (Panel-12M) through a two-stage feature selection process (Figure 5a). This panel integrated six metabolites with high sensitivity for risk differentiation (Panel-6M) and six metabolites showing distinct expression patterns between risk groups (Panel-6SM). The integrated Panel-12M achieved an AUC of 0.856, significantly outperforming imaging-based assessment (AUC=0.627) and providing a powerful tool for clinical decision-making (Figure 5b).

The metabolic alterations observed in TETs patients reflect fundamental changes in cellular metabolism. Downregulation of pyruvate and lactate suggests altered energy metabolism, while changes in glycerolipid and fatty acid metabolites indicate membrane remodeling and signaling alterations (Figure 5c). These metabolic signatures not only serve as biomarkers but also provide insights into the molecular mechanisms driving TETs progression, potentially revealing new therapeutic targets.

The clinical implementation of this platform offers numerous advantages over current standards. The non-invasive nature of blood sampling enables repeated monitoring, facilitating treatment response assessment and disease surveillance. The rapid analysis time (minutes versus days for pathology) supports timely clinical decisions, while the minimal sample requirement makes it suitable for patients with limited venous access. Most importantly, the metabolic information provides functional insights complementary to anatomical imaging, creating a more comprehensive diagnostic picture[20].

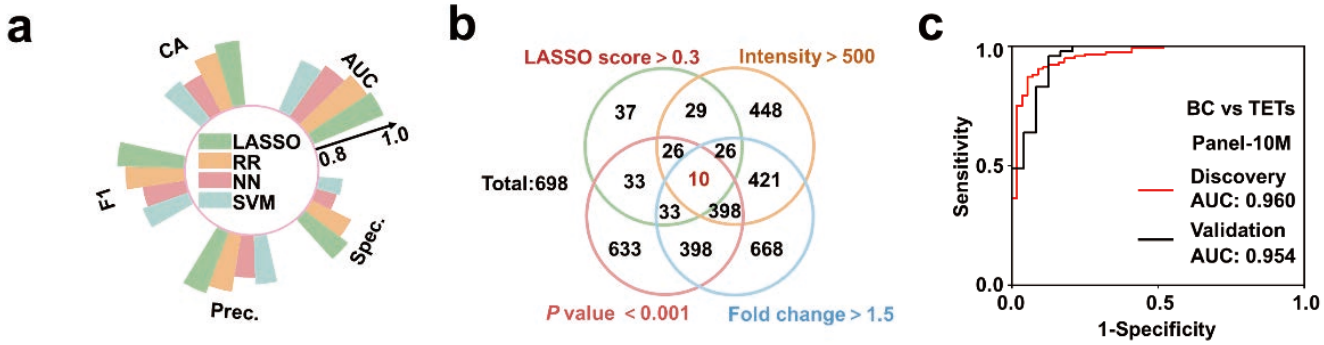

Figure 4 Diagnosis of TET-associated serum metabolic fingerprints. (a) Performance evaluation of different machine learning algorithms in distinguishing between benign control and TETs patients. (b) Venn diagram of 10 m/z features selected as diagnosis biomarker panel following multiple screening rounds. (c) Diagnostic model constructed using Panel-10M for discovery and validation cohorts.

Conclusion and Future Perspectives

The development of the Fe-MOF-derived heterojunction platform represents a significant advancement in metabolic diagnostics, addressing critical limitations in current TETs management. The integration of materials science, analytical chemistry, and machine learning has created a powerful tool that combines high sensitivity, specificity, and clinical practicality. The 1,000-fold improvement in detection sensitivity compared to conventional matrices enables identification of metabolic alterations at earlier disease stages, while the robust classification algorithms ensure reliable diagnostic decisions.

The clinical validation across 243 participants demonstrates the real-world utility of this approach. The consistent performance across discovery and validation cohorts, with AUC values exceeding 0.95 for diagnosis and 0.85 for risk stratification, meets the rigorous standards required for clinical implementation. The metabolic panels identified through rigorous feature selection provide biological insights while maintaining analytical simplicity, balancing depth of information with practical applicability.

Several aspects of this platform are particularly noteworthy for future development. The modular design allows adaptation to other cancer types by adjusting the metabolic panels, while the minimal sample requirement enables application in pediatric and critically ill patients. The cost-effectiveness (approximately US $0.03 per test compared to approximately US $4 per test for LC-MS/

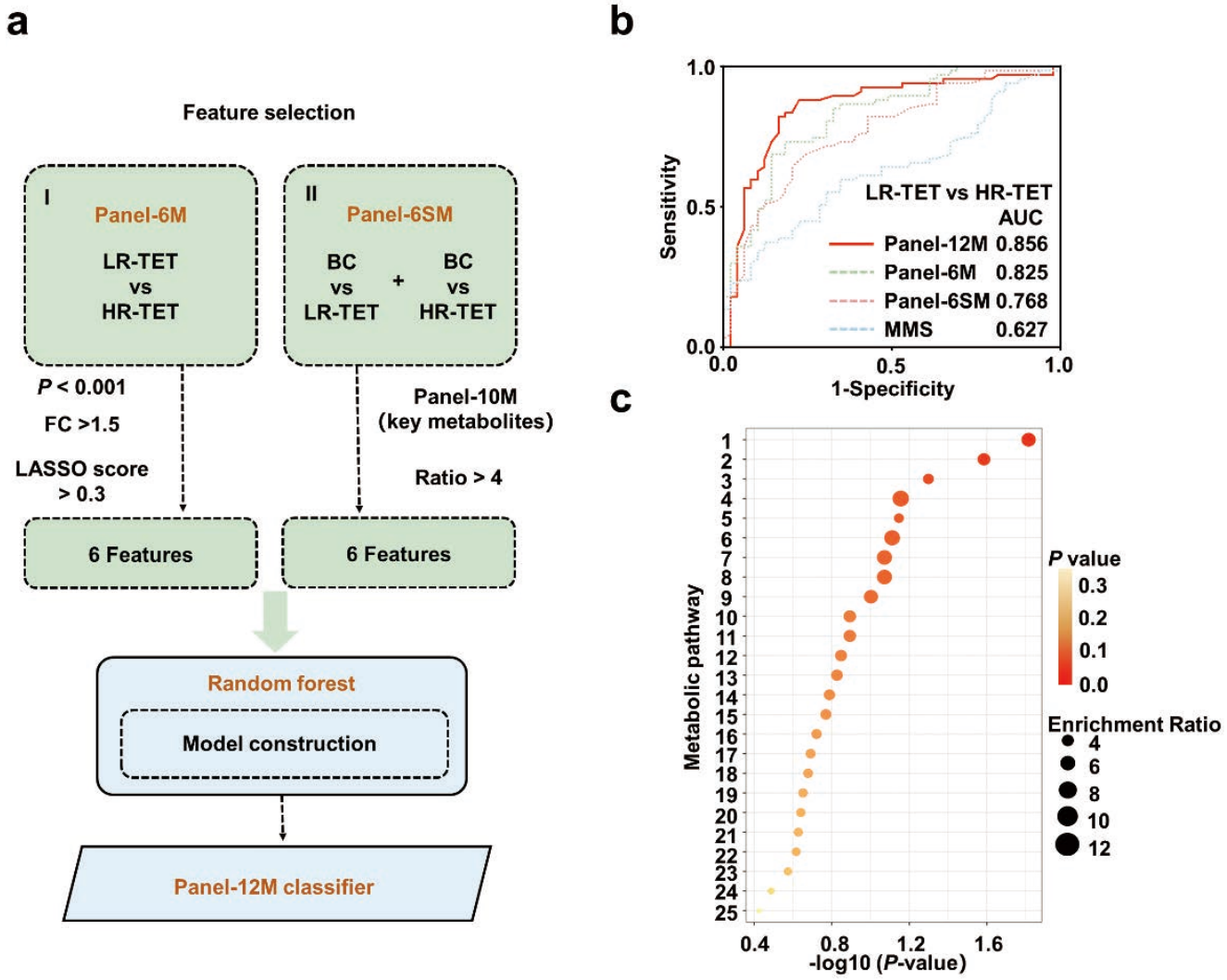

Figure 5 Serum metabolic fingerprint-based risk stratification of TETs. (a) Schematic workflow for classifier construction. Feature selection (green): Stages I identifying key metabolites to form the Panel-6M that met statistical criteria of P < 0.001, FC > 1.5, and LASSO score > 0.3 in the comparison of LR-TET vs HR-TET; and II identifying metabolites from the Panel-10M to form the 6 score metabolites panel (Panel-6SM) with a ratio (LASSO score from BC vs LR-TET divided by LASSO score from BC vs HR-TET) greater than 4. Classifier building (blue): The 12 metabolites from stages I and II are integrated into the final classifier of Panel-12M using a random forest algorithm. (b) Relative importance of specific metabolic pathways in TET progression, ranked by their contribution. 1: Glycerolipid metabolism; 2: Gluconeogenesis; 3: Pyruvate metabolism; 4: De novo triacylglycerol biosynthesis; 5: Warburg effect; 6: Pyruvaldehyde degradation; 7: Glycerol phosphate shuttle; 8: Cardiolipin biosynthesis; 9: Glucose-alanine cycle; 10: Alpha linolenic acid and linoleic acid; 11: Alanine metabolism; 12: Mitochondrial electron transport chain; 13: Glutathione metabolism; 14: Transfer of acetyl groups; 15: Glycolysis; 16: Cysteine metabolism; 17: Urea cycle; 18: Phospholipid biosynthesis; 19: Ammonia recycling; 20: Citric acid cycle; 21: Amino sugar metabolism; 22: Beta-alanine metabolism; 23: Galactose metabolism; 24: Glutamate metabolism; 25: Pyrimidine metabolism.

MS) makes it suitable for widespread screening programs, potentially transforming cancer detection in resource-limited settings.

Future research directions should focus on several key areas. Multi-center validation across diverse populations will establish generalizability, while longitudinal studies can assess utility for monitoring treatment response and disease recurrence. Technical enhancements could include integration with other omics technologies and development of point-of-care devices. Additionally, exploration of the identified metabolic pathways may reveal new therapeutic targets and mechanistic insights into TETs biology.

The implications of this work extend beyond TETs diagnostics. The material design principles, creating heterojunctions through controlled pyrolysis, can be applied to other analytical challenges, while the computational framework for metabolic feature selection and model building can be adapted to various disease states. This interdisciplinary approach serves as a blueprint for developing next-generation diagnostic platforms that leverage advances in multiple scientific fields.

References

[1] Y. Bai, Y. Nan, T. Wu, A. Zhu, X. Xie, Y. Sun, Y. Deng, Z. Dou, X. Hu, R. Zhou, S. Xu, Y. Zhang, J. Fan, D. Ju, *Adv Sci* 2024, 11, e2400493.

[2] C. Zhang, L. Xu, Q. Huang, Y. Wang, H. Tang, *J Am Chem Soc* 2023, 145, 25513.

[3] X. Li, J. Yang, X. Zhou, C. Dai, M. Kong, L. Xie, C. Liu, Y. Liu, D. Li, X. Ma, Y. Dai, Y. Sun, Z. Jian, X. Guo, X. Lin, Y. Li, L. Sun, X. Liu, L. Jin, H. Tang, Y. Zheng, S. Hong, *Nat Metab* 2024, 6, 1397.

[4] G. K. Parida, S. Mitra, A. Suman, G. S. Muthu, *Clin Nucl Med* 2021, 46, e61.

[5] W. Xu, J. Lin, M. Gao, Y. Chen, J. Cao, J. Pu, L. Huang, J. Zhao, K. Qian, *Adv Sci* 2020, 7, 2002021.

[6] H. Su, X. Li, L. Huang, J. Cao, M. Zhang, V. Vedarethinam, W. Di, Z. Hu, K. Qian, *Adv Mater* 2021, 33, e2007978.

[7] J. Cao, Q. J. Yao, J. Wu, X. Chen, L. Huang, W. Liu, K. Qian, J. J. Wan, B. O. Zhou, *Cell Metab* 2024, 36, 209.

[8] K. Mosupi, M. Masukume, G. Weng, N. M. Musyoka, H. W. Langmi, *Coordin Chem Rev* 2025, 529, 216467.

[9] M. De Martino, J. C. Rathmell, L. Galluzzi, C. Vanpouille-Box, *Nat Rev Immunol* 2024, 24, 654.

[10] J. Yang, X. Yin, L. Zhang, X. Zhang, Y. Lin, L. Zhuang, W. Liu, R. Zhang, X. Yan, L. Shi, W. Di, L. Feng, Y. Jia, J. Wang, K. Qian, X. Yao, *Adv Mater* 2022, 34, 2201422.

[11] Z. Li, W. Peng, J. Zhou, S. Shui, Y. Liu, T. Li, X. Zhan, Y. Chen, F. Lan, B. Ying, Y. Wu, *Adv Mater* 2024, 36, 2312799.

[12] W. Chen, H. Yu, Y. Hao, W. Liu, R. Wang, Y. Huang, J. Wu, L. Feng, Y. Guan, L. Huang, K. Qian, *ACS Nano* 2023, 17, 19779.

[13] R. Wang, S. Yang, M. Wang, Y. Zhou, X. Li, W. Chen, W. Liu, Y. Huang, J. Wu, J. Cao, L. Feng, J. Wan, J. Wang, L. Huang, K. Qian, *Nat Sustain* 2024, 7, 602.

[14] A. Yiming, Y. Zhao, H. Meng, S. Yang, C. Ding, R. Wang, H. Su, W. Chen, W. Liu, Y. Zhou, X. Li, H. Jin, J. Wang, K. Qian, L. Huang, *Adv Funct Mater* 2025, 35, 2417474.

[15] C. Pei, C. Liu, Y. Wang, D. Cheng, R. Li, W. Shu, C. Zhang, W. Hu, A. Jin, Y. Yang, J. Wan, *Angew Chem Int Ed Engl* 2020, 59, 10831.

[16] a) M. S. Tsao, A. G. Nicholson, J. J. Maleszewski, A. Marx, W. D. Travis, *J Thorac Oncol* 2022, 17, e1; b) N. Girard, F. Mornex, P. Van Houtte, J. F. Cordier, P. van Schil, *J Thorac Oncol* 2009, 4, 119.

[17] R. Wang, Z. Gu, Y. Wang, X. Yin, W. Liu, W. Chen, Y. Huang, J. Wu, S. Yang, L. Feng, L. Zhou, L. Li, W. Di, X. Pu, L. Huang, K. Qian, *Adv Funct Mater* 2022, 32, 2206670.

[18] Y. Chen, W. Xu, W. Zhang, R. Tong, A. Yuan, Z. Li, H. Jiang, L. Hu, L. Huang, Y. Xu, Z. Zhang, M. Sun, X. Yan, A. F. Chen, K. Qian, J. Pu, *Cell Rep Med* 2023, 4, 114.

[19] Z. M. El-Zaatari, J. Y. Ro, *Adv Anat Pathol* 2021, 28, 335.

[20] Y. Huang, H. Yang, J. Li, F. Wang, W. Liu, Y. Liu, R. Wang, L. Duan, J. Wu, Z. Gao, J. Cao, F. Bian, J. Zhang, F. Zhao, S. Yang, S. Cao, A. Yang, X. Wang, M. Geng, A. Hao, J. Li, J. Cao, C. Li, Z. Zhang, N. Zhang, Y. Huang, Y. Zhang, K. Qian, F. Zhou, *Small Methods* 2024, 8, 2301046.

Dr. Lin Huang

Assistant Professor
School of Medicine
Shanghai Jiao Tong University

* This article is an English translation of the original Japanese version published in Readout No. 61.

Elucidating Novel Regulatory Mechanisms for Metabolic Systems of Cancers by Imaging Metabolomics and Their Medical Applications

Makoto Suematsu

Director
Central Institute for Experimental Medicine and Life Science
Professor Emeritus
Keio University

Regulation of cancer metabolic systems is crucial for understanding the molecular mechanisms of cancer cell proliferation and chemoresistance to anticancer drugs. Post-translational modifications (PTMs) of enzyme proteins represent a domain that cannot be explored through comprehensive analyses of the transcriptome or epigenetics. Among these, the methylation and demethylation of arginine residues serve as a 'signpost' that determines the metabolic fate of glucose uptake in cancer cells. Developing methods to artificially control these modifications may present novel targets for cancer therapy.

Introduction

It has long been known that cancer cells actively take up glucose and enhance glycolysis, thereby vigorously producing lactate, regardless of whether the oxygen supply is sufficient or insufficient. This phenomenon is called the Warburg effect, named after its discoverer (Figure 1). Analyses of intracellular metabolism in many solid tumors over the past 15 years have revealed that this metabolic phenotype is produced by the combined action of several mechanisms. These include enhanced glucose uptake via the upregulated expression of glucose transporter 1 (GLUT1); increased activity of phosphofructokinase-1 (PFK-1), a rate-limiting enzyme of glycolysis; the acquisition of transcriptional regulatory factor function through the nuclear translocation of pyruvate kinase M2; and the inhibition of conversion to acetyl CoA through the regulation of pyruvate dehydrogenase kinase (PDK), which phosphorylates pyruvate dehydrogenase and controls the flux from glycolysis to mitochondrial metabolism. The experimental results described below represent mechanisms that are extremely important for activating cancer cell proliferation and acquiring resistance to chemotherapy.

1. Discovery of a Sophisticated Mechanism for Glycolytic Regulation via Protein Methylation

Traditionally, the metabolic trait of enhancing glycolysis regardless of the oxygen environment was considered to be utilized in cancer progression as a means of maintaining ATP levels in tumor cells. Focusing on the fact that glucose metabolized through glycolysis is bio-transformed into a variety of metabolites via branching metabolic pathways, we hypothesized that this process may be involved in the manifestation of diverse biological effects in cancer, and have conducted our research accordingly.

In 2014, Yamamoto from our research group discovered a novel regulatory mechanism of PFK-1, a rate-limiting enzyme in glycolysis. Specifically, it was found that PFKFB3, the enzyme responsible for generating fructose 2,6-bisphosphate (F2,6BP), an allosteric activator of PFK-1, is methylated at arginine residues 131 and 134 by the action of protein arginine methyltransferase-1 (PRMT1), which specifically methylates arginine residues in proteins. This increases F2,6BP production and consequently enhances PFK-1 activity[1].

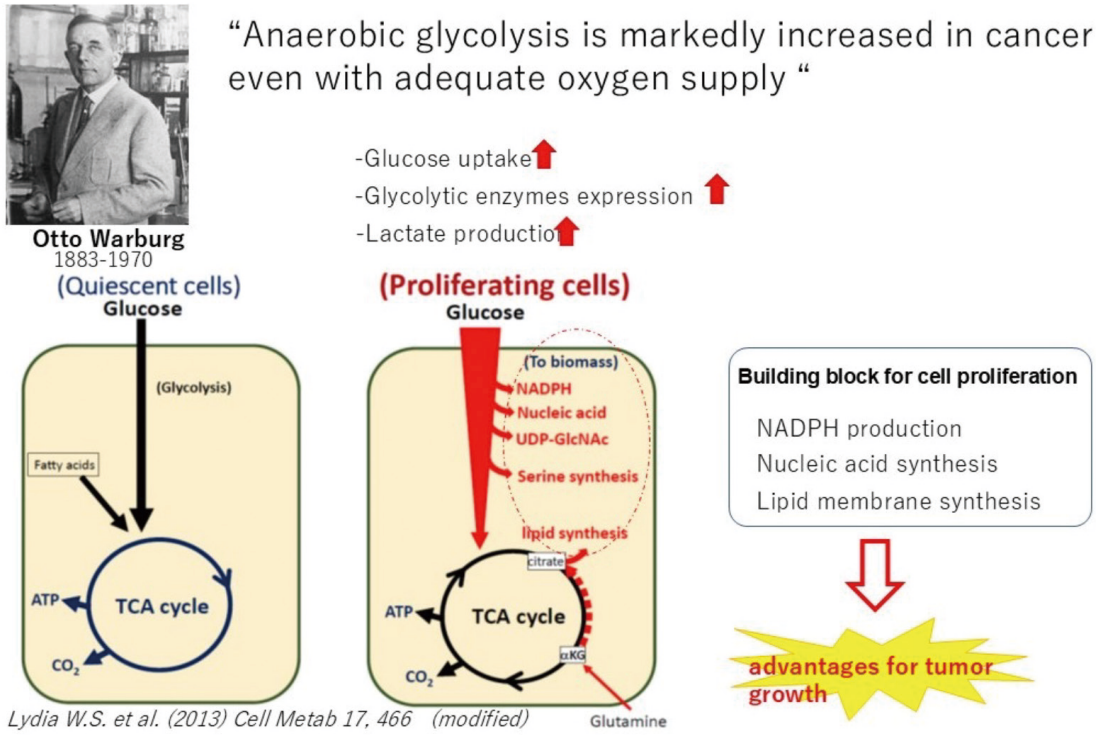

Figure 1 Differences in cancer cell metabolism of glycolysis and the Warburg effect.

Metabolome analysis further revealed that when PFKFB3 is in an unmethylated state, PFK-1 is relatively inhibited. This leads to an increase in upstream fructose 6-phosphate (F6P), an increased flux through the pentose phosphate pathway (a branch of glycolysis), and enhanced synthesis of NADPH (which is required for glutathione production), as well as increased production of ribose 5-phosphate (which is required for nucleic acid synthesis).

2. PHGDH: Gateway to Serine Synthesis

We clarified that methylation modifications of glycolytic enzymes mediated by PRMT1 also occur in pyruvate kinase M2 (PKM2) (Figures 2, 3). PKM2 is highly expressed in cancer cells and embryonic cells, and it has been considered to exert diverse biological effects by translocating between the cytoplasm and the nucleus, although

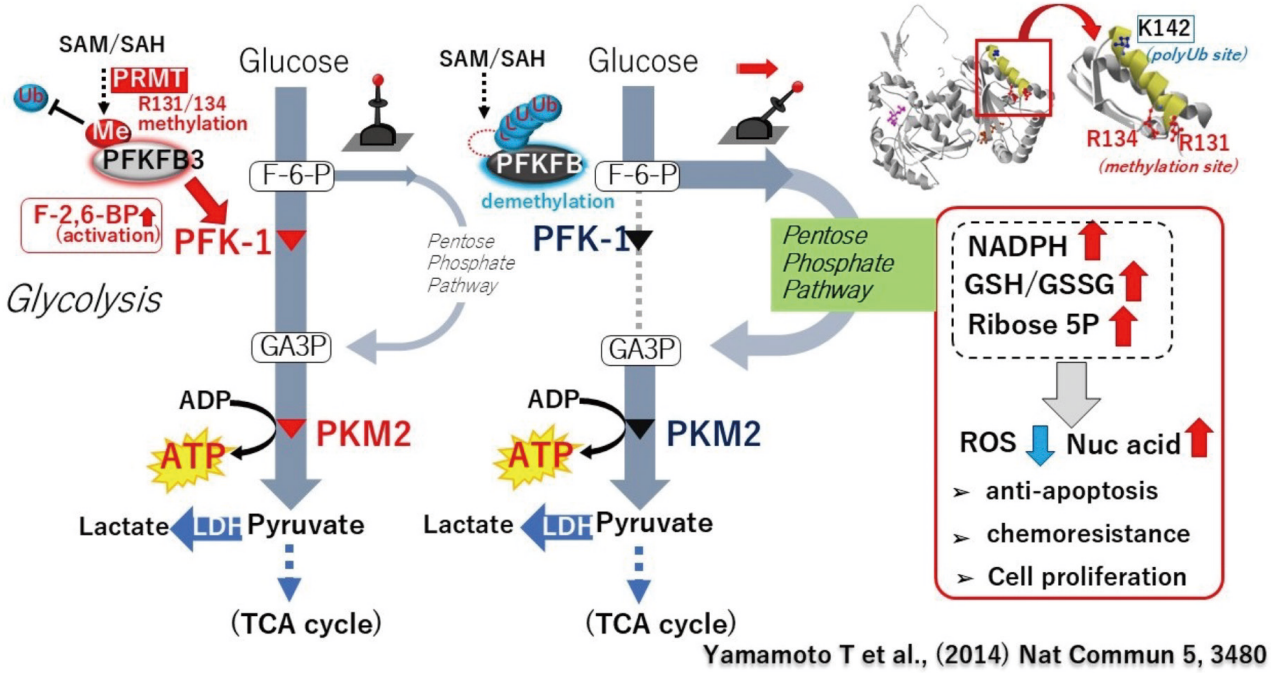

Figure 2 Roles of methylation of PFKFB3 and PKM2 in regulating glycolysis.

the full picture of its regulatory mechanism remains unknown. PKM2 ordinarily exists as a tetramer in the cytoplasm and exhibits enzymatic activity, whereas the stabilization of its dimer form promotes nuclear translocation. In this process, its enzymatic activity is relatively suppressed, and it acquires function as a transcriptional regulatory factor (Figure 3).

PFKFB3 methylation and PKM2 methylation occurring simultaneously via PRMT1 would increase metabolites located upstream of glycolysis and decrease those located downstream. However, because glycolysis includes multiple branch pathways, we administered 13C-labeled glucose to multiple distinct breast cancer cell lines (a paclitaxel-sensitive line and a resistant line) and quantitatively traced the metabolic flux using metabolome analysis to identify which pathways the carbon was actually entering (Figure 3). As a result, we found an increase in 3-phosphoglycerate (3-PG), an intermediate metabolite of glycolysis, as well as an increase in flux from 3-PG into the serine synthesis pathway. We therefore examined modifications of phosphoglycerate dehydrogenase (PHGDH), the rate-limiting enzyme of the 3-PG-to-serine synthesis pathway, in its enzyme protein form, and found that arginine residues such as R20 and R54 are methylated as target molecules of PRMT1. PHGDH methylation is enhanced in paclitaxel-resistant breast cancer cell lines. Furthermore, upon examining the functional role of each amino acid residue, it was revealed that the methylation of R20 suppresses ubiquitination mediated through the adjacent lysine residue (K21), and that the methylation of R54 activates the chemical reaction of negatively charged 3-PG; together, these effects activate the enzymatic reaction. In chemotherapy-resistant breast cancer cell lines, PRMT1 is upregulated. As a result, PFKFB3, PKM2, and PHGDH are coordinately activated, leading to an increase in flux through the serine synthesis pathway.

3. Biological Significance of Serine Synthesis Pathway Activation in Cancer

PHGDH converts 3-PG to phosphohydroxypyruvate, which is further converted to α-ketoglutarate (αKG) by phosphoserine aminotransferase-1 (PSAT1). Although αKG is normally a product of the citric acid cycle, this series of metabolic reactions is localized in the cytoplasm, from where it is supplied as a substrate required for fatty acid synthesis. The saturated fatty acids produced are not only used as building blocks for the cancer cell membrane structure but also activate fatty acid synthase (FASN) by *S*-palmitoylating the FASN enzyme protein, thereby further promoting fatty acid synthesis. Second, the activation of PHGDH activates the serine-glycine cleavage system, which serves as a source of methyl group generation and may therefore sustain PRMT-mediated methylation as a post-translational modification. Third, it promotes the

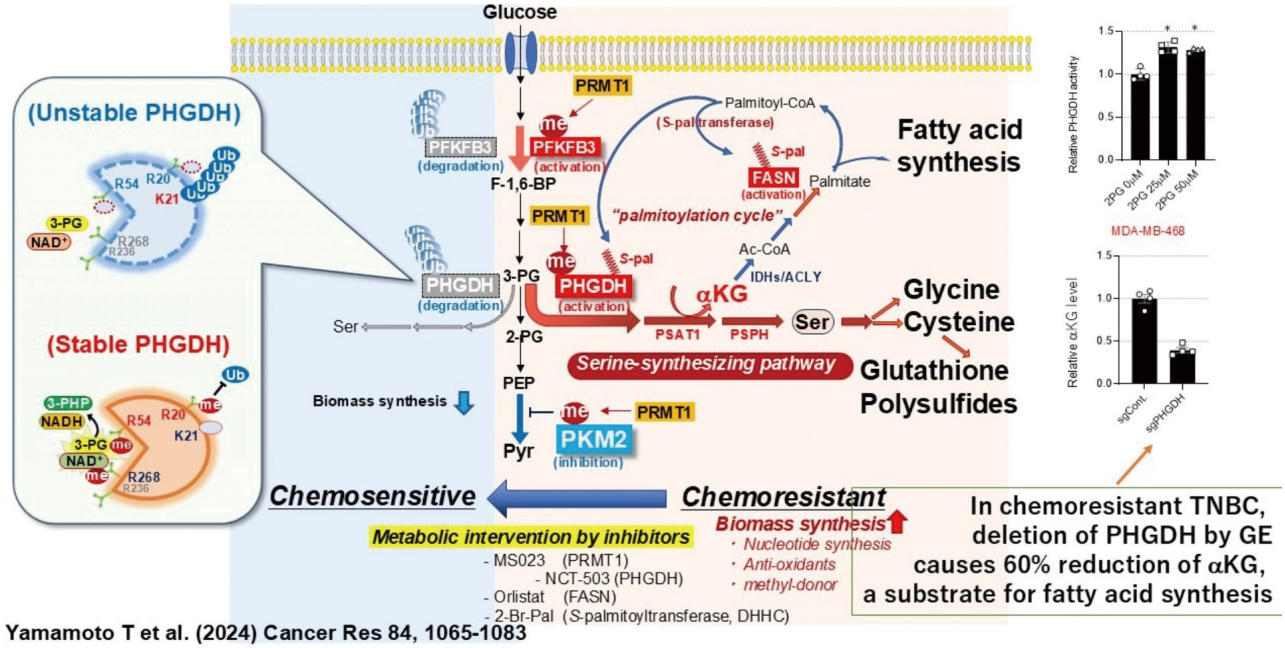

Yamamoto T et al. (2024) Cancer Res 84, 1065-1083

Figure 3 Roles of methylation of PHGDH, a gateway enzyme of serine synthesis, in the donation of methyl carbons and the generation of free fatty acids and reactive sulfur species in cancer cells. Arginine methylation of PHGDH renders the protein less sensitive to polyubiquitination and thereby increases the catalytic activity of the enzyme. Loss of PHGDH function causes a 60% reduction in fatty acid synthesis in cancer cells, suggesting that the pathway through serine synthesis constitutes a major supplier of lipid components.

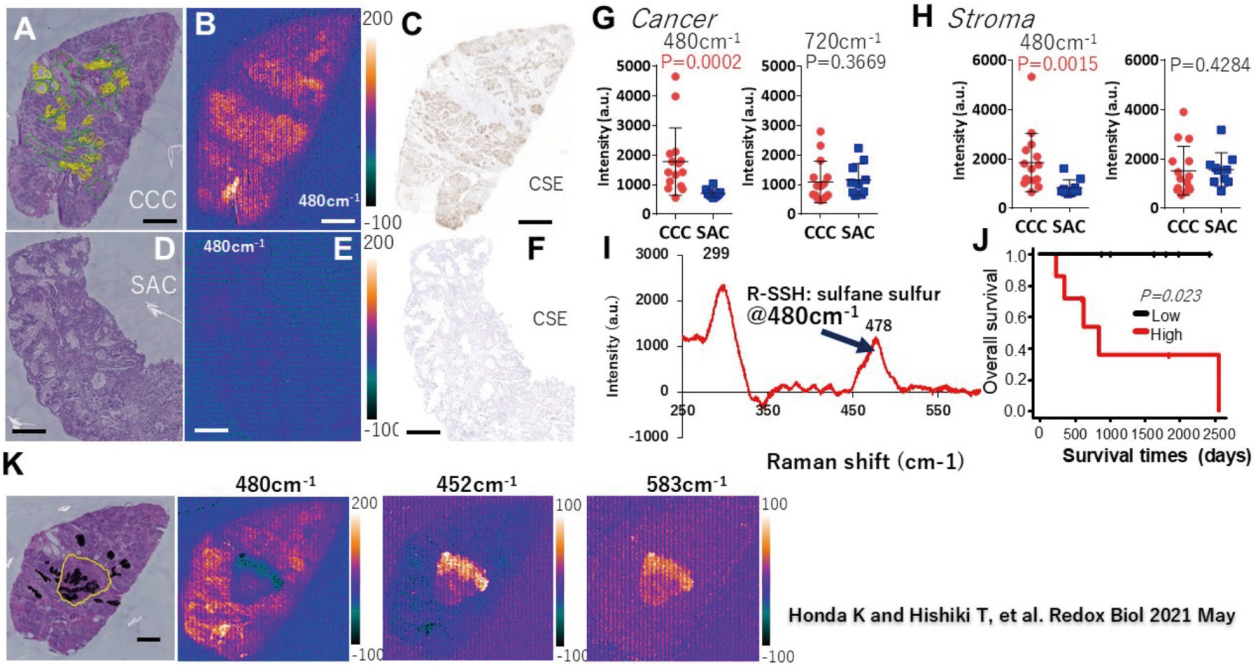

Figure 4 On-tissue visualization of polysulfides in frozen tissue of ovarian carcinoma (Clear cell carcinoma; CCC, and Serous adenocarcinoma; SCC) by Au-nanoparticle-based SERS imaging. Shows the relationship between polysulfide signals at 480 cm^{-1} and post-operative prognosis. Yellow and green annotations correspond to cancer cell clusters and stromal regions, respectively. K: Effects of topical application of bimane, a reagent that breaks down polysulfides to sulfodibimane, generating new Raman peaks at 452 and 583 cm^{-1}.

synthesis of cysteine and glutathione as antioxidant defense systems, thereby suppressing ferroptosis and other cytotoxic mechanisms in cancer cells. These antioxidants are involved in the generation of polysulfides, which contain multiple sulfur atoms within a single molecule. Polysulfides have the ability to "detoxify" electrophilic species inside cells as nucleophilic metabolites (Figure 4). Many of the drugs used to treat solid tumors are electrophilic reagents, and polysulfides possess a biological activity that neutralizes their effects. For this reason, we have used clinical surgical specimens and employed surface-enhanced Raman spectroscopy (SERS) as a technique for detecting polysulfides to investigate whether resistance to anticancer drugs in actual patients can be predicted.

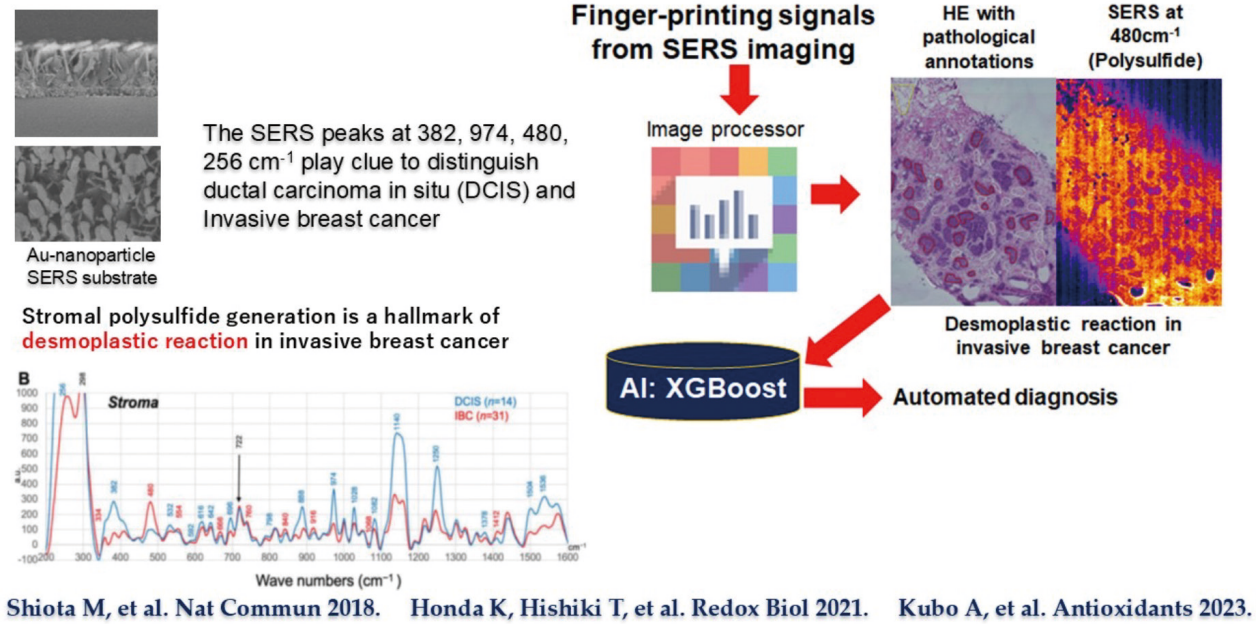

Figure 5 Use of Au nanoparticle-based SERS substrates (scanning electron micrographs) to visualize polysulfides in needle-biopsied tissues of breast cancers. Representative pictures indicating Hematoxylin-Eosin staining and SERS imaging at 480 cm^{-1} in invasive breast cancer. Note that the cancer stroma, rather than cancer cell nests, indicates greater polysulfide signals at 480 cm^{-1}. AI (XGBoost) allows us to automatically differentiate ductal carcinoma in situ (DCIS) and invasive breast cancer (IBC).

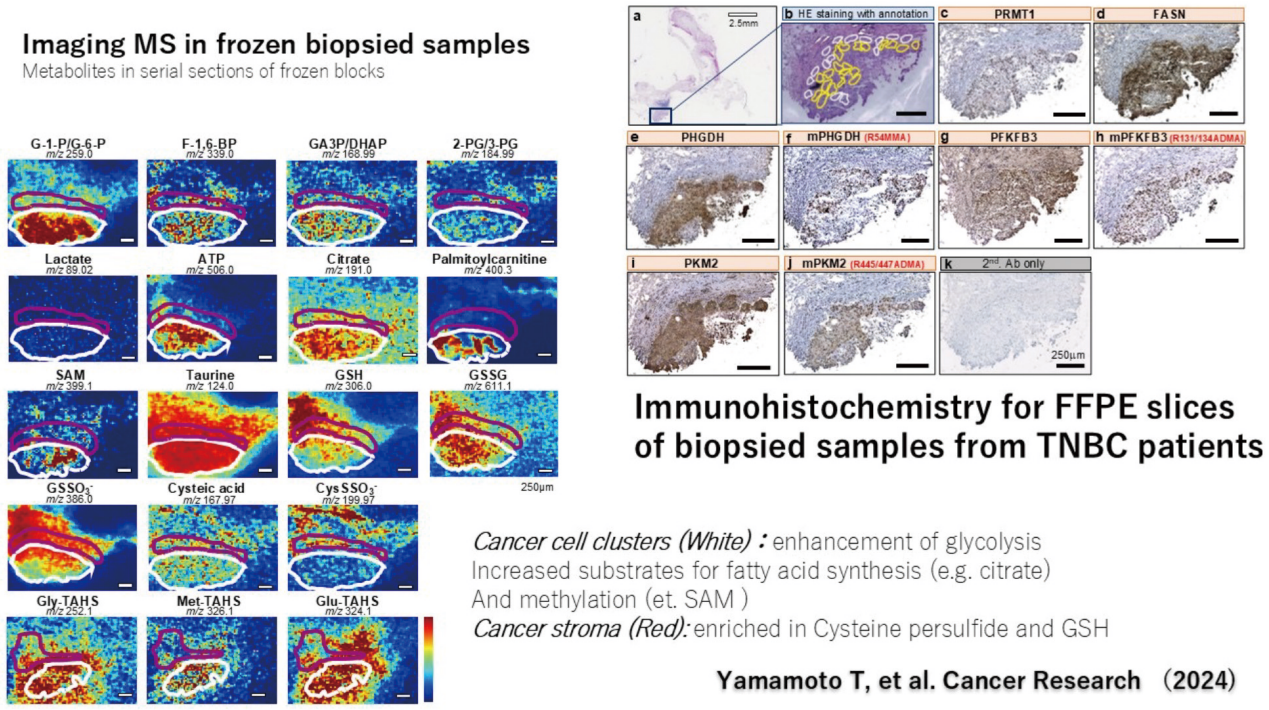

Figure 6 Representative pictures of imaging mass spectrometry of needle-biopsied frozen tissues of breast cancer (left) and immunohistochemistry using different antibodies recognizing methylated glycolytic enzymes.

4. Enhanced Polysulfide Production in Tumor Tissues of Patients with Anticancer Drug Resistance and Prognosis

In breast cancer, it is essential to perform a needle biopsy at the suspicious lesion and to establish a classification that reflects the pathological findings and genotype. Based on these findings, the lesion is diagnosed as either ductal carcinoma in situ (DCIS) or invasive breast cancer (IBC) with evidence of invasion into the surrounding tissue. In the latter case, consideration is then given to surgical indications. In some cases, preoperative chemotherapy is administered to shrink the primary tumor before surgery. We reported that DCIS and IBC, which are sometimes difficult to distinguish even for specialized pathologists, can be differentiated with high accuracy by SERS-based image analysis of needle biopsy specimens (frozen sections) using AI (Figure 5).

As shown in Figure 5, polysulfide levels are particularly elevated in the cancer stromal region in IBC; therefore, even if a drug reaches the peritumoral area during anticancer therapy, it is thought that inactivation occurs readily. We also consider that such a desmoplastic reaction correlates with drug resistance in breast cancer.

5. Metabolite Mapping in Frozen Breast Cancer Tissue by Mass Spectrometry Imaging

It has been revealed that the regulatory mechanism of metabolism—flowing from glucose through glycolysis and the serine synthesis pathway to the sulfur-containing amino acid metabolism pathway—is controlled by methyl group transfer reactions. However, in actual cancer tissues, completely different metabolic profiles can be detected between cancer cell clusters and the surrounding stromal regions, and many questions remain regarding how the cancer and stroma maintain biological homeostasis through their interactions. Figure 6 shows data obtained by analyzing the metabolic profile of a thin section taken from a frozen breast cancer needle biopsy specimen (left), as well as the adjacent section processed by FFPE and stained with various antibodies. As shown on the left, the cancer cell cluster (white) exhibited high levels of 3-PG, lactate, ATP, citrate, glutathione, and palmitic acid, whereas the surrounding stromal region (red) showed relatively high levels of cysteine persulfide, glutathione persulfide, and related species. Although metabolite imaging is not possible in FFPE specimens, immunostaining with a monoclonal antibody specific to methylation enzymes revealed (as shown on the right in Figure 6) that site-specific utilization of metabolites is occurring within the cancer tissue.

Conclusion

We would like to express our sincere gratitude to HORIBA, Ltd. for providing us with the opportunity to deliver this lecture and to write this special contribution.

* A portion of the article was previously published in reference [2].

References

[1] WARBURG O. On the origin of cancer cells. Science. 1956, 123(3191), p. 309-314. doi:10.1126/science.123.3191.309.

[2] Yamamoto T., Hayashida T., Masugi Y., Oshikawa K., Hayakawa N., Itoh M., Nishime C., Suzuki M., Nagayama A., Kawai Y., Hishiki T., Matsuura T., Naito Y., Kubo A., Yamamoto A., Yoshioka Y., Kurahori T., Nagasaka M., Takizawa M., Takano N., Kawakami K., Sakamoto M., Wakui M., Yamamoto T., Kitagawa Y., Kabe Y., Horisawa K., Suzuki A., Matsumoto M., and Suematsu M. PRMT1 sustains de novo fatty acid synthesis by methylating PHGDH to drive chemoresistance in triple-negative breast cancer. Cancer Research. 2024, 84(7), p. 1065-1083. doi:10.1158/0008-5472.CAN-23-2266.

Liquid Biopsy in Cancer Management: Advances, Challenges, and Emerging Clinical Applications

Prof. Dr. Catherine Alix-Panabières

Professor of Oncology
University of Montpellier
Faculty of Medicine of Montpellier
Director of the Liquid Biopsy Laboratory
University Medical Center of Montpellier
Montpellier, FRANCE

Doryan Masmoudi

Hospital Engineer
Research and Innovation Department
University Hospital of Montpellier
Laboratory of Human Rare Circulating Cells and Liquid Biopsy
PhD Student, University of Montpellier

Liquid biopsy analyzes tumor-derived components, including circulating tumor DNA (ctDNA), circulating tumor cells (CTCs), and extracellular vesicles (EVs) in blood and other body fluids. Unlike traditional tissue biopsies, it provides a minimally invasive, dynamic view of tumor heterogeneity and disease evolution. Advances in detection technologies have improved sensitivity and broadened applications, from early cancer detection and minimal residual disease monitoring to treatment response assessment and therapy-guided strategies. Nevertheless, biological constraints, technical variability, and the lack of standardized workflows limit routine clinical implementation. This review summarizes current methodologies, clinical applications, and the complementary value of circulating analytes, highlights emerging innovations such as multi-omics integration and AI-driven analysis, and outlines future directions including standardization and harmonization, multicenter interventional trials, and integration into standard oncology practice.

Introduction

Cancer diagnosis and monitoring have traditionally relied on tissue biopsies, which, while informative, are invasive, often risky, and may not fully capture tumor heterogeneity. A tissue biopsy provides a snapshot of the tumor at a single time point, whereas cancer evolves dynamically over time. Under therapeutic pressure, certain tumor cell populations may be eliminated, while others emerge, and resistant clones can arise after the initial biopsy.

Because tissue biopsies cannot be repeatedly performed at each stage of treatment for molecular monitoring, early detection of therapeutic resistance is often precluded.

Liquid biopsy, the analysis of tumor-derived components

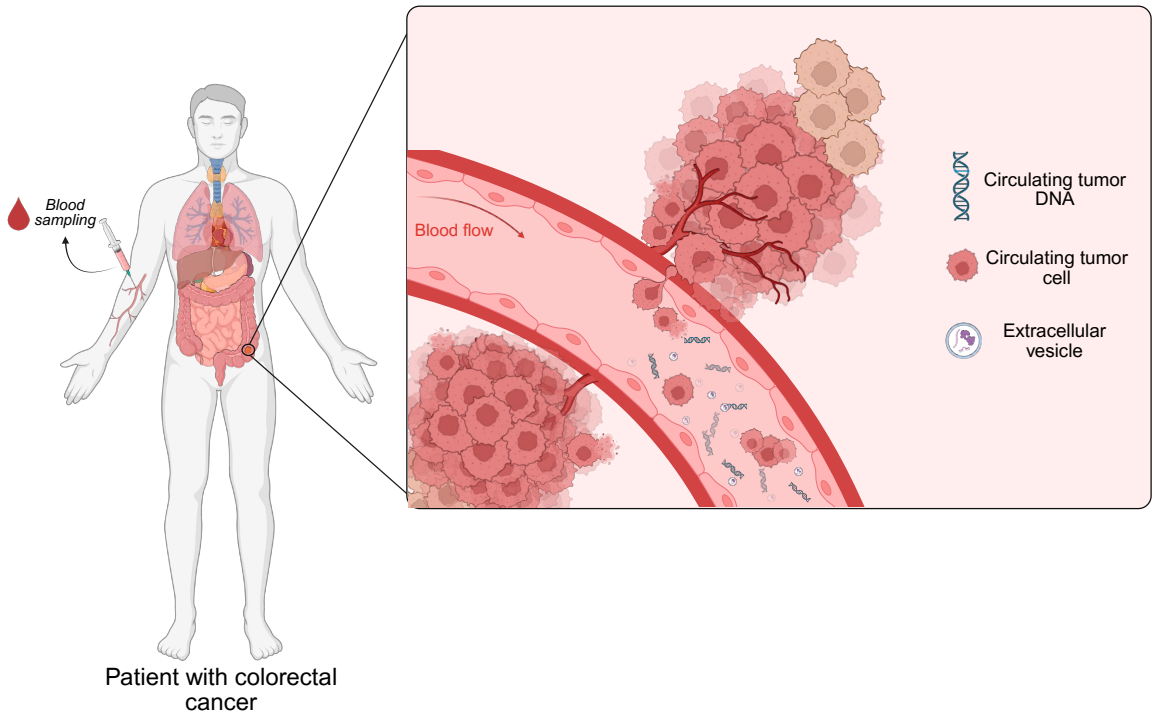

Figure 1 Blood-Based Tumor Biomarkers. Schematic representation of ctDNA, CTCs, and EVs circulating in the bloodstream.

in body fluids, has emerged as a minimally invasive alternative, offering the potential for real-time monitoring of tumor progression and response to therapy (Figure 1). Key analytes in liquid biopsy include circulating tumor DNA (ctDNA), which are fragments of DNA released into the bloodstream by apoptotic or necrotic tumor cells[1].

They reflect the genetic make-up of tumors and can provide information about mutations and tumor burden[1]. Circulating tumor cells (CTCs), which are intact tumor cells shed from primary tumors or metastases[2]. They are capable of revealing genomic, transcriptomic, and functional characteristics at the single-cell level[2]. They also offer single-cell insights into tumor heterogeneity and metastatic potential[2]. Extracellular vesicles (EVs), which include exosomes and microvesicles, are membrane-bound vesicles containing DNA, RNA, and proteins secreted by tumor cells[3]. The integration of these analytes provides a more comprehensive picture of tumor biology and facilitates the development of personalized treatment strategies.

From an analytical perspective, these different biomarkers impose distinct technical constraints that ultimately condition their clinical applicability. For each of these analytes, signal rarity, inter-laboratory variability, required sensitivity and specificity, as well as workflow complexity, constitute major barriers to their routine clinical implementation[4]. In recent years, substantial improvements in the sensitivity and specificity of liquid biopsy assays have enabled their application across a wide range of cancer types and clinical scenarios. These advances benefit all major analytes. ctDNA, for sensitive detection of tumor mutations and minimal residual disease. CTCs, for single-cell characterization of tumor heterogeneity and metastatic potential; and EVs, for stable molecular profiling and insights into the tumor microenvironment.

These improvements have been made possible thanks to recent and specific technological advances. Next-Generation Sequencing (NGS) allows the simultaneous detection of multiple mutations at very low frequencies, thereby improving the sensitivity and accuracy of tumor genetic profiling. Methods such as digital PCR (dPCR) enable ultra-sensitive detection of known mutations. Recent advances in microfluidic enrichment, immunomagnetic isolation, and single-cell sequencing now enable the capture of extremely rare cells, such as CTCs. These techniques also allow detailed genomic, transcriptomic, and functional characterization at the single-cell level. Improved isolation methods such as ultracentrifugation, microfluidic platforms, and immunoaffinity-based capture now enable the analysis of EVs. To obtain a more comprehensive view of tumor biology, it is also possible to integrate multi-omics data from these different biomarkers. All of these analyses and technologies generate large and complex datasets, often containing noise as well as weak signals. The integration and interpretation of these data have been made possible by the recent advent of artificial intelligence (AI) and advanced bioinformatics, which enable the fusion of multiple data types, the computation of molecular signatures, and integrated visualization[5]-[7].

These technological innovations now allow liquid biopsy to be applied across a wider range of cancer types, including early-stage tumors where the tumor signal is low. They pave the way for dynamic and repeated monitoring of minimal residual disease (MRD) and for the personalized adaptation of therapies based on molecular evolution. In this way, liquid biopsy is transitioning from a research tool to a reliable and repeatable clinical tool, capable of supporting decision-making in precision oncology. This manuscript provides a comprehensive overview of the current state of liquid biopsy technologies, their clinical applications, limitations, and future perspectives, focusing on their transformative potential in precision oncology.

Technology approaches

Technological innovations have greatly enhanced the analytical performance of liquid biopsy, enabling sensitive and specific detection of tumor-derived analytes including ctDNA, CTCs, and EVs (Figure 2). ctDNA analysis strategies can be broadly classified into tumor-informed and tumor-agnostic approaches. Tumor-informed assays rely on prior sequencing of tumor tissue to identify patient-specific mutations, which are then tracked in plasma, allowing high sensitivity and specificity. Tumor-agnostic approaches, in contrast, use predefined gene panels or genomic features without prior tumor knowledge, enabling broader applicability but typically with lower sensitivity, especially in low-burden disease.

The detection of ctDNA presents several analytical challenges. First, it represents a small fraction of the total circulating DNA in the blood, especially in early-stage cancers or after treatment. In addition, to accurately capture tumor heterogeneity, methods capable of detecting multiple mutations simultaneously are required. Various technological approaches are available to address these challenges. ctDNA can be detected using dPCR. The sample is partitioned into several million microscopic compartments (or droplets in the case of ddPCR). A PCR amplification is then performed independently in each compartment. This approach transforms quantitative detection into direct counting: the number of positive compartments corresponds exactly to the number of copies of the targeted mutation. It provides analytical precision that cannot be achieved with conventional PCR. Notably, it allows the detection of rare mutations, even when their frequency in ctDNA is very low (<0.1% of total DNA). Additionally, it provides absolute quantification, which is essential for dynamic disease monitoring. dPCR is particularly suitable for known mutations. After

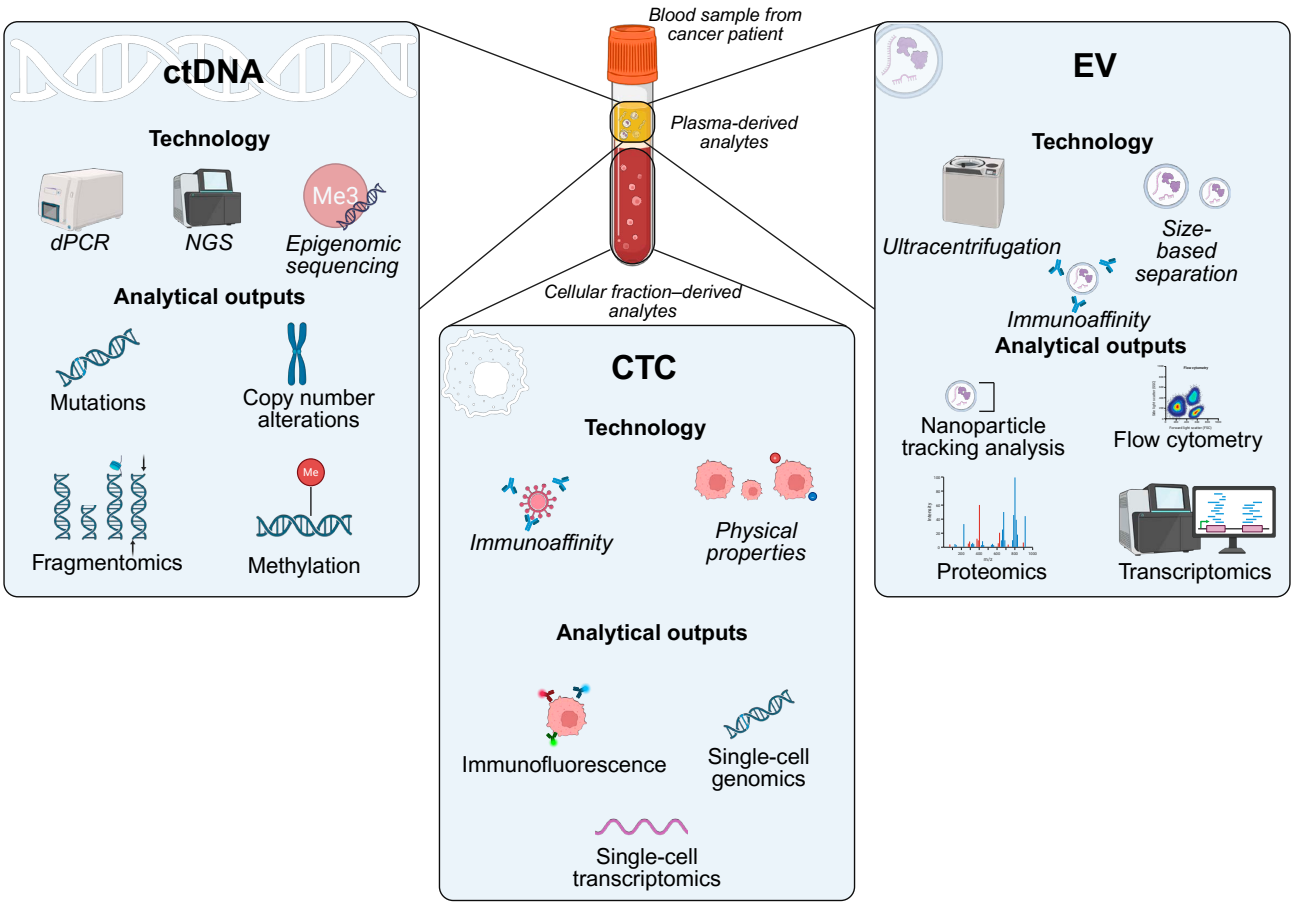

Figure 2 Technological approaches for circulating biomarker detection and characterization.

sequencing tumors via tissue biopsy to identify mutations, these same mutations can be detected in ctDNA using dPCR at very sensitive levels (VAF <1.5%)[8]. dPCR can also be used to target cancer-specific DNA methylation sequences[9].

With strong analytical linearity, detection rates ranging from 38.7% to 46.8% can be achieved in non-metastatic disease[9]. In metastatic patients, detection rates increase to 70.2% and 83.0%[9]. Multiplexing, by combining different markers or mutations, increases the probability of detecting ctDNA, thereby mitigating variability related to tumor heterogeneity and low signal abundance[9]. However, this approach does not yet provide sufficient sensitivity for comprehensive early cancer detection and requires validation in larger and more heterogeneous patient cohorts.

It also is possible to perform NGS to sequence millions of DNA fragments simultaneously. This enables highly precise identification of mutations, insertions, deletions, and copy number variations. NGS allows the detection of very low-frequency mutations, sometimes present in less than 0.1% of circulating DNA fragments, and also permits simultaneous detection of multiple mutations. Multi-site evaluations have shown that it is possible to detect mutations present at ≥0.5% allele frequency[10]. However, the detection of rare variants remains a major analytical challenge[10]. In a large prospective study in advanced non-small-cell lung cancer, ctDNA sequencing could identify actionable genomic alterations that were not detected by contemporaneous tissue sequencing[11]. Patients whose treatment was guided by these ctDNA findings had significantly longer overall survival compared with those not treated according to ctDNA results[11]. These results illustrate that NGS panels allow the simultaneous analysis of multiple genes and mutations efficiently, making them well-suited for dynamic disease monitoring[11]. They also provide semi-quantitative measurements of mutation levels[11]. NGS panels exhibit fairly good analytical specificity, with very few false positives, and good sensitivity when the variant allele frequency (VAF) is ≥ 0.5%[12]. However, for rare variants (VAF ≤ 0.2%), sensitivity varies considerably between assays and across laboratories[12]. dPCR appears to be more sensitive than NGS panels due to droplet partitioning and absolute quantification[13]. The costs are also lower than those of NGS panels; however, dPCR requires prior knowledge of tumor-specific mutations[13].

CTCs represent a major analytical challenge in liquid biopsy due to their extreme rarity in the bloodstream, often limited to only a few cells among millions of normal blood cells. Their abundance varies widely depending on cancer type, disease stage, and therapeutic pressure. In addition, CTCs exhibit marked phenotypic and molecular heterogeneity, encompassing epithelial, mesenchymal, or hybrid states, which limits the effectiveness of approaches relying on single markers. It is possible to use magnetic beads coupled with antibodies targeting specific CTC markers (e.g., EpCAM or other tumor antigens). This method provides good specificity and allows for cell recovery, although its performance can be limited by antigen expression heterogeneity. From 7.5 mL of blood, the CellSearch® system (the FDA-cleared clinical standard) also uses CellSave tubes, which stabilize CTCs for up to 96 hours after collection, a crucial step for multicenter or clinical studies[14]. This method provides high specificity and standardized measurement suitable for clinical contexts, but it may be less sensitive than approaches based on multiple molecular markers[14].

Microfluidic devices exploit the physical properties of CTCs, such as their size, deformability, or hydrodynamic behavior, to separate them from blood cells. These approaches enable marker-independent capture of CTCs[15],[16]. In a preclinical comparison, the CROSS chip detected additional CTC subpopulations not always captured by the CellSearch® system, highlighting potential complementary use[16]. Microfluidic chips demonstrate continuous improvements in the isolation and analysis of CTCs and enable single-cell analyses. However, in the future, these chips will need to address challenges related to purity, full workflow integration, and high throughput for clinical sample volumes. Moreover, size-based isolation methods may fail to detect smaller CTCs, which can be the most aggressive[17].

After enrichment by filtration, microfluidic or immunomagnetic methods, the DNA or RNA from a single cell can be uniformly amplified to generate sufficient material for sequencing. The RNA or DNA can then be analyzed to identify mutations, observe copy number variations (CNVs), assess clonal heterogeneity, monitor tumor evolution, and evaluate the expression of immune or epithelial/mesenchymal markers[18],[19].

Extracellular vesicles (EVs) also represent a major technical challenge in liquid biopsy due to the complex cargo they carry, their stability, which varies depending on storage or handling conditions, and their variability in terms of concentration, tumor type, and disease stage. Moreover, circulating tumor-derived EVs are highly outnumbered by EVs originating from normal cells. This extreme dilution necessitates the use of highly sensitive and specific methods for their detection and enrichment. EVs can be isolated and separated based on their size and density using high-speed ultracentrifugation. Their physical properties can also be exploited for isolation using micro-

fluidic devices. The use of microfluidic chips integrating functionalized nanointerfaces has demonstrated higher isolation efficiency than ultracentrifugation and may help overcome the challenge posed by the extreme dilution of tumor-derived EVs in the circulation[20]. Additionally, magnetic beads or functionalized surfaces coupled to antibodies or ligands targeting tumor-specific EV surface proteins can be employed. The efficiency of this approach depends on the expression of surface markers, which can vary across EV subpopulations and tumor types.

It is notably possible to isolate EVs using aptamers conjugated with a fluorophore that are specific to surface proteins of tumor-derived EVs[21]. After isolation, EVs are analyzed for their DNA, RNA, proteins, and sometimes metabolites, allowing multiple types of data to be integrated from a single sample. Plasma EV proteomics goes beyond the mere quantification of EVs by providing access to qualitative and discriminative molecular information[22]. Beyond proteomic analysis, the transcriptomic profiling of EVs faithfully reflects tumor-specific molecular signatures, including molecular subtypes, expression programs associated with tumor progression, and relevant oncogenic alterations[23].

Data derived from ctDNA, CTCs, and EVs are large, heterogeneous, and complex, encompassing genomic, transcriptomic, proteomic, and sometimes metabolomic information. Integrating these diverse data sources requires managing both inter-laboratory variability and very weak signals often buried in noise. To address this, pipelines can be implemented to normalize, filter, and merge different types of data (NGS sequencing, dPCR, EV proteomics, EV transcriptomics, single-cell sequencing)[24],[25]. The combination of two to four analytes increases the proportion of patients with "actionable" signals (potentially usable to guide therapeutic decisions) compared to the analysis of individual biomarkers[24]. AI and machine learning further enable the identification of combined signatures, the detection of subtle patterns, and the prediction of tumor evolution[5],[26]. These integrated, multi-analyte pipelines, empowered by artificial intelligence, are critical for translating complex liquid biopsy data into clinically actionable insights, laying the groundwork for personalized cancer management.

Clinical applications

Early cancer detection remains a major challenge, and liquid biopsy has shown promising potential for identifying tumors at an early stage in lung, colorectal, and pancreatic cancers through the analysis of circulating ctDNA and EVs[27]-[31]. Targeted sequencing of frequently mutated genes in ctDNA from lung cancer (EGFR, KRAS, PIK3CA, TP53) enables the early identification of lung cancers[27]. Combined with whole-genome sequencing, ctDNA assays can detect ctDNA in the plasma of early lung cancer patients in an ultrasensitive and personalized manner[32]. The combination of whole-genome sequencing of cell-free DNA and machine learning also optimizes the early detection of colorectal cancer[33]. Early cancer detection is also enabled through the detection of EV surface-specific markers, such as GPC1[30],[31]. The proteomic content of circulating tumor-derived EVs also enables early cancer detection[34]. The detection of CTCs is particularly challenging in early-stage cancer due to their extreme rarity in the bloodstream.

Moreover, due to their ability to reflect the inherent aggressiveness of the tumor, ctDNA, CTCs, and EVs have prognostic value. Indeed, the total amount of ctDNA in plasma often reflects tumor size and extent, and high levels of ctDNA are generally associated with more aggressive disease and poorer prognosis[35]-[37]. ctDNA also enables the identification of more invasive molecular subtypes with distinct prognostic outcomes[38]. Similarly, the number of CTCs is directly correlated with tumor aggressiveness and, consequently, patient survival across multiple cancer types[39]-[41]. The expression of certain markers, such as PD-L1, identifying more aggressive subtypes, can also predict poor prognosis under immunotherapy[42]-[44]. EV concentration is also associated with more aggressive disease and, consequently, poorer prognosis[45]. The expression of specific proteins on the surface of EVs can identify more aggressive subpopulations[46]. Furthermore, analysis of EV cargo provides signatures related to tumor aggressiveness, proliferation, and angiogenesis, which can be correlated with survival[47],[48].

After curative treatment (surgery, radiotherapy, chemotherapy), the presence of minimal residual disease (MRD), including circulating tumor cells or tumor-derived fragments, may indicate a high risk of relapse before imaging. Thus, the detection of ctDNA after curative treatment significantly predicts metastatic relapse in patients with various cancer such as breast, colorectal or lung cancer[49]-[52]. The presence of CTCs is also an indicator of relapse after treatment and is associated with a significant decrease in both recurrence-free and overall survival, particularly in breast, lung, pancreatic cancers, and melanoma[53]-[57]. Similarly, the expression of specific surface markers on EVs may indicate tumor recurrence, such as CD31 in patients with hepatocellular carcinoma[58]. In addition, EV concentrations during therapy have been associated with treatment failure and reduced survival[59]. Despite their promising biological relevance, EV-based approaches for MRD monitoring are currently less mature than ctDNA- and CTC-based assays, with fewer large prospective stud-

ies and limited clinical standardization.

Beyond quantitative monitoring, ctDNA analysis also enables the early identification of resistance mechanisms induced by therapeutic pressure, such as the emergence of secondary mutations on the treatment target or the activation of alternative signaling pathways[60],[61]. CTCs can also dynamically modulate the expression of EMT- and immune evasion–related surface markers, such as PD-L1, under therapeutic pressure[62]. CTCs exhibiting stem-like and EMT-associated phenotypes are more chemoresistant and correlate with poorer clinical outcomes[63]. In addition, longitudinal monitoring of ctDNA can predict early response to immunotherapies, such as checkpoint inhibitors, and identify non-responders before conventional imaging[64]-[67]. For example, decreases in ctDNA levels early after initiation of PD-1/PD-L1 blockade correlate with radiologic response and improved progression-free and overall survival in non-small cell lung cancer and other tumor types[64],[65]. Similarly, dynamic profiling of CTCs, including immune checkpoint expression like PD-L1, may help guide adjustments in immunotherapy strategies, potentially optimizing patient outcomes[68]-[70].

Thus, liquid biopsy demonstrates its wide range of applications, including early cancer detection, monitoring of relapse, assessment of immunotherapy efficacy, and patient prognosis (Figure 3). It also holds the potential to guide therapeutic decisions. Therefore, using post-surgical ctDNA status to guide the initiation of adjuvant chemotherapy significantly reduces the use of chemotherapy in low-risk patients while maintaining recurrence-free survival outcomes comparable to those based on standard criteria[71]. Post-surgical ctDNA status can be used to stratify patients and personalize the use of adjuvant chemotherapy[71],[72]. Today, several clinical trials are ongoing to use ctDNA to guide the initiation of immunotherapy (eg. NCT04093167 or NCT04660344). CTC phenotyping may also be useful for guiding therapeutic stratification in metastatic breast cancer[73]. Thus, CTC phenotyping can identify patients who might benefit from anti-HER2 therapy even though their primary tumor is HER2-negative[73]. Moreover, the CTC count–guided management strategy in breast cancer has shown a significant improvement in overall survival[74]. Several groups, including the LCCRH at the CHU of Montpellier, are working on national and European projects (EPILUNAR; https://transcan.eu/output-results/funded-projects/epilunar.kl and CURE, ARC founded) aimed at guiding immunotherapy by integrating multiple biomarkers, such as CTCs, EVs, and ctDNA.

Nevertheless, EVs are still primarily being explored as prognostic markers or therapeutic vehicles, rather than as direct decision-making tools for treatment modifications.

Challenges and Limitations

Despite the promise of liquid biopsy, significant biological, technical, and economic challenges remain. Some tumor-derived DNA alterations, including subclonal or

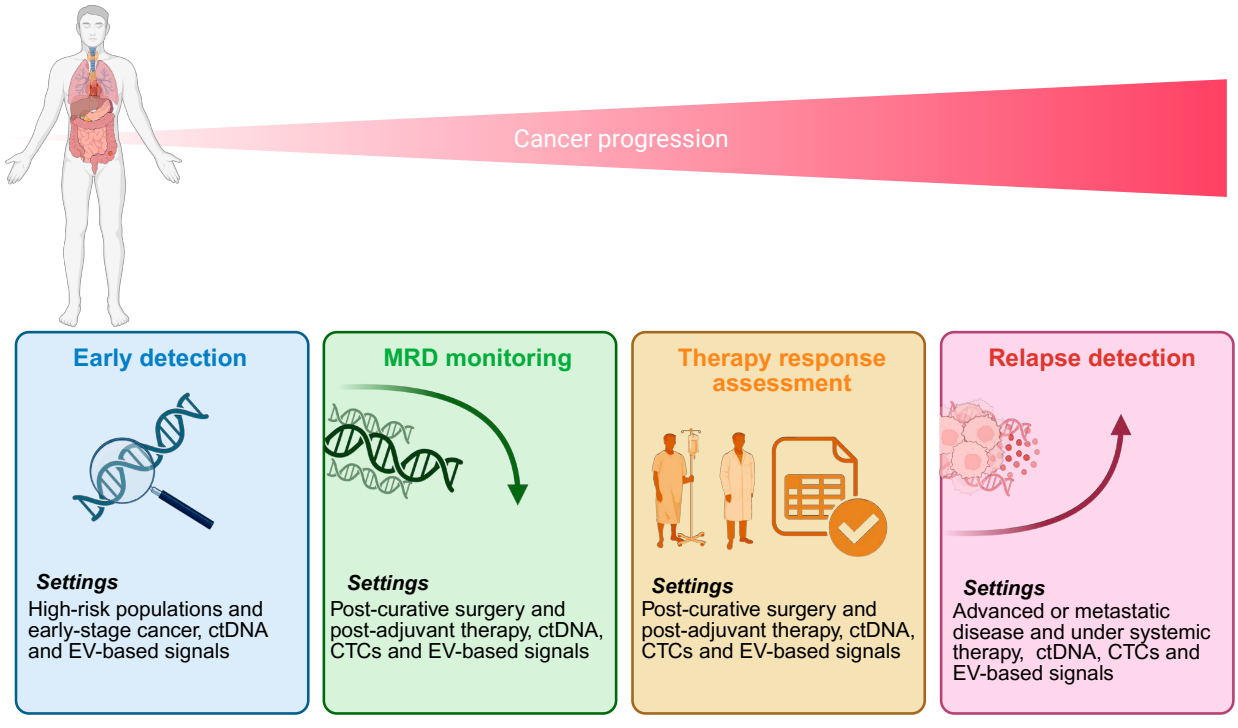

Figure 3 Clinical Applications of liquid biopsy. Liquid biopsy applications across disease stages: early detection, minimal residual disease monitoring, therapy response assessment, and relapse detection.

low-frequency mutations, are inherently difficult to detect, particularly in early-stage cancers where ctDNA levels are extremely low. CTCs are often rare in localized disease and may not capture the full heterogeneity of the tumor, while their dynamic phenotypes can complicate interpretation. EVs are heterogeneous, and their content is influenced by multiple cell types and immune status, with a lack of standardized isolation, quantification, and characterization protocols. Across all analytes, technical variability including differences in extraction methods, library preparation, sequencing depth, and detection platforms limits comparability between studies. Pre-analytical factors such as sample collection, processing, and storage, as well as inconsistent timing of longitudinal sampling in clinical trials, can further affect analyte abundance and interpretability. Technologically, ultra-sensitive and harmonized platforms are needed to detect low-abundance analytes, but these remain complex and resource-intensive, limiting broad adoption. From an economic standpoint, cost and feasibility influence the ability of centers to implement liquid biopsy systematically; although it can be cost-effective in some settings when guiding therapy or complementing tissue biopsy, heterogeneity between cancer types and limited data on response monitoring remain challenges[75]. Addressing these biological, methodological, technological, and economic limitations is essential to ensure the reliable integration of liquid biopsy into clinical practice and its translation into actionable patient care.

Future directions

Emerging directions in liquid biopsy focus on technological innovation, analytical refinement, and broader clinical integration. Multi-omics approaches combining DNA, RNA, protein, lipid, and metabolite analyses promise a more comprehensive view of tumor biology and its dynamic evolution. Advances in ultra-sensitive detection technologies and error-suppression strategies will further improve the detection of low-abundance analytes, particularly in early-stage disease and minimal residual disease settings. AI and machine learning models are increasingly applied to integrate complex liquid biopsy datasets, improve early detection, predict treatment response, and support personalized therapeutic decision-making. Today, several research groups are pursuing early detection of pancreatic cancer using liquid biopsy approaches, such as the PANLIPSY project (ARC foundation and Fonds Pour Bertrand Kamal) and PANCAID (https://pancaid-project.eu/), which aims to define and validate an AI-integrated multimarker blood signature combining CTCs, ctDNA, and other circulating biomarkers across patients, benign pancreatic disease, and healthy cohorts[76].

Beyond technological advances, a major future direction lies in the transition of liquid biopsy from a primarily prognostic tool to a truly actionable and decision-guiding platform, enabling treatment initiation, adaptation, or de-escalation based on real-time molecular dynamics. This shift will require large-scale, multicenter, interventional clinical trials to validate liquid biopsy–guided strategies, define clinically meaningful thresholds, and demonstrate patient benefit. Longitudinal and adaptive monitoring approaches will further allow early identification of response trajectories and resistance mechanisms, supporting dynamic treatment optimization.

Standardization and harmonization of pre-analytical and analytical workflows across centers will be critical to enable inter-study comparability and widespread adoption. In this regard, the European Liquid Biopsy Society (ELBS) actively promotes such standardization by providing guidelines, recommendations, and best practices, facilitating the translation of liquid biopsy technologies into clinical practice (https://www.elbs.eu).

The development of point-of-care and miniaturized platforms may facilitate rapid, near-patient liquid biopsy testing, accelerating clinical decision-making. Pan-cancer ctDNA panels, as well as fragmentomic and epigenomic signatures, aim to enable broad, tumor-agnostic early cancer detection. Furthermore, integration of liquid biopsy data with advanced imaging modalities, such as radiomics and functional imaging, immunomonitoring, and clinical parameters may provide synergistic insights into tumor biology and host–tumor interactions. Collectively, these innovations, supported by robust multicenter clinical evidence, have the potential to transform cancer diagnosis, longitudinal monitoring, and treatment personalization (Figure 4).

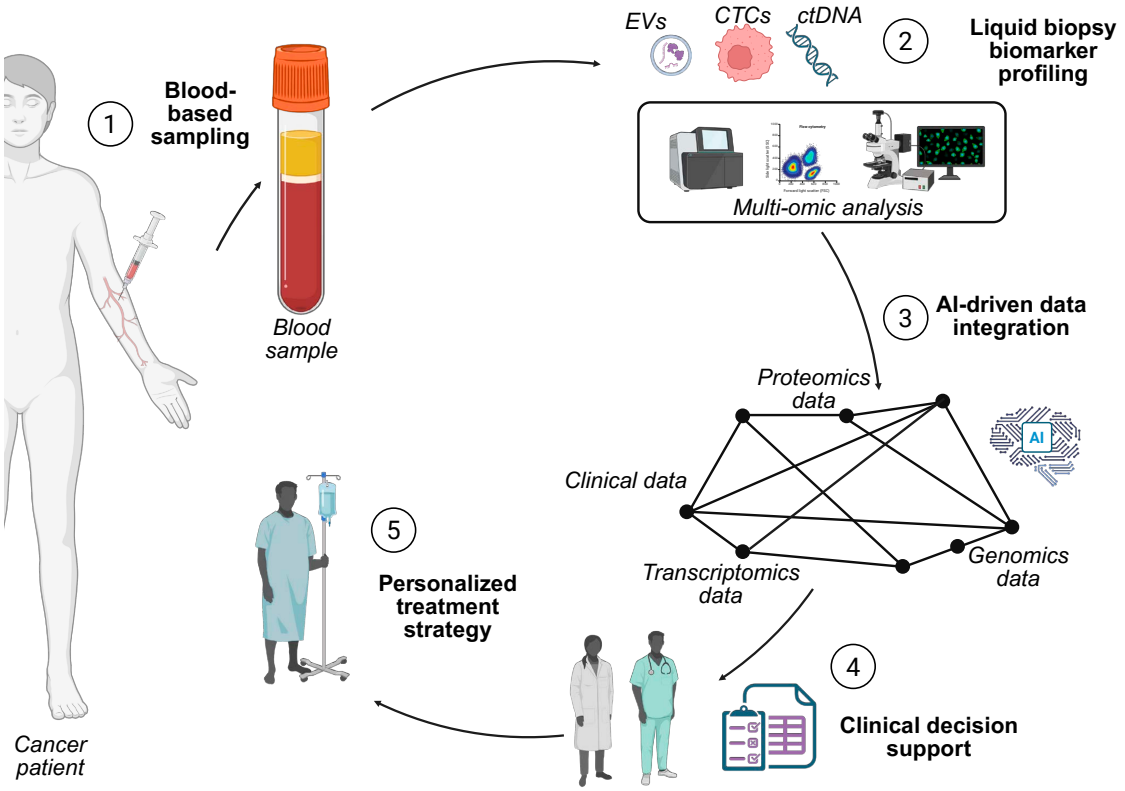

Figure 4 Multi-Omics and AI integration. Workflow schematic showing integration of ctDNA, CTCs, EVs, multi-omics data, and AI-driven analytics to guide personalized cancer therapy and decision-making.

Conclusion

Liquid biopsy represents a paradigm shift in cancer management, enabling minimally invasive, real-time monitoring of tumor progression and response to therapy. Advances in detection technologies, multi-omic integration, and AI-driven analysis have expanded clinical applications from early diagnosis to therapy monitoring and personalized treatment guidance. By providing complementary information through ctDNA, CTCs, and EVs, liquid biopsy offers a dynamic view of tumor biology that is not achievable with tissue biopsies alone. Looking forward, continued efforts toward standardization of pre-analytical and analytical workflows, enhanced sensitivity for early-stage disease and minimal residual disease detection, and harmonization of technologies across centers will be essential for robust clinical implementation. Importantly, the transition of liquid biopsy from a predominantly prognostic approach to a truly actionable decision-support tool will require large-scale, multicenter interventional clinical trials demonstrating clear clinical utility and patient benefit. Ultimately, liquid biopsy has the potential to revolutionize personalized cancer therapy by enabling earlier detection of relapse, real-time treatment adaptation, and improved patient outcomes. As analytical platforms continue to evolve and integrate multi-omic and clinical data within routine oncology workflows, liquid biopsy is poised to become a cornerstone of precision oncology in the coming years.

References

[1] Qin, Z., Ljubimov, V. A., Zhou, C., Tong, Y. & Liang, J. Cell-free circulating tumor DNA in cancer. *Chinese journal of cancer* 35, 36 (2016).

[2] Visal, T. H., den Hollander, P., Cristofanilli, M. & Mani, S. A. Circulating tumour cells in the-omics era: how far are we from achieving the 'singularity'? *British journal of cancer* 127, 173-184 (2022).

[3] Gai, C., Pomatto, M. A., Grange, C., Deregibus, M. C. & Camussi, G. Extracellular vesicles in onco-nephrology. *Experimental & Molecular Medicine* 51, 1-8 (2019).

[4] Coppola, C. A. et al. Liquid Biopsy: The Challenges of a Revolutionary Approach in Oncology. *International Journal of Molecular Sciences* 26, 5013 (2025).

[5] Wang, Y. et al. PRIME: an interpretable artificial intelligence model based on liquid biopsy improves prediction of progression risk in non-small cell lung cancer. *Military Medical Research* 12, 94 (2025).

[6] Hussain, M. S. et al. AI-powered liquid biopsy for early detection of gastrointestinal cancers. *Clinica Chimica Acta*, 120484 (2025).

[7] Pastuszak, K. et al. Detection of circulating tumor cells by means of machine learning using Smart-Seq2 sequencing. *Scientific Reports* 14, 11057 (2024).

[8] Gassa, A. et al. Detection of circulating tumor DNA by digital droplet PCR in resectable *lung cancer* as a predictive tool for recurrence. Lung Cancer 151, 91-96 (2021).

[9] Jacobsen, C. M. et al. Development and validation of a methylation-specific droplet digital PCR multiplex for lung cancer detection. *Scientific Reports* 15, 32305 (2025).

[10] Deveson, I. W. et al. Evaluating the analytical validity of circulating tumor DNA sequencing assays for precision oncology. *Nature biotechnology* 39, 1115-1128 (2021).

[11] Jee, J. et al. Overall survival with circulating tumor DNA-guided therapy in advanced non-small-cell lung cancer. *Nature medicine* 28, 2353-2363 (2022).

[12] Li, W. et al. Analytical evaluation of circulating tumor DNA sequencing assays. *Scientific Reports* 14, 4973 (2024).

[13] Szeto, S. et al. Performance Comparison of Droplet Digital PCR and Next-Generation Sequencing for Circulating Tumor DNA Detection in Non-Metastatic Rectal Cancer. *Cancer Medicine* 14, e70943 (2025).

[14] Van der Auwera, I. et al. Circulating tumour cell detection: a direct comparison between the CellSearch System, the AdnaTest and CK-19/mammaglobin RT–PCR in patients with metastatic breast cancer. *British journal of cancer* 102, 276-284 (2010).

[15] Lin, M. et al. Nanostructure embedded microchips for detection, isolation, and characterization of circulating tumor cells. *Accounts of chemical research* 47, 2941-2950 (2014).

[16] Ribeiro-Samy, S. et al. Fast and efficient microfluidic cell filter for isolation of circulating tumor cells from unprocessed whole blood of colorectal cancer patients. *Scientific reports* 9, 8032 (2019).

[17] Wenta, R. et al. Size Matters: Small Circulating Tumor Cells Indicate Worse Therapy Response in Breast Cancer. *MedComm* 6, e70468 (2025).

[18] Childs, A. et al. Whole-genome sequencing of single circulating tumor cells from neuroendocrine neoplasms. *Endocrine-related cancer* 28, 631-644 (2021).

[19] Kojima, M. et al. Single-cell next-generation sequencing of circulating tumor cells in patients with neuroblastoma. *Cancer science* 114, 1616-1624 (2023).

[20] Reátegui, E. et al. Engineered nanointerfaces for microfluidic isolation and molecular profiling of tumor-specific extracellular vesicles. *Nature communications* 9, 175 (2018).

[21] Tian, F. et al. Protein analysis of extracellular vesicles to monitor and predict therapeutic response in metastatic breast cancer. *Nature communications* 12, 2536 (2021).

[22] Tamarindo, G. et al. Distinct proteomic profiles of plasma-derived extracellular vesicles in healthy, benign, and triple-negative breast cancer: candidate biomarkers for liquid biopsy. *Scientific Reports* 15, 12122 (2025).

[23] Bahrambeigi, V. et al. Transcriptomic profiling of plasma extracellular vesicles enables reliable annotation of the cancer-specific transcriptome and molecular subtype. *Cancer research* 84, 1719-1732 (2024).

[24] Keup, C. et al. Integrative statistical analyses of multiple liquid biopsy analytes in metastatic breast cancer. *Genome Medicine* 13, 85 (2021).

[25] Keup, C. et al. Longitudinal multi-parametric liquid biopsy approach identifies unique features of circulating tumor cell, extracellular vesicle, and cell-free DNA characterization for disease monitoring in metastatic breast cancer patients. *Cells* 10, 212 (2021).

[26] Bu, J. et al. Tri-modal liquid biopsy: Combinational analysis of circulating tumor cells, exosomes, and cell-free DNA using machine learning algorithm. *Clinical and translational medicine* 11, e499 (2021).

[27] Chen, K.-Z. et al. Circulating tumor DNA detection in early-stage non-small cell lung cancer patients by targeted sequencing. *Scientific reports* 6, 31985 (2016).

[28] Yang, Y.-C. et al. Circulating tumor DNA detectable in early-and late-stage colorectal cancer patients. *Bioscience reports* 38, BSR20180322 (2018).

[29] Macgregor-Das, A. et al. Detection of circulating tumor DNA in patients with pancreatic cancer using digital next-generation sequencing. *The Journal of Molecular Diagnostics* 22, 748-756 (2020).

[30] Melo, S. A. et al. Glypican-1 identifies cancer exosomes and detects early pancreatic cancer. *Nature* 523, 177-182 (2015).

[31] Yoshioka, Y. et al. Circulating cancer-associated extracellular vesicles as early detection and recurrence biomarkers for pancreatic cancer. *Cancer Science* 113, 3498-3509 (2022).

[32] Black, J. R. et al. Ultrasensitive ctDNA detection for preoperative disease stratification in early-stage lung adenocarcinoma. *Nature medicine* 31, 70-76 (2025).

[33] Wan, N. et al. Machine learning enables detection of early-stage colorectal cancer by whole-genome sequencing of plasma cell-free DNA. *BMC cancer* 19, 832 (2019).

[34] Hinestrosa, J. P. et al. Development of a blood-based extracellular vesicle classifier for detection of early-stage pancreatic ductal adenocarcinoma. *Communications Medicine* 3, 146 (2023).

[35] Martello, M. et al. High level of circulating cell-free tumor DNA at diagnosis correlates with disease spreading and defines multiple myeloma patients with poor prognosis. *Blood Cancer Journal* 14, 208 (2024).

[36] Zhao, X., Hou, S., Hao, R., Zang, Y. & Song, D. Prognostic significance of circulating tumor DNA detection and quantification in cervical cancer: a systematic review and meta-analysis. *Frontiers in Oncology* 15, 1566750 (2025).

[37] Gao, Y. et al. Diagnostic and prognostic value of circulating tumor DNA in gastric cancer: a meta-analysis. *Oncotarget* 8, 6330 (2016).

[38] Prat, A. et al. Circulating tumor DNA reveals complex biological features with clinical relevance in metastatic breast cancer. *Nature communications* 14, 1157 (2023).

[39] Giuliano, M. et al. Circulating tumor cells as prognostic and predictive markers in metastatic breast cancer patients receiving first-line systemic treatment. *Breast Cancer Research* 13, R67 (2011).

[40] Volovetsky, A. B. et al. Prognostic Value of the Number of Circulating Tumor Cells in Patients with Metastatic Non-Small Cell Lung Cancer. *Micromachines* 16, 470 (2025).

[41] Cohen, S. et al. Prognostic significance of circulating tumor cells in patients with metastatic colorectal cancer. *Annals of oncology* 20, 1223-1229 (2009).

[42] Kong, D. et al. Correlation between PD-L1 expression ON CTCs and prognosis of patients with cancer: a systematic review and meta-analysis. *Oncoimmunology* 10, 1938476 (2021).
[43] Sinoquet, L. et al. Programmed cell death ligand 1-expressing circulating tumor cells: a new prognostic biomarker in non-small cell lung cancer. *Clinical Chemistry* 67, 1503-1512 (2021).
[44] Guibert, N. et al. PD-L1 expression in circulating tumor cells of advanced non-small cell *lung cancer* patients treated with nivolumab. Lung Cancer 120, 108-112 (2018).
[45] Ricklefs, F. L. et al. Circulating extracellular vesicles as biomarker for diagnosis, prognosis, and monitoring in glioblastoma patients. *Neuro-oncology* 26, 1280-1291 (2024).
[46] Herzog, M., Verdenik, I., Kobal, B. & Černe, K. Higher EpCAM-positive extracellular vesicle concentration in ascites is associated with shorter progression-free survival of patients with advanced high-grade serous carcinoma. *International Journal of Molecular Sciences* 25, 6780 (2024).
[47] Bukva, M. et al. Machine learning-based analysis of cancer cell-derived vesicular proteins revealed significant tumor-specificity and predictive potential of extracellular vesicles for cell invasion and proliferation–A meta-analysis. *Cell Communication and Signaling* 21, 333 (2023).
[48] Han, Y. et al. Plasma extracellular vesicle messenger RNA profiling identifies prognostic EV signature for non-invasive risk stratification for survival prediction of patients with pancreatic ductal adenocarcinoma. *Journal of hematology & oncology* 16, 7 (2023).
[49] Garcia-Murillas, I. et al. Mutation tracking in circulating tumor DNA predicts relapse in early breast cancer. *Science translational medicine* 7, 302ra133-302ra133 (2015).
[50] Garcia-Murillas, I. et al. Assessment of molecular relapse detection in early-stage breast cancer. *JAMA oncology* 5, 1473-1478 (2019).
[51] Kotani, D. et al. Molecular residual disease and efficacy of adjuvant chemotherapy in patients with colorectal cancer. *Nature medicine* 29, 127-134 (2023).
[52] Zhong, R. et al. Accuracy of minimal residual disease detection by circulating tumor DNA profiling in lung cancer: a meta-analysis. *BMC medicine* 21, 180 (2023).
[53] Hall, C. S. et al. Prognostic value of circulating tumor cells identified before surgical resection in nonmetastatic breast cancer patients. *Journal of the American College of Surgeons* 223, 20-29 (2016).
[54] Lucci, A. et al. Presence of circulating tumor cells predates imaging detection of relapse in patients with stage III melanoma. *Cancers* 15, 3630 (2023).
[55] Matikas, A. et al. Detection of circulating tumour cells before and following adjuvant chemotherapy and long-term prognosis of early breast cancer. *British journal of cancer* 126, 1563-1569 (2022).
[56] Yeo, D. et al. Portal venous circulating tumor cells as a biomarker for relapse prediction in resected pancreatic cancer. *Cellular and Molecular Life Sciences* 82, 1-12 (2025).
[57] Wankhede, D., Grover, S. & Hofman, P. Circulating tumor cells as a predictive biomarker in resectable lung cancer: a systematic review and meta-analysis. *Cancers* 14, 6112 (2022).
[58] Juratli, M. A. et al. Extracellular vesicles as potential biomarkers for diagnosis and recurrence detection of hepatocellular carcinoma. *Scientific reports* 14, 5322 (2024).
[59] König, L. et al. Elevated levels of extracellular vesicles are associated with therapy failure and disease progression in breast cancer patients undergoing neoadjuvant chemotherapy. *Oncoimmunology* 7, e1376153 (2018).
[60] Tsui, D. W. Y. et al. Dynamics of multiple resistance mechanisms in plasma DNA during EGFR-targeted therapies in non-small cell lung cancer. *EMBO molecular medicine* 10, e7945 (2018).
[61] Ma, F. et al. ctDNA dynamics: a novel indicator to track resistance in metastatic breast cancer treated with anti-HER2 therapy. *Oncotarget* 7, 66020 (2016).
[62] Ntzifa, A. et al. Gene expression in circulating tumor cells reveals a dynamic role of EMT and PD-L1 during osimertinib treatment in NSCLC patients. *Scientific Reports* 11, 2313 (2021).
[63] Papadaki, M. A. et al. Circulating tumor cells with stemness and epithelial-to-mesenchymal transition features are chemoresistant and predictive of poor outcome in metastatic breast cancer. *Molecular Cancer Therapeutics* 18, 437-447 (2019).
[64] Goldberg, S. B. et al. Early assessment of lung cancer immunotherapy response via circulating tumor DNA. *Clinical Cancer Research* 24, 1872-1880 (2018).
[65] Cabel, L. et al. Circulating tumor DNA changes for early monitoring of anti-PD1 immunotherapy: a proof-of-concept study. *Annals of Oncology* 28, 1996-2001 (2017).
[66] Kansara, M. et al. Early circulating tumor DNA dynamics as a pan-tumor biomarker for long-term clinical outcome in patients treated with durvalumab and tremelimumab. *Molecular Oncology* 17, 298-311 (2023).
[67] Tolmeijer, S. H. et al. Early on-treatment circulating tumor DNA measurements and response to immune checkpoint inhibitors in advanced urothelial cancer. *European Urology Oncology* 7, 282-291 (2024).
[68] Khattak, M. A. et al. PD-L1 expression on circulating tumor cells may be predictive of response to pembrolizumab in advanced melanoma: results from a pilot study. *The Oncologist* 25, e520-e527 (2020).
[69] Zhou, Q. et al. Circulating tumor cells PD-L1 expression detection and correlation of therapeutic efficacy of immune checkpoint inhibition in advanced non-small-cell lung cancer. *Thoracic Cancer* 14, 470-478 (2023).
[70] Tan, Z. et al. Assessment of PD-L1 expression on circulating tumor cells for predicting clinical outcomes in patients with cancer receiving PD-1/PD-L1 blockade therapies. *The Oncologist* 26, e2227-e2238 (2021).
[71] Tie, J. et al. Circulating tumor DNA analysis guiding adjuvant therapy in stage II colon cancer. *New England Journal of Medicine* 386, 2261-2272 (2022).
[72] Nakamura, Y. et al. ctDNA-based molecular residual disease and survival in resectable colorectal cancer. *Nature medicine* 30, 3272-3283 (2024).
[73] Fehm, T. et al. Efficacy of lapatinib in patients with HER2-negative metastatic breast cancer and HER2-positive circulating tumor cells—the DETECT III clinical trial. *Clinical Chemistry* 70, 307-318 (2024).
[74] Bidard, F.-C. et al. Overall survival with circulating tumor cell count–driven choice of therapy in advanced breast cancer: a randomized trial. *Journal of Clinical Oncology* 42, 383-389 (2024).
[75] Fagery, M., Khorshidi, H. A., Wong, S. Q., Vu, M. & IJzerman, M. Health economic evidence and modeling challenges for liquid biopsy assays in cancer management: a systematic literature review. *Pharmacoeconomics* 41, 1229-1248 (2023).
[76] Bardol, T. et al. Early detection of pancreatic cancer by liquid biopsy "PANLIPSY": a French nation-wide study project. *Bmc Cancer* 24, 709 (2024).

Column

* This article is an English translation of the original Japanese version published in Readout No. 61.

Keeping the Light of Hope Alive
Bringing Retinal Regenerative Therapies to Patients: Social Implementation and New Business Models

Masayo Takahashi

"Incurable diseases" deprive people of their "lives": retinal disorders as a societal challenge

Vision profoundly influences human quality of life. Losing vision is not merely a functional impairment of "not being able to see"; it also undermines the foundations of social life, including employment, education, mobility, and communication. In particular, blindness caused by retinal diseases constitutes a serious challenge in developed countries facing rapid population aging. In Japan as well, retinal degenerative diseases—such as age-related macular degeneration (AMD), diabetic retinopathy, and retinitis pigmentosa (RP)—are major causes of visual impairment. Because the retina does not spontaneously regenerate once it degenerates and therapeutic options are limited, these diseases have long been regarded as "incurable."

Ten years since the world's first iPS-RPE transplantation: safety and "sustaining visual function"

Against this backdrop, the advent of induced pluripotent stem (iPS) cell technology brought about a major turning point in ophthalmology. It remains fresh in our memory that Professor Shinya Yamanaka received the Nobel Prize in 2012, drawing global attention to iPS cell research. Subsequently, in 2014, the world's first transplantation of a retinal pigment epithelium (RPE) cell sheet derived from iPS cells was performed, making the potential of regenerative medicine a reality[1] (Figure 1).

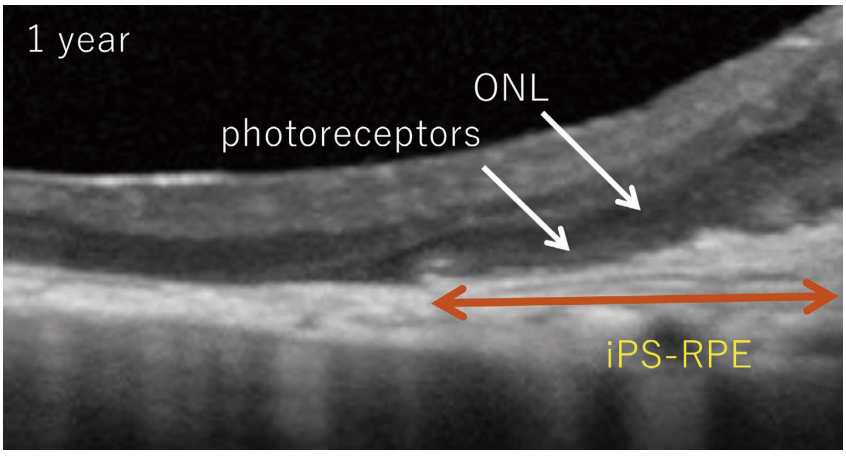

Figure 1 Optical coherence tomography image from the first clinical application of iPS cells. At 1 year after transplantation, the photoreceptor layer is preserved only above the iPS cell–derived RPE cell sheet, and visual function is maintained.

The first clinical study of iPS cell–derived RPE transplantation was designed to demonstrate the safety of iPS cells, which the world had regarded as potentially dangerous because of their resemblance to infinitely proliferating cancer cells. To this end, we generated more than 200 iPS cell lines and conducted exhaustive safety verification[2]. The therapy itself was also designed and implemented as the scientifically best, highly symbolic treatment. Its success became major news worldwide at the time[3]. Ten years later, it has been shown that the transplanted cells engraft safely over the long term and maintain the survival of photoreceptors—which cannot survive in areas where the RPE has atrophied and disappeared—thereby preserving visual function. In other words, a single transplantation of an iPS cell–derived RPE sheet reconstructs retinal structure and sustains retinal function permanently, conferring substantial clinical value from the perspective of "prolonging" visual function. Notably, beyond the medical domain, this was also the year in which the Act on the Safety of Regenerative Medicine and the Pharmaceuticals and Medical Devices Act were formulated alongside the progress of our project and subsequently came into force. These were the world's first laws specialized for regenerative medicine, and the year also impressed upon us the societal power of science—namely, that a technology such as iPS cells could even give rise to new legislation.

"Cells as products" are not sufficient: the "healthcare system" that determines standard-of-care adoption

However, this success does not immediately translate into establishment as standard-of-care. To deliver therapy broadly, not only "cells as products" but also a development model as a medical treatment is indispensable. The success factors for regenerative medicine are not limited to the cell product as one key success factor; rather, success is achieved only when optimization of clinical protocols and surgical techniques, an explanatory framework that supports patients' understanding and informed acceptance, postoperative follow-up, and linkage to insurance systems are all in place. Put differently, regenerative medicine is not a "product" but a "treatment," and social implementation is itself the construction of a comprehensive healthcare system. In other words, it is necessary to transform treatment development from a focus on "things" to a focus on "services/experiences."

The path by which new technologies reach social implementation is never smooth. As illustrated by Gartner's hype cycle, innovative technologies attract excessive expectations, then pass through a trough of disillusionment, and only later mature into practical use through steady, incremental applications. Regenerative medicine is no exception; scientific success alone is insufficient. Multifaceted challenges—such as safety, manufacturing stability, cost, institutional design, patient care, and technology transfer to healthcare professionals—must be addressed (Figure 2).

This reflects the difficulty of developing a new modality—surgical regenerative medicine using cells—which differs fundamentally from pharmaceuticals.

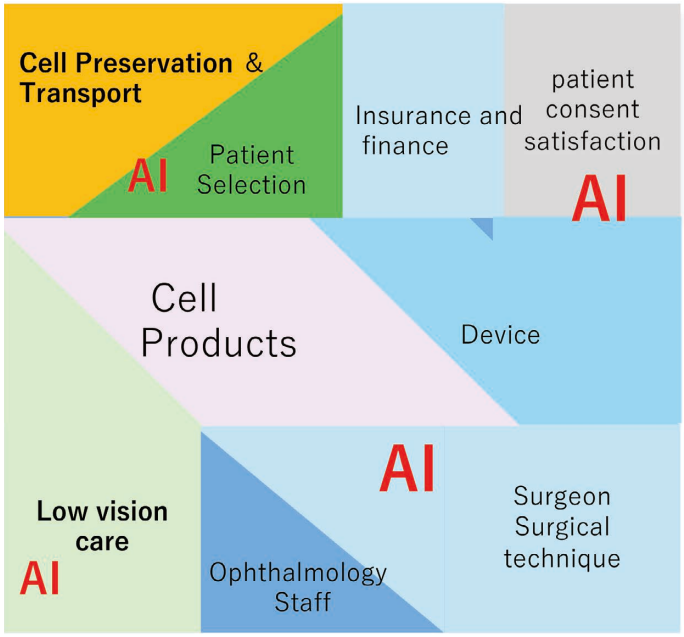

Figure 2 Elements required for the success of surgical regenerative medicine.

Scaling up cell manufacturing and ensuring uniform quality: automation and AI-driven process optimization

One of the critical challenges for accelerating implementation is scaling up cell manufacturing and ensuring uniform quality. Traditionally, cell manufacturing has tended to depend heavily on the skills of experienced technicians; this not only increases labor costs but also makes it difficult to ensure reproducibility. In this context, manufacturing automation using the humanoid robot "Maholo"[4] and process optimization through AI-based analysis improved yield and opened a path to manufacturing cells for 700–800 people per batch. This is not merely labor saving; it resolves the instability inherent in manufacturing in which individual staff members—each with different tendencies—culture cells that are constantly changing, thereby contributing to product stabilization. It may also help suppress future treatment prices and represents a key to evolving regenerative medicine from "advanced medicine for a limited number of people" into "standard medicine disseminated throughout society."

Improving the formulation of transplant products: reducing surgical and immunosuppression risks

In addition, improving the formulation of transplant products was also important. Since the first autologous iPS cell–derived RPE sheet transplantation, formulations have evolved to an allogeneic (donor-derived) iPS cell–derived RPE suspension and further to an RPE aggregate strip, thereby reducing surgical risk and immunosuppression risk[5]. To date, long-term engraftment has been achieved in a total of 10 cases without serious complications, and maintenance of visual function has been confirmed in all cases. In particular, in two cases, improvements were observed that would be impossible under the natural course of the disease, strongly indicating the clinical potential of regenerative medicine. Overall, a characteristic of our therapy development has been that improvements derived from information obtained from each individual case have enabled both reduction of surgical risk and greater certainty of efficacy.

Institutional innovation for dissemination: beyond conventional clinical trial–approval pathways

Meanwhile, innovation in institutional design is also necessary for regenerative medicine to become widespread. Surgical regenerative medicine tends to be costly, and relying solely on conventional clinical trial and approval models carries risks of failure midstream and prolonged timelines before reaching the full population of patients in need. Therefore, we are pursuing treatment development that is not limited to conventional clinical trials, based on the view that new development tracks are important to deliver therapies to patients earlier by leveraging mechanisms such as the Advanced Medical Care system, combined use of insured and uninsured medical services, and combinations of public and private insurance. In regenerative medicine, rather than "entering clinical trials quickly," there are cases in which it has greater societal value—similar to surgical treatments—to "deliver better treatments while continuously improving them." Institutional design to enable this is required.

The reality beyond treatment: low vision care and designing "expectations"

Now that regenerative medicine—once a "dream therapy"—has become "reality," in both positive and challenging senses, patient care is indispensable. Visual impairment cannot be resolved by treatment alone; support is also required to help patients reconstruct daily life beyond the medical domain (low vision care). In particular, what is expected from the term "regenerative medicine" is "seeing well," yet in reality, recovery of visual function is limited. Expecting "seeing well" is akin to expecting a bedridden person to sprint 100 meters; however, in the case of vision, such expectations are often placed on patients, with a high risk of disappointment. Accordingly, we established the Kobe Eye Center and built an integrated framework that unifies healthcare, research, support, and social implementation: patient follow-up by the Public Interest Incorporated Association NEXT VISION; introduction of devices that people with visual impairment can use, which often advance faster than medical care; optimization of surgical methods and clinical protocols by Kobe Eye Center Hospital; and the development of Kobe i Clinic (KiC), which provides online medical care primarily for overseas patients. Now in its eighth year since establishment, each division is operated autonomously and has received a certain level of recognition in its respective field (Figure 3).

From Japan to the world: an international dissemination model built on hospital leadership × local regulations

Broadening our perspective further, collaboration not only within Japan but also with Asia, Europe, and the United States will become increasingly important. Plans to advance outbound and inbound treatments through partnerships with overseas medical institutions—such as Thomas Jefferson University and Wills Eye Hospital in the United States, and a stem cell center in Indonesia—hold the potential to expand regenerative medicine originating in Japan to the world. By conducting hospital-led clinical practice in compliance with local regulations and further supporting the transition to clinical trials, it is possible to form an international dissemination model for the therapy.

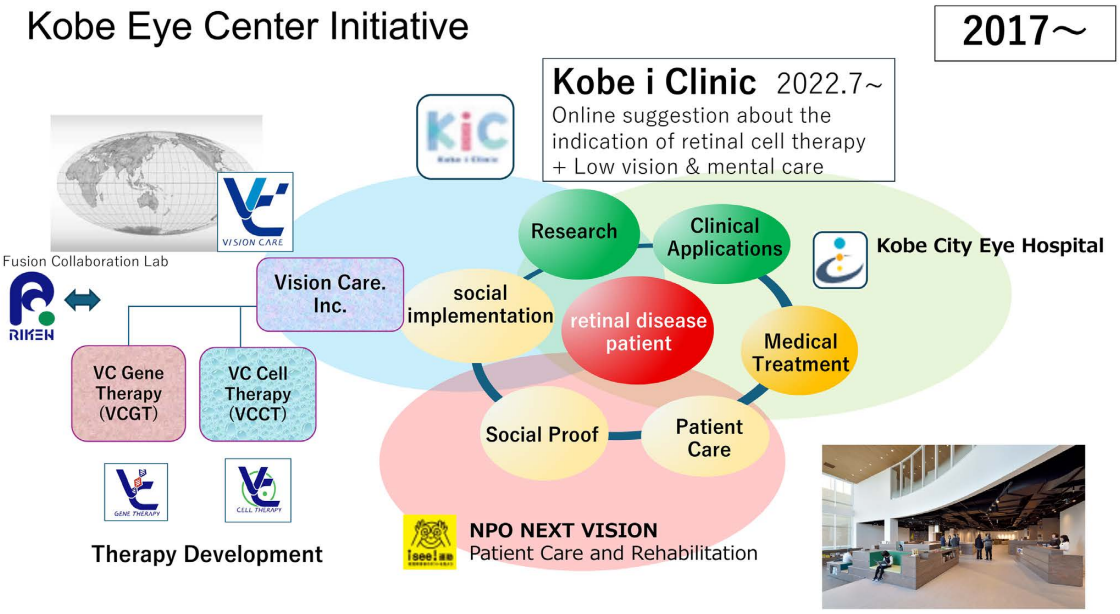

Figure 3 Structure of the Kobe Eye Center.

In 2025, *Nature* reported that "Japan's big bet on stem-cell therapies might soon pay off"[6]. This is not mere optimism; it reflects the cumulative result of many years of research, trial and error, and challenges toward social implementation

Conclusion

To ensure that the "medicine of dreams" does not extinguish the light of hope even after it becomes reality, it is necessary to build a comprehensive medical-economic ecosystem that encompasses not only innovation in cell technologies but also manufacturing, institutions, insurance, patient support, and international expansion. When science and society function as two aligned wheels, regenerative medicine will, for the first time, shift from a "special treatment" to an "ordinary treatment." Going forward, we will continue to build new business models that connect the clinical frontlines with industrial frontlines, in order to realize a society in which patients can live without giving up on the future.

References

[1] Mandai M, et al. Autologous Induced Stem-Cell–Derived Retinal Cells for Macular Degeneration. *New England Journal of Medicine*. 2017
[2] Kamao H, et al. Characterization of human induced pluripotent stem cell-derived retinal pigment epithelium cell sheets aiming for clinical application. *Stem Cell Reports*. 2014.
[3] Nature's 10 mattered in 2014, *Nature* 516: 287-444, 2014
[4] ロボティック・バイオロジー・インスティテュート株式会社,「CONCEPT(コンセプト)」 https://rbi.co.jp/concept/, accessed 2026-03-30. (in Japanese)
[5] Sakai et al. *Ophthalmology Sci*. 5:100770, 2025
[6] "JAPAN's big bet on stem-cell therapies might soon pay off." *Nature*. 640:04-17, 2025

Masayo Takahashi
President
Vision Care Inc.*1
VCCT Inc.*2

*1 Vision Care Co., Ltd. official website
https://www.vision-care.jp/
*2 VC Cell Therapy Co., Ltd. official website
https://www.vcct.jp/

HORIBA's Biohealthcare Technologies Supporting Drug Discovery, Diagnosis, and Treatment

Kosuke Tsujita

The healthcare journey, which covers prevention, diagnosis, treatment, and prognosis management as a continuous process, is facing a strong need for transformation due to the pandemics such as COVID-19 and the rapid aging of society. Fast and simple testing methods, early detection of diseases, the development of new biopharmaceuticals and cell therapies, and advanced process technologies for their stable production and supply are all essential. This article introduces HORIBA's biohealthcare business from two perspectives—diagnostic devices and analytical instruments—and presents the technologies it has developed to date, their future directions, and how they will contribute to improving the quality of the healthcare journey.

Keywords
liquid biopsy, biopharmaceuticals, process monitoring

Introduction

The healthcare journey—from prevention to diagnosis, treatment, and prognosis management—is entering a major period of transformation due to the global spread of COVID-19 and the acceleration of population aging and declining birthrates. During COVID-19, large numbers of patients presenting with fever and fatigue emerged, creating an urgent need to deliver medical care while preventing droplet/aerosol transmission; this situation exceeded the assumptions underlying the healthcare system at that time. Challenges in healthcare response to pandemics became evident, including the supply of in vitro diagnostic testing analyzers and reagents; the provision of locations and opportunities for testing, clinical care, and emergency patient care; the early provision of vaccines and therapeutics; and the monitoring and control of outbreaks. Consequently, nationwide efforts are underway to prepare for the next pandemic. At present, Japan is also facing increasingly severe problems such as soaring medical expenditures and strain on the healthcare delivery system due to the rapid progression of population aging and declining birthrates. Medical expenditures have increased year by year (Figure 1). As the elderly population grows, the burden on the working-age population becomes even heavier and further increases in medical expenditures may undermine the sustainability of the social security system. Structural challenges, including shortages of physicians and healthcare workers and their uneven distribution between urban and rural areas, are also intensifying. In small- and medium-sized hospitals, there are increasing cases in which deteriorating management makes it difficult to maintain emergency medical care systems. Addressing these issues is an urgent matter.

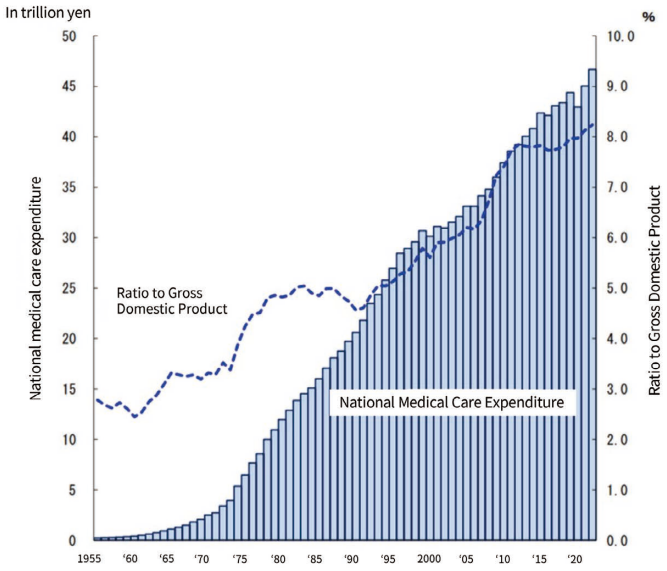

Figure 1 Annual trends in national medical expenditures and the ratio to gross domestic product.
Source: Ministry of Health, Labour and Welfare, "Overview of National Medical Expenditures in FY2022 (Summary of Results)" [1], [2].

In this social context, there is a growing demand for measurement technologies that enable simple testing without large systems or specialists and that contribute to rapid and accurate diagnosis, as well as analytical technologies useful for developing new therapeutics and vaccines and measurement technologies that support their stable, highly efficient production and supply. The following sections introduce HORIBA's initiatives and future developments in its biohealthcare business related to these needs.

HORIBA's Biohealthcare Business Initiatives

HORIBA's biohealthcare business comprises two domains: "medical devices used for diagnosis" and "analytical systems used in drug development." The former contributes by supporting clinical settings, whereas the latter contributes by supporting research and development settings.

HORIBA's medical devices are primarily deployed as clinical laboratory systems for hematology, immunology, and clinical chemistry. Through the provision of compact Point-of-Care Testing (POCT) systems for clinics (including pediatrics), laboratories in small- and medium-sized hospitals, and bedside use, HORIBA supports routine clinical practice.

The Hematology and CRP analyzer (Figure 2) was developed 27 years ago as system capable of simultaneously measuring complete blood count (CBC) and C-reactive protein (CRP*1) using whole blood samples. Subsequently, it has achieved specimen miniaturization, shorter turnaround time (TAT), reduced infection risk for operators, and downsizing of the device, and it is now widely adopted, particularly in clinics. Because it can simultaneously measure different test items that are important for infectious disease screening, it provides data that support rapid on-site decision-making in screening tests aimed at differentiating viral infection from bacterial infection in febrile patients.

Figure 2 Automated Hematology and CRP analyzer.

*1 CRP (C-Reactive Protein): a type of protein that increases in serum when acute inflammation or tissue injury is present in the body.

Figure 3 Glucose analyzer.

Figure 4 Centrifugal blood analyzer.

Figure 5 Laser diffraction and dynamic imaging particle size and shape analyzer.

Figure 6 Raman microscope.

In Japan, the prevalence of chronic diseases such as diabetes has increased, and there is a growing need to measure blood glucose and HbA1c[*2] not only at specialized facilities but also under the care of primary care physicians. HORIBA provides a solution that enables in-house diabetes testing by combining the glucose analyzer "ANTSENSE" (Figure 3) with the centrifugal blood analyzer "Banalyst" (Figure 4), which measures HbA1c with high accuracy using μTAS technology. In addition to enabling measurement of whole-blood samples through simple operation, shorter TAT makes it possible to efficiently conduct diagnosis and prognosis monitoring of chronic diseases within the limited time available for outpatient practice.

*2 Hemoglobin A1c (HbA1c): hemoglobin bound to glucose in the blood, representing the average blood glucose level over the past 1–2 months.

In recent years, with the widespread adoption of Electronic Medical Records (EMR), HORIBA has developed solutions not only for analyzers themselves but also for automatically integrating and linking data to EMR. These solutions support improvements in the quality of medical care by streamlining testing operations, reducing input errors, and centrally managing historical data. Such "analyzer + data integration" initiatives also constitute an important foundation for work-style reforms and for coordination in home care, both of which are being promoted in clinical settings.

Meanwhile, HORIBA's analytical systems originated from its founding product, the pH meter, and have been widely used from basic to applied research through pH measurement of various solutions in laboratories. Subsequently, HORIBA expanded into the particle measurement field and achieved particle size distribution measurement over an extremely wide range—from several tens of nm to several mm—by combining multiple measurement principles such as laser diffraction and dynamic light scattering. In particular, the laser diffraction and dynamic imaging particle size and shape analyzer (Figure 5) has been used to evaluate particle size distributions of raw materials for pharmaceuticals, foods, cosmetics, and other products, and has made substantial contributions to optimizing particle design that directly affects formulation uniformity and dissolution properties.

In addition, Raman microscopes (Figure 6) and transmission Raman spectrometers leveraging spectroscopic technologies have supported quality improvement of tablets by visualizing the dispersibility of specific components in small-molecule drug tablets and evaluating crystal polymorphs, thereby ensuring content uniformity.

In recent years, in response to increasing societal demands for medical safety, the importance of ensuring data integrity (DI) for manufacturing and quality control data has further increased. Because pharmaceutical manufacturers require systems that ensure data authenticity and consistency, HORIBA, in addition to providing analytical instruments, has deployed "HORIBA PLATINALINK" as a DI-compliant platform that can be utilized across HORIBA products, thereby ensuring data traceability and preventing falsification, among other measures.

Future Business Initiatives

In recent years, the forms of diagnosis demanded in clinical settings and of drug development and manufacturing have been changing substantially. In the diagnostic domain, earlier detection of diseases such as cancer is expected to become increasingly important. Accordingly, in addition to conventional pathological examinations that collect tissue, a shift toward liquid biopsy—using body fluids such as blood that is simpler and less invasive—is expected to progress.

For example, research on early diagnosis targeting miRNA (RNA that plays a role in regulating gene function) in exosomes released from cancer cells, as well as prognosis management and monitoring of treatment effects through analysis of trace amounts of Circulating Tumor Cells (CTCs) present in blood, has been advancing. These approaches are expected to provide important clues for future applications ranging from early cancer diagnosis to treatment monitoring.

To contribute to such future healthcare, HORIBA is leveraging technologies cultivated in medical devices and analytical instruments. For instance, HORIBA is also engaged in technology development related to liquid biopsy, including analysis of exosomes using the simultaneous multi-laser nanoparticle tracking analyser "ViewSizer 3000" (Figure 7), which applies particle tracking—one of the particle size distribution measurement techniques—and capturing CTCs by applying blood sampling technologies cultivated in hematology analyzers. These technologies are currently utilized mainly for research purposes; however, in the future, it is expected that, by integrating them with diagnostic medical devices, they will evolve into next-generation diagnostic solutions that can also be used in clinical settings.

In the domain of drug development and manufacturing, the development of biopharmaceuticals and vaccines using proteins such as antibodies and nucleic acids has been accelerating. Biopharmaceuticals mainly consist of macromolecules with molecular weights ranging from several thousand to several hundred thousand, and their manufacturing differs substantially from that of small-molecule drugs based primarily on chemical synthesis, as it depends on cell culture processes. Minor fluctuations in raw materials, culture conditions, and cell states can significantly affect the quality attributes of the final product. Consequently, compared with small-molecule drug manufacturing, biopharmaceutical manufacturing places greater importance on thorough process design as well as real-time control and management. Among pharmaceutical manufacturers and Contract Development and Manufacturing Organizations (CDMOs), there is a strong demand not only for final product quality evaluation but also for continuous monitoring of in-process conditions and for initiatives to enhance visualization and control of manufacturing processes.

Manufacturing and quality control technologies that precisely analyze products and medium components during cell culture are important for achieving both improved production efficiency and stable quality of biopharmaceuticals. The importance of the concept of QbD (Quality by Design), which realizes product quality through manufacturing processes designed to meet quality requirements, and of PAT (Process Analytical Technology), which visualizes and analyzes manufacturing processes in real time and builds quality through process control, has been increasing in recent years.

Figure 7 Simultaneous multi-laser nanoparticle tracking analysis system.

Figure 8 Process Raman.

Figure 9 Fluorescence spectroscopy analyzer.

To address these needs, HORIBA is advancing the deployment of process measurement solutions aimed at implementation in production environments, not only for research and development purposes, based on its core technologies such as Raman spectroscopy and fluorescence analysis. In particular, the process Raman system "PI-200 series" (Figure 8) and the Fluorescence spectroscopy analyzer "Veloci A-TEEM BioPharma Analyzer" (Figure 9) monitor, in real time, product and raw material concentrations, glucose, lactate, and other metabolism-related components in cell culture, thereby contributing to optimization of culture conditions. This contributes to improved production efficiency, while initiatives are also underway to support the design and verification of manufacturing processes by leveraging the acquired data.

Conclusion

HORIBA's biohealthcare business is also at a major turning point. In the field of diagnostic devices, HORIBA has thus far provided value primarily through screening tests in clinical settings; however, going forward, through integration with advanced analytical and measurement technologies cultivated in analytical systems, HORIBA will evolve toward next-generation diagnostic solutions that support prevention, early diagnosis, and monitoring. In the field of analytical systems as well, HORIBA will promote the development of process measurement technologies that consistently support the drug development environment not only in basic research and formulation evaluation but also from basic research through to actual production processes.

HORIBA's biohealthcare business aims to contribute to qualitative improvements across the entire healthcare journey—from diagnosis to treatment and prognosis management—and to create new value. In subsequent articles, as specific examples, we will introduce in detail the centrifugal blood analyzer Raman analytical technologies supporting culture and manufacturing processes, the fluorescence spectroscopy biopharma analyzer, and the fluorescence lifetime imaging microscope.

* Editorial note: This content is based on HORIBA's investigation at the year of publication unless otherwise stated.

References

[1] 厚生労働省,「令和4年度 国民医療費の概況(結果の概要)」(in Japanese),
https://www.mhlw.go.jp/toukei/saikin//hw/k-iryohi/22/dl/kekka.pdf
Accessed February 12, 2026
[2] 厚生労働省,「令和６年度 医療費の動向」(in Japanese),
https://www.mhlw.go.jp/topics/medias/year/24/dl/iryouhi_data.pdf
Accessed February 12, 2026

Kosuke Tsujita
Business Planning Dept.
Bio & Healthcare Technology Division
HORIBA, Ltd.

Visualizing 'Invisible Fluctuations' on the Manufacturing Site
—Optimizing Process Control through Raman Spectroscopy—

Takashi Kinoshita

Yutaro Hirose

Shohei Miyamoto

Hirotaka Yabushita

In pharmaceutical manufacturing, product quality is strongly influenced by process conditions and process progression, making real-time monitoring essential to continuously observe and control the internal process state without interrupting operation. This is particularly important in biopharmaceutical cell culture, where variability is high and cellular metabolic and nutritional states directly determine final product quality and yield. Raman spectroscopy enables direct online measurement of key metabolites in bioreactors --such as glucose and lactate --because it is non-destructive and non-contact, requires little to no sampling or sample preparation, and is relatively insensitive to water interference. When combined with chemometrics (multivariate analysis such as Partial Least Squares, PLS), it can estimate metabolite concentrations and cell states with high accuracy, enabling applications such as automated nutrient feed control and quality prediction. Looking ahead, further advances are expected toward implementing more sophisticated Process Analytical Technology (PAT) by integrating AI and digital twins.

Keywords
Raman spectroscopy, process monitoring, biopharmaceuticals, pharmaceuticals, chemometrics

Introduction

To ensure a stable supply of high-quality and low-cost pharmaceuticals, innovation in analytical technologies for quality control is indispensable. The U.S. Food and Drug Administration (FDA) and the International Council for Harmonisation of Technical Requirements for Pharmaceuticals for Human Use (ICH), which promotes harmonisation of pharmaceutical regulations across Japan, the United States, and Europe, strongly call for innovation in scientifically evidence-based quality and manufacturing management systems. Rather than testing only the final product as in conventional approaches, the concept of "Quality by Design (QbD)," in which the manufacturing process itself is designed and appropriately managed and controlled so that the intended quality is consistently achieved, is becoming increasingly important for ensuring product quality.

In this article, we introduce real-time monitoring of pharmaceutical manufacturing processes using Raman spectroscopy, covering topics from the principles of Raman spectroscopy to specific measurement case examples.

1. Fundamentals of Raman Spectroscopy

Raman spectroscopy has the advantage of requiring no sample pretreatment and being well suited to in situ observation, thereby offering high ease of measurement. In the following, we describe the principles of Raman spectroscopy, and the types of Raman spectroscopic instruments used in manufacturing processes.

1.1. Principle

When incident light interacts with matter, inelastically scattered light is generated (Figure 1a). This inelastic scattered light has a wavelength different from that of the excitation light and is referred to as Raman-scattered light. Because the wavelength of Raman-scattered light is shifted from the excitation wavelength by an amount corresponding to the molecular vibrational energy of the material being measured, it is used to obtain information on molecular structure and compositional characteristics (Figure 1b). Among the scattered light produced upon irradiation, scattered light having the same wavelength as the excitation light is also obtained; this is referred to as Rayleigh-scattered light. Because Rayleigh scattering is approximately 10^6 times more efficient than Raman scattering, it acts as background relative to Raman scattering and thus constitutes an inhibiting factor for compositional evaluation by Raman spectroscopy. Therefore, it is necessary to remove Rayleigh scattering using an optical filter and allow only Raman scattering to pass through[1].

1.2. Types

General-purpose Raman spectrometers can be broadly classified into a macro *type, intended for measurements over regions on the order of millimeters, and a micro type, which is integrated with an optical microscope to* measure local structures on the order of micrometers. Many macro-type instruments are portable and compact and are used, for example, for incoming inspection of raw materials. Transmission Raman spectroscopy, which is used for the quantification of active pharmaceutical ingredients (APIs) in tablets as described later, as well as probe Raman instrumentation for process monitoring, also fall into this category. By contrast, micro-type systems are characterized by high spatial and wavenumber resolution and the capability for imaging, and they are used mainly

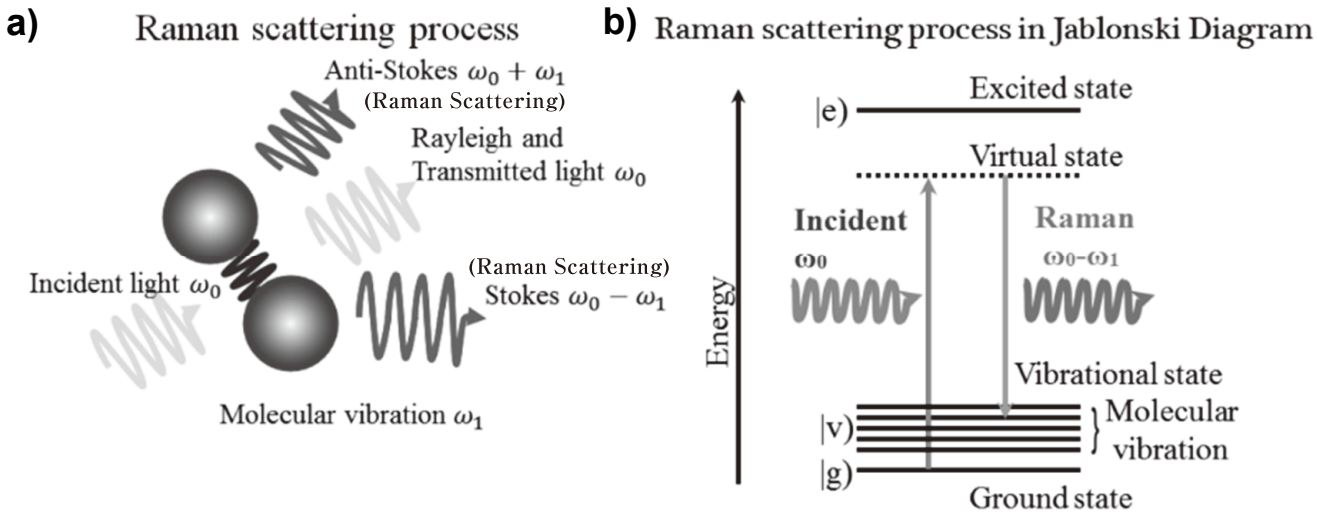

Figure 1 Conceptual diagram of molecular vibration (a), explanatory diagram of the Raman effect (b).

in pharmaceutical manufacturing development and quality control. Below, we describe two macro-type Raman analytical instruments that are primarily used in pharmaceutical production.

1.2.1. Transmission Raman

In transmission Raman spectroscopy, a laser is irradiated onto one side of a sample, and among the Raman-scattered light generated as the light undergoes diffuse reflection within the sample, the light transmitted through the sample is measured. Accordingly, an average Raman spectrum from the entire sample can be obtained. In addition, because Raman spectroscopy can provide sharp peaks and thus offers high chemical discriminative capability, it is less susceptible to the effects of changes in physical parameters (e.g., granule size and tablet thickness). For these reasons, transmission Raman spectroscopy has attracted attention as a method for quantitative determination of components in bulk samples.

1.2.2. Probe Raman

In recent years, with the shift toward continuous manufacturing of pharmaceutical tablets, there has been increasing demand to monitor their crystallinity and concentration. Compared with conventional methods, Raman spectroscopy—being non-destructive, non-contact, and non-invasive, enabling sample evaluation without pretreatment—has attracted attention as a technique that can be integrated into production processes for in-process evaluation. To incorporate a Raman spectrometer into a manufacturing line, a fiber-optic probe is used as the light-delivery/collection interface, and it is connected to a spectrometer and a detector. By adopting a fiber-optic configuration, remote measurements become possible, for example by separating the light source, spectrometer, and instrument control unit from the probe placed near the sample by several hundred meters. Probe designs include those that measure by direct contact with powders or solutions, as well as those that enable non-contact measurements through an observation window by using an objective lens at the probe tip. The use of probe Raman facilitates discrimination in-process among different polymorphic forms during manufacturing, detection of hydration states and phase transitions, and characterization of processes such as kneading (mixing) and drying.

2. Real-Time Monitoring Technologies Using Raman Spectroscopy

2.1. Advantages of Applying Raman Spectroscopy to Continuous Manufacturing Processes

Raman spectroscopy has recently become an important means of real-time monitoring in continuous manufacturing processes, as an analytical technique capable of obtaining chemical-structure information at the molecular level in a non-destructive and non-contact manner. Whereas laboratory analysis tends to focus on single measurements and short-term operation, continuous manufacturing sites require more advanced operation, including long-term stable operation of instruments and analytical methods, data reliability, and multipoint monitoring that provides an overview of the entire process. A key feature of Ramans instrumentation is that it requires little to no sample pretreatment and can be applied to samples in diverse states, including liquids, solids, and gases. Moreover, because water exhibits weak Raman scattering, Raman spectroscopy has the advantage of being readily applicable to processes that use water, such as those in the pharmaceutical and chemical industries. Against this background, Raman systems are rapidly becoming widespread in the field of process analysis.

2.2. Status Monitoring and Anomaly Detection to Support Continuous and Stable Instrument Operation

To operate Raman spectroscopic instrumentations stably over long periods in continuous manufacturing environments, it is essential not only to ensure instrument robustness but also to implement a real-time monitoring system that continuously tracks fluctuations in the instrument's internal status and the external environment. This enables early detection of potential failures or performance degradation, thereby allowing preventive maintenance and rapid response.

2.2.1. Specific Examples of Monitoring Parameters

Internal temperature of the instrument enclosure: Because excessively high or low temperatures can contribute to deterioration of electronic and optical components, the temperature should be continuously monitored using temperature sensors.

Laser status: The oscillation current, voltage, power, wavelength, and related parameters are measured in real time, and warnings are issued when abnormalities are detected.

Temperature of the spectrometer and detector: To prevent expansion of the spectrometer and optical components

due to temperature fluctuations, as well as increases in detector dark current, cooling mechanisms and temperature-control systems are implemented.

2.2.2. Anomaly Detection and Alert System

By monitoring these parameters, abnormalities in the instrument and changes in the external environment can be detected immediately. When an abnormality occurs, the system outputs alerts or error messages and is designed so that operators can respond promptly. This enables minimization of downtime and maintenance of data reliability.

2.3. Instrument and Data Protection Through Redundant Design

In continuous manufacturing processes, instrument failures can have a major impact on production efficiency and quality. Accordingly, Raman spectroscopic instrumentation incorporates redundant designs that assume the possibility of failures and component degradation, thereby enhancing system fault tolerance.

2.3.1. Instrument Redundancy (Example: Lasers)

Semiconductor lasers, which serve as the primary light source, inevitably undergo aging-related degradation due to heat and light exposure. Therefore, two lasers are installed, and automatic switching is performed at fixed intervals, enabling continued operation with the other laser even if one fails.

2.3.2. Redundancy for Data Protection (Example: Storage)

Loss of measurement data affects traceability and quality assurance. The instrument's hard disks are redundantly configured via mirroring (RAID configuration), thereby reducing the risk of data loss and system downtime in the event of disk failure. This improves data integrity and ensures the safety of critical process data.

2.4. Ensuring Long-Term Spectral Stability

In real-time monitoring, it is important to suppress the effects of day-to-day environmental changes and instrument aging on spectra and to continue acquiring data of equivalent quality over extended periods.

2.4.1. Temperature Control of Optical Components

Optical devices such as the laser, spectrometer, and detector are sensitive to changes in ambient temperature, and temperature fluctuations directly lead to spectral fluctuations. For example, temperature-induced changes in the emission wavelength of a semiconductor laser and thermal expansion of components in the spectrometer optics can shift the wavelength axis of Raman spectra. In addition, increases in detector temperature affect the S/N ratio of spectra. To maximize the performance of each component, it is desirable that the laser, spectrometer, and detector can each be independently regulated at their respective optimal temperatures.

2.4.2. Online Automatic Calibration Technology

Process Raman spectrometers are equipped with an internal reference light source, such as a noble-gas lamp, and include a function that periodically measures emission lines to automatically calibrate the spectrometer's wavelength axis. In addition, calibration of the laser emission wavelength is performed using known peaks of the sample, thereby enabling long-term stable management of both the spectrometer and the laser. As a result, highly accurate spectral data can be obtained without being affected by environmental changes or instrument aging.

2.5. Visualization of the Entire Process Through a Multipoint Measurement System

In continuous manufacturing, there is a strong need to manage multiple processes and multiple locations. In Raman spectroscopy, incorporating a multipoint measurement scheme makes it possible to grasp the status of the entire process and to further enhance quality control.

2.5.1. Multipoint Measurement Using a Multiplexer

In Raman spectroscopy, multipoint measurement can be achieved with a single instrument by using a multiplexer to switch among multiple measurement channels. This reduces instrument costs while enabling real-time understanding of the status of the overall process.

2.5.2. Operational Benefits of Multipoint Measurement

Multipoint measurement enables fine-grained monitoring of quality variations at each process and location, thereby allowing early detection of process abnormalities and process optimization. It also enables centralized monitoring of the entire production line and contributes to strengthening traceability and quality assurance.

3. Spectral Analysis Methods (Chemometrics)

3.1. Information Contained in Raman Spectra and the Importance of Analysis

Raman spectra directly and indirectly contain diverse information, including the concentrations of chemical components in a sample and physical properties (e.g., boiling point and density), as well as sensory attributes such as color and odor, mechanical strength, and other characteristics. In process monitoring, it is important to extract such information from spectra and utilize it for process control and quality control. However, Raman spectra constitute multidimensional data comprising hundreds to thousands of intensity values, and extracting the information of interest requires advanced data processing and analytical techniques.

3.2. Development of Calibration Models

3.2.1. Workflow for Building Calibration Models

A calibration model is a mathematical model that relates spectral data to calibration targets (e.g., component concentrations). Model development proceeds through the following steps: data collection, preprocessing, regression model construction, and validation.

3.2.2. Data Collection Methods

Measurement of process samples: Samples from the production line are measured using a Raman spectrometer, and, in parallel, target reference values for calibration (e.g., component concentrations) are obtained by offline analysis.

Data acquisition using design of experiments: To improve the generality and robustness of the calibration model, another approach is to prepare in-house samples with known concentrations and use them as model-building data. A method known as Design of Experiments (DoE) is employed, in which factors and levels are set in a planned manner to construct the model with as few experiments as possible.

Dataset splitting: The collected data are split into training data and test data in order to appropriately evaluate generalization performance on unseen data. The training data are used for hyperparameter selection and model fitting, whereas the test data are used to estimate the final generalization error.

3.2.3. Spectral Data Preprocessing Techniques

In addition to Raman-scattered light, spectral data include fluorescence, Rayleigh-scattered light, instrument-derived noise, and other components. To develop a high-accuracy model, preprocessing of spectral data to appropriately remove or reduce these effects is indispensable.

Wavenumber selection: Only wavenumber regions that are highly sensitive to the calibration target are selected. Effective wavenumber regions are explored using methods such as MWPLS, thereby improving model accuracy[2],[3].
Baseline correction: Flexible baseline estimation methods, such as the ALS method[4], are used to remove complex baselines. Polynomial correction, MSC, and derivative processing using a Savitzky–Golay filter[5] are also employed.

Normalization: To remove the influence of laser-intensity fluctuations, normalization is performed using the spectral area or the intensity of a specific peak.

Noise reduction and correction for interfering components: Methods such as binning, Savitzky–Golay filtering, and the GLSW method[6] are used to reduce random noise and suppress the influence of interfering components. In recent years, end-to-end preprocessing using deep learning has also been investigated[7],[8].

3.2.4. Construction of Regression Models

Regression algorithms are applied to the preprocessed spectral data (X) and the calibration target values (y) to build calibration models. In spectral analysis, PLS is widely used.

PLS: Spectral X, which exhibits strong collinearity, is projected onto a latent space that maximizes covariance with y, and y is regressed using a small number of variables. The dimensionality of the latent space (K) is optimized by cross-validation (CV). PLS includes PLS1, which corresponds to a single calibration target, and PLS2, which corresponds to multiple calibration targets.

Cross-validation (CV): The training data are divided into multiple subsets, and models are built and evaluated while holding out a portion of the data. The dimensionality of the latent variables is determined using RMSECV (the Root Mean Squared Error of Cross-Validation) as an index, thereby preventing overfitting.

Outlier removal: Abnormal data are detected and removed using distributions such as the Q statistic and Hotelling's

T2. This improves model accuracy and robustness.

Other regression methods: Machine-learning methods based on decision trees, such as GBM (gradient boosting machines), as well as nonlinear regression using deep learning, have also been actively studied in recent years.

3.2.5. Model Validation Methods

The developed calibration model is applied to a test dataset that was not used for training, and the prediction error, RMSEP, is evaluated. If RMSEP is confirmed to fall within a pre-specified acceptable range, generalization performance to unseen data is ensured.

3.2.6. Model Transfer and Calibration Techniques

Because developing calibration models entails substantial cost, reuse of models is desirable. In general, even instruments of the same model often do not exhibit identical spectral characteristics. Therefore, model reuse is achieved by applying techniques such as CCD channel sensitivity calibration using a standard light source[9], SBC (Slope/Bias Correction), PDS (Piecewise Direct Standardization), and TOP (Transfer by Orthogonal Projection), which transform the data to enable model transfer[10], [11].

3.2.7. Continuous Model Maintenance

Because calibration models are built based on training data, prediction accuracy may deteriorate when process conditions or sample composition change. It is important in practice to periodically compare offline analytical results for samples with the values predicted by the Raman spectrometer and, as needed, to update the model by adding or modifying training data. This approach enables maintenance of accuracy and reliability in long-term process monitoring.

3.3. Evolution of Analytical Methods and Future Perspectives

3.3.1. Utilization of Deep Learning and Machine Learning

In addition to conventional linear regression models such as PLS, deep learning and decision-tree-based machine-learning methods have recently begun to be applied to the analysis of Raman spectroscopic data[12],[13]. These methods are well suited to capturing nonlinearity and complex correlations and may enable end-to-end automation of the multi-step preprocessing traditionally required.

3.3.2. Improving Robustness and Generality

To maintain high-accuracy predictions even under diverse process conditions and sample variability, there is a growing need to improve the robustness and generality of analytical methods. Through technological innovations in noise reduction, outlier detection, and wavenumber selection the scope of Raman spectroscopy applications continues to expand.

4. Case Studies

4.1. Management of Active Pharmaceutical Ingredients Using Transmission Raman

For the quantification of pharmaceutical active ingredients, analysis is typically performed by dissolving tablets and then applying high-performance liquid chromatography (HPLC) or ultra-performance liquid chromatography (UPLC). Analysis by transmission Raman enables quantitative determination of the drug substance comparable to that achieved by UPLC, using a method in which tablets or powders are measured without pretreatment and without the use of organic solvents (Figure 2). In addition, measurement is completed within a few seconds per tablet, providing high throughput. Furthermore, transmission Raman is useful not only for quantifying drug substances but also for determining the contents of crystalline polymorphs[14],[15], amorphous forms[16], and cocrystals[17].

Ohashi et al. reported that a calibration model for a drug developed using transmission Raman is robust to variations in process parameters in wet granulation and tableting processes, and that it can be applied to non-destructive analysis of tablets even at low drug concentrations[18]. Superiority over existing technologies such as

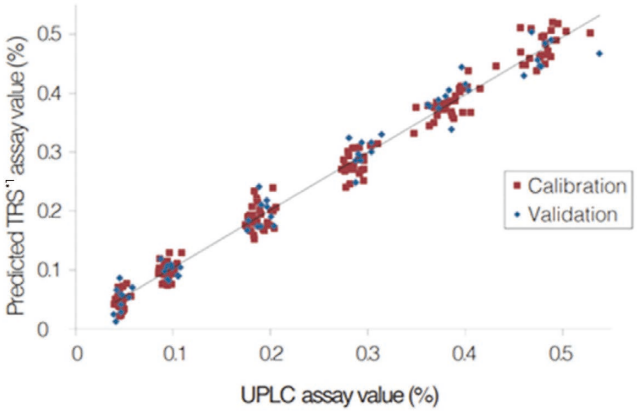

Figure 2 Correlation between Raman spectra and UPLC for tablets with different active ingredient concentrations (Provided by Professor Fukami, Meiji Pharmaceutical University).

*1 Transmission Raman spectroscopy

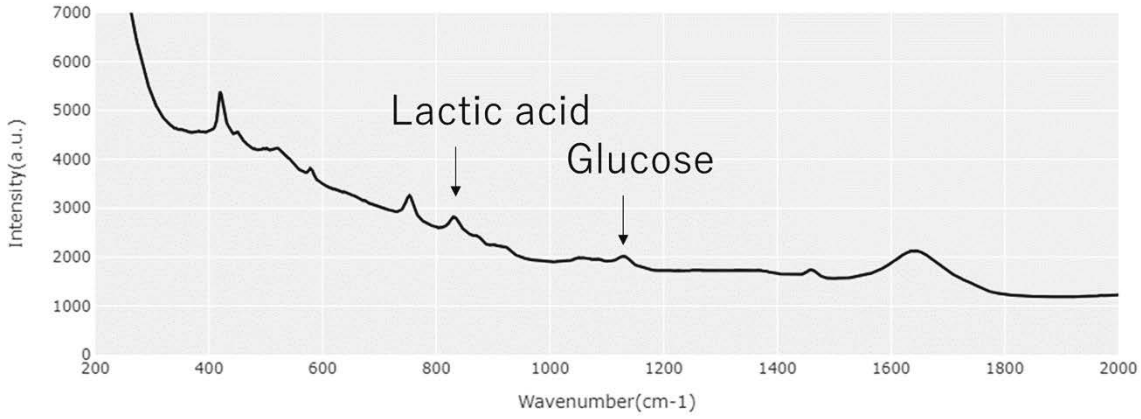

Figure 3 Raman Spectra of Cell Culture Medium.

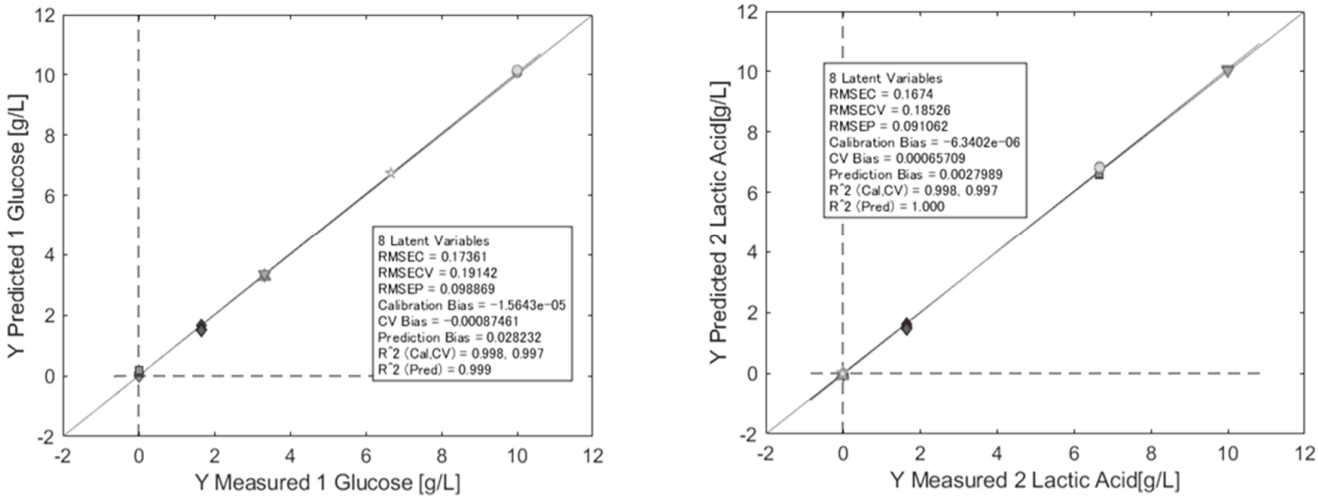

Figure 4 Prediction of Glucose and Lactic Acid concentrations from Raman Spectra using Chemometrics.

near-infrared spectroscopy has been demonstrated, and the use of transmission Raman as a process analytical technology (PAT) tool is expected to contribute to improving the robustness of continuous manufacturing.

4.2. Culture Process Monitoring

Monoclonal antibodies (mAbs) as therapeutic antibodies accounted for the majority of the biopharmaceutical industry in 2019, representing 70% of total sales. As demand for mAb products increases year by year and biosimilars[*2] are introduced, competition among industrial pharmaceutical companies is intensifying, with emphasis placed on maximizing production volume while reducing both manufacturing and development costs and shortening manufacturing lead times

In recent years, substantial improvements have been observed in bioreactor cell density, product yield, and process efficiency. Intensification and optimization of upstream processes are mainly associated with cell line development and media optimization, and in recent years, new strategies based on PAT and QbD have gained popularity.

*2 Biosimilar: Unlike generics (follow-on drugs) for low-molecule pharmaceuticals, a biosimilar is a follow-on version of a biopharmaceutical with a complex molecular structure.

Because it is difficult to produce an identical structure, “similarity” to and “equivalence” with the reference (originator) product are demonstrated through rigorous testing.

In cell-culture operations, particularly during cell proliferation, appropriate management of glucose feeding is critical. As shown in Figure 3, components such as lactate and glucose can be spectrally separated and assigned even in mixed solutions. Accordingly, by applying the techniques introduced in 3. Spectral Analysis Methods (Chemometrics), the concentrations of these components in culture media can be determined[18],[19] (Figure 4). If the glucose concentration is not properly maintained, the culture-medium environment deteriorates, leading to a decline in product quality. Similarly, excessive accumulation of lactate can also degrade the culture environment and may result in reduced cell growth and productivity. The introduction of PAT that combines Raman spectroscopy with chemometrics is considered to promote process

intensification and to be useful for shortening the development timeline of pharmaceuticals and enabling stable manufacturing.

Indeed, according to a report by Gibbons et al.[19], in batch cultures in which glucose concentration was controlled using Raman spectroscopy, the accuracy of glucose feeding improved, cell growth rate and viability increased, and the final product titer increased. They further reported that glycation was substantially reduced in some batches, resulting in improved product quality. These results demonstrate the effectiveness of process monitoring by Raman spectroscopy in cell culture.

Conclusion

In this article, we discussed practical considerations for applying Raman spectroscopy to real-time process monitoring, as well as data-analysis techniques. We also presented examples in which these approaches have been implemented in practice, namely, management of active pharmaceutical ingredients and monitoring of culture processes.

As a vibrational spectroscopic technique that is non-destructive and non-invasive and provides rich information, Raman spectroscopy is expected to continue to develop. In particular, recent years have seen rapid advances not only in laser, spectrometer, and detector technologies but also in data-analysis methods, including machine learning. By combining the various measures for stable long-term operation introduced in this article with these technological advances, we anticipate that Raman spectroscopy will be broadly applied to diverse industrial processes, including those involving previously uncharacterized composite materials and complex biological samples.

* Editorial note: This content is based on HORIBA's investigation at the year of publication unless otherwise stated.

References

[1] HORIBA, Ltd., " What is Raman Spectroscopy?" https://www.horiba.com/jpn/scientific/technologies/raman-imaging-and-spectroscopy/raman-spectroscopy/

[2] R. Hara et al., Development of Raman Calibration Model Without Culture Data for In-Line Analysis of Metabolites in Cell Culture Media, *Applied Spectroscopy*, 77(5), 521-533(2023)

[3] J.H. Jiang, R.J. Berry, H.W. Siesler, Y. Ozaki. Wavelength Interval Selection in Multicomponent Spectral Analysis by Moving Window Partial Least-Squares Regression with Applications to Mid-Infrared and Near-Infrared spectroscopic Data, *Analytical Chemistry*, 74(14), 3555–3565(2002)

[4] Gallagher, NB," Fitting Smooth Curves Part III: Baselining with an Asymmetric Least-Squares Algorithm," [white paper] Eigenvector Research, Inc., www.eigenvector.com

[5] Gallagher, NB," Savitzky-Golay Smoothing and Differentiation Filter," [white paper] Eigenvector Research, Inc., www.eigenvector.com

[6] Gallagher, NB et al., Generalized Weighting to Account for Sampling Artifacts, [white paper] Eigenvector Research, www.eigenvector.com

[7] Corner C. Horgan et al., High-Throughput Molecular Imaging via Deep-Learning-Enabled Raman Spectroscopy, *Analytical Chemistry*, 93, 15850-15860(2021)

[8] Hao He et al, Noise learning of instruments for high-contrast, high-resolution and fast hyperspectral microscopy and nanoscopy, *Nature communications*, 15, 754(2024)

[9] KRISTIN J. FROST, Calibration of Raman Spectrometer Instrument Response Function with Luminescence Standards: An Update, *Applied Spectroscopy*, 52(12), 1614-1618(1998)

[10] J.J.Workman Jr., A Review of Calibration Transfer Practices and Instrument Differences in Spectroscopy, Applied Spectroscopy, 72(3), 340-365(2018)

[11] L. Salguero-Chaparro et al., Calibration transfer of intact olive NIR spectra between a pre-dispersive instrument and a portable spectrometer, *Computers and Electronics in Agriculture* 96, 202–208(2013)

[12] Weng et al., Deep learning networks for the recognition and quantitation of surface-enhanced Raman spectroscopy, *Analyst*, 145, 4827-4835(2020) (in Japanese)

[13] Gao et al., Machine learning algorithms for rapid estimation of holocellulose content of poplar clones based on Raman spectroscopy, *Carbohydrate Polymers*, 292, 119635(2022)

[14] 柏木ら, 医薬品固形製剤の生産におけるラマン分光法の活用, *製剤機械技術学会誌*, 27(2), 42-51(2018) (in Japanese)

[15] Griffen JA et al., Rapid quantification of low level polymorph content in a solid dose form using transmission Raman spectroscopy, *J.Pharma. Biomed. Anal.*, 128, 35-45(2016)

[16] Terada H et al., Quantitation of trace amorphous solifenacin succinate in pharmaceutical formulations by transmission Raman spectroscopy, Int. *J.Pharm.*, 565, 325-332(2019)

[17] Koide T et al., Quantification of a cocrystal and its dissociated compounds in solid dosage form using transmission Raman spectroscopy, *J.Pharma. Biomed. Anal.*, 177, 112886(2020)

[18] Ohashi R et al., Effects of wet granulation process variables on the quantitative assay model of transmission Raman spectroscopy for pharmaceutical tablets, Euro. *J.Pharma. Biopharma.* 191,276-289(2023)

[19] L. Gibbons et al., An assessment of the impact of Raman based glucose feedback control on CHO cell bioreactor process development, *Biotechnol. Prog*, 39(5), e3371(2023)

Takashi Kinoshita
Biomedical Science Solution Dept.,
Bio & Healthcare Technology Division,
HORIBA, Ltd.

Yutaro Hirose
Bio & Health Care Field Dept.,
Sales Promotion Center,
Sales Division,
HORIBA, Ltd.

Shohei Miyamoto
IoT & Data Analytics Dept.,
Design Engineering Center,
R&D Division,
HORIBA, Ltd.

Hirotaka Yabushita
Data Science Manager
HORIBA Instruments Incorporated (HII)

Development of Centrifugal Blood Analyzer "Yumizen Banalyst M120" for Point-of-Care Testing

Takashi Nagai

Due to factors such as the increase in the number of patients with diabetes and revision of the medical care act, demand for point-of-care testing (POCT) and for greater accuracy and faster turnaround times in clinics is increasing. In response, we developed a blood analyzer that enables immediate testing at the point of care for analytes such as Hemoglobin A1c, CRP,and high-sensitivity CRP, which are used for screening diabetes and infectious diseases, using only a small volume of blood. In this device, a dedicated reagent chip designed by applying μTAS technology is loaded into the instrument, allowing processes equivalent to those performed by large-scale analyzers—from centrifugation and reagent reactions to optical measurement—to be reproduced within a small chip. This enables highly accurate measurements despite the analyzer's small footprint. Furthermore, the analyzer reduces the measurement time by up to approximately 2 minutes and 30 seconds (about 33%) compared with the conventional analyzer. This paper describes the development process and key features of the centrifuge-based analyzer.

Keywords
μTAS, POCT(Point-of-Care Testing), HbA1c, CRP

Introduction

Due to changes in lifestyle habits and the social environment, the number of patients with diabetes visiting clinics has increased rapidly in recent years[1]. In addition, amid market changes such as the aging of the patient population and revisions to the Medical Care Act in Japan[2], community healthcare settings are being required to establish systems that can perform highly accurate testing efficiently with limited time and personnel. Our company has long offered a broad range of blood-testing systems for the clinic market that support point-of-care testing (POCT), enabling rapid testing in close proximity to patients[3]. The widespread adoption of POCT makes test results available immediately, thereby shortening the time from diagnosis to initiation of treatment and contributing to improvements in the quality of healthcare and in patients' quality of life (QOL). Expectations for POCT systems have increased, there are concerns that their data accuracy may be inferior to that of large analyzers used in hospitals.

In particular, Hemoglobin A1c*1 (HbA1c), which is also used as an indicator for monitoring patients with diabetes, requires measurement results with high stability and accuracy[4]. In response to requests from clinical settings for a system that can perform testing in a simpler manner and in an even shorter measurement time—while maintaining the high-accuracy measurement enabled by the μTAS*2 technology that is a key feature of our conventional system[5]—we developed the centrifugal blood analyzer Yumizen Banalyst M120 (Figure 1).

*1 Hemoglobin A1c (HbA1c): HbA1c indicates the proportion (%) of hemoglobin in red blood cells that is bound to glucose and reflects the average blood glucose level over the past 1–2 months.

*2 μTAS: An abbreviation for Micro Total Analysis System. It is a system in which fluidic devices are integrated on a chip measuring from several millimeters to several centimeters on a side, enabling a series of chemical operations—such as chemical reactions and biochemical analyses—to be performed efficiently in a short time.

Overview of the Reagent Chip

The YM-120 uses a disposable plastic chip based on μTAS technology (hereafter, the reagent chip) . The reagent chip contains sealed liquid reagents and a series of analytical operations—such as centrifugation of blood, reaction with reagents, and optical measurement—are performed using μTAS technology. At present, four

Figure 1 Yumizen Banalyst M120(YM-120).

reagent chips are available for the following analytes: HbA1c, a marker of diabetes; C-reactive protein (CRP)[*3], an inflammation marker; high-sensitivity CRP (hs-CRP)[*4], which provides enhanced sensitivity in the low-concentration range of CRP; and cystatin C[*5], a marker of renal function. By selecting the reagent chip according to the item to be tested, multiple analytes can be measured with a single instrument. Figure 2 shows the functional sections of the HbA1c reagent chip.

Within a compact chip measuring 40.0×50.0×4.5 mm, each section performs its intended function, allowing the entire analytical workflow to be completed within the reagent chip. To achieve this, "control of centrifugal force" on the instrument side is a key point.

*3 CRP (C-reactive protein): A type of protein that increases in serum when there is acute inflammation or tissue damage in the body.

*4 High-sensitivity CRP: Has sensitivity at least 100-fold higher than that of a conventional CRP test, making it possible to measure trace amounts of CRP that cannot normally be detected.

*5 Cystatin C: One of the serum proteins used mainly as a marker for renal function testing.

Instrument Overview

Figure 3 shows the internal structure of the instrument. Inside the measurement chamber, a rotating table is installed, and stages on which the reagent chip and the balancer chip are placed are arranged on the table, respectively. The rotating table is driven by a motor at up to 3,000 rpm, thereby applying centrifugal force to the reagent chip. Using this centrifugal force, liquids within the reagent chip (blood and reagents) are transported, and the pretreatment required for measurement is performed automatically. In addition, by rotating the stages on the rotating table, the orientation of the reagent chip is switched, thereby controlling the direction of the centrifugal force acting on the liquid moving within the reagent chip. By repeatedly applying centrifugal force through rotation of the table and switching direction through rotation of the stages, the liquid is metered and mixed, and a series of analyses is performed. In this instrument, we re-examined the internal mechanisms and operating sequence relative to our conventional instrument, and, by improving the rotation time of the rotating table and increasing the speed of reagent-chip orientation switching, we reduced the measurement time for all four assays while maintaining measurement accuracy. In particular, we achieved measurement time reductions[*6] of approximately 2 min 30 s (approximately 33%) for HbA1c and approximately 1 min 20 s (approximately 17%) for CRP (Table 1).

*6 Compared with our conventional instrument and based on our internal evaluation. The effect may vary depending on the method of use and conditions.

In optical measurement, light emitted from an illumination LED (wavelength: 635 nm) installed inside the measurement chamber passes through the optical measurement section of the reagent chip, is reflected by a mirror, and

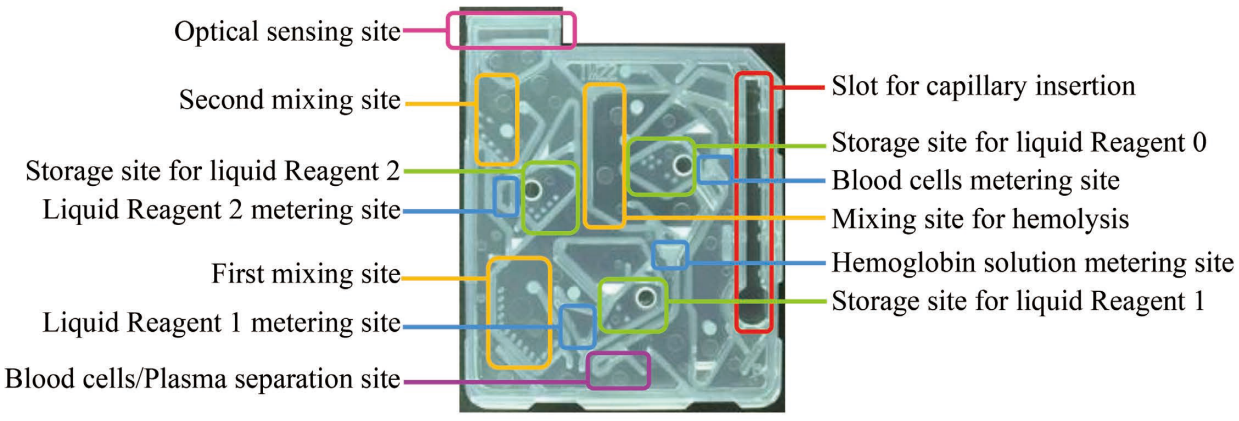

Figure 2 Functional sites of HbA1c reagent chip.

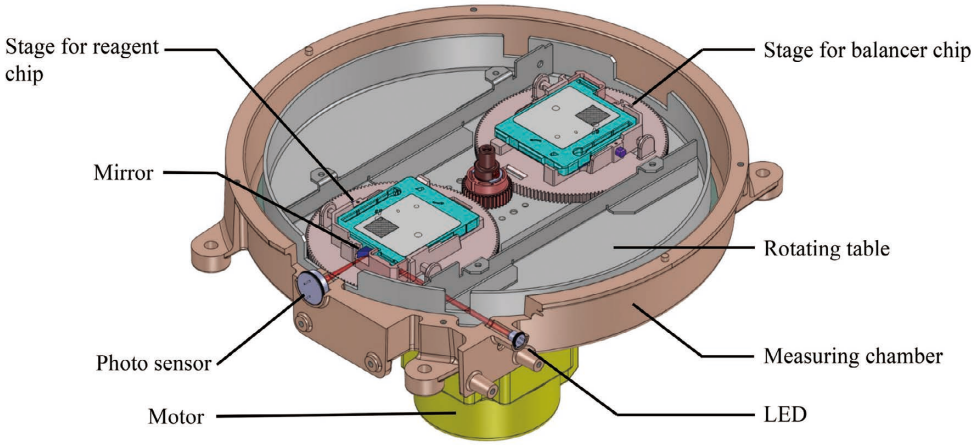

Figure 3 Structure of YM-120.

Table 1 Measurement time.

Assay item	Our conventional instrument	YM-120	Time reduction
HbA1c	7 min 40 sec	5 min 10 sec	2 min 30 sec
CRP	7 min 40 sec	6 min 20 sec	1 min 20 sec
High-sensitivity CRP	7 min 40 sec	7 min 20 sec	20 sec
Cystatin C	8 min	7 min 50 sec	10 sec

enters a photodiode. By shortening, relative to conventional approaches, the time required for absorbance photometry in this optical measurement and acquiring calibration-curve information, we achieved both high-accuracy measurement and reduced measurement time.

How to Use the YM-120

Figure 4 shows the user operating procedure. First, whole blood is collected using a dedicated capillary (HbA1c: approximately 4.0 µL; CRP: approximately 4.4 µL; high-sensitivity CRP: approximately 9.5 µL; cystatin C: approximately 6.0 µL). Next, the capillary is loaded into the reagent chip. When the reagent chip is set in the instrument's measurement chamber and the cover is closed, measurement starts automatically.

All information required for measurement—including identification of the test item, reagent-chip lot information, and calibration-curve information—is consolidated in a two-dimensional code affixed to the surface of the reagent chip.

A camera installed inside the instrument automatically reads the two-dimensional code, the measurement sequence is executed according to the test item, and concentration calculations are performed based on the corresponding calibration-curve information. When measurement is complete, the results are displayed on the instrument screen.

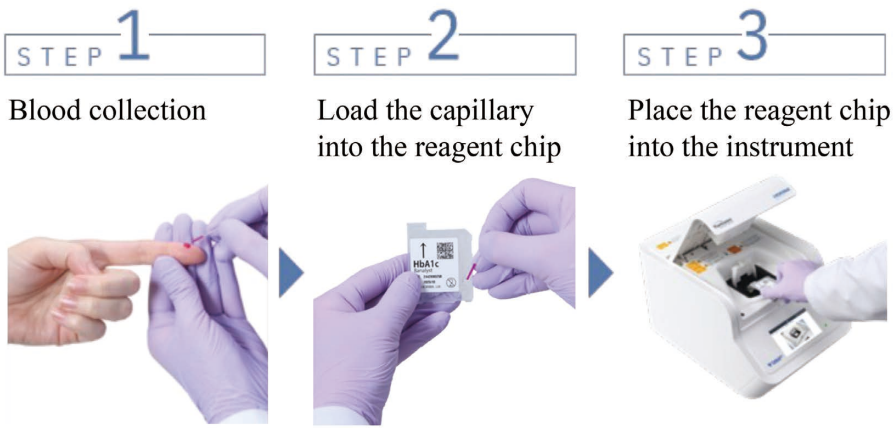

Figure 4 Measurement procedure of YM-120.

The YM-120 eliminates the need for centrifugation, cumbersome replenishment of reagents, waste-liquid handling, and other procedures that are commonly required with large instruments in clinical laboratories, and it can be used easily even by users who are not proficient in operating analytical equipment. In addition, because testing is possible even when blood is collected from a fingertip using a lancet, the burden of blood sampling on patients can be reduced, and the system can also be used in pediatrics and neonatal intensive care units (NICUs).

Performance Evaluation

HbA1c is used in routine clinical practice as an important indicator of glycemic control in patients with diabetes, and there is a strong demand for measurement system that are rapid, simple, and highly accurate. To confirm traceability to the international reference method for HbA1c, we participated in the NGSP certification study, which is conducted to verify such traceability, and assessed correlation with a secondary reference measurement laboratory (Figure 5). To obtain NGSP certification, it is required that, when 40 certification-study specimens provided by the certifying organization are measured over a period of 5 days, at least 36 specimens fall within ±5% of the values measured by the secondary reference measurement laboratory. The YM-120 produced results within ±5% for all specimens, confirming small deviations and high correlation.

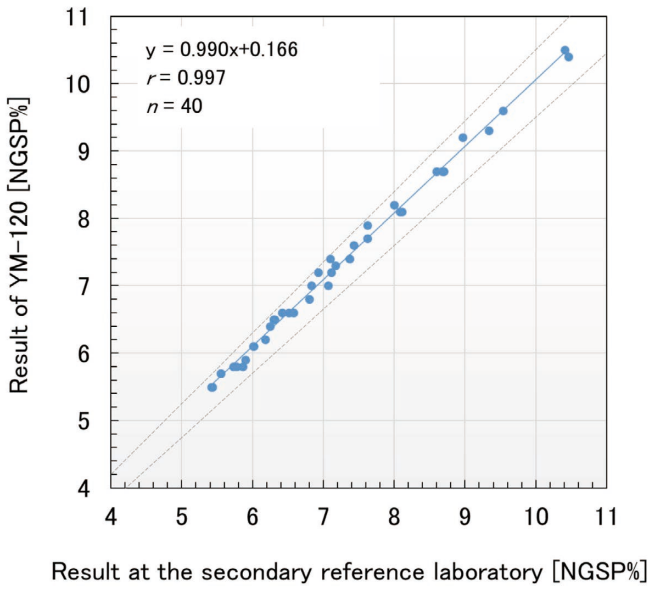

The dotted line shows the ± 5% of the result at the secondary reference laboratory.

Figure 5 NGSP Certification Test Results for HbA1c.

Improved Usability

To improve operational efficiency in healthcare settings by increasing testing throughput, reducing waiting time other than the measurement time is also a key consideration. With our conventional analyzer, a waiting period was required from the end of a measurement until the next measurement could be performed; this waiting time was eliminated, enabling continuous measurements. In addition, we enabled analyzer start-up and shutdown to be executed by a timer and allowed users to configure public holidays and unscheduled clinic-closure days, thereby improving operability and workflow convenience.

Figure 6 illustrates integration with our electronic medical record (EMR) linkage software, "GATELINK."[*1] Through this integration, measurement results can be automatically transmitted to the EMR. Furthermore, by integrating with our comprehensive maintenance-service support system for our analyzers, "HORIBA MEDISIDE LINKAGE next"[*7][6], monthly aggregation of measurement data acquired from this instrument can be performed, and documents such as

Figure 6 GATELINK connection configuration diagram.

measurement standard operating procedures, which are required to be prepared under revisions to the Medical Care Act in Japan, can be generated automatically. These functions contribute to reducing the burden of data management and mitigating risks arising from data-entry errors.

*7 Product availability varies by country. This product is not available in all markets.

Conclusion

In this article, we described the YM-120, which enables immediate on-site testing within medical facilities using only a small volume of blood, focusing on the structure of the μTAS-technology-based reagent chip and the instrument, as well as high-accuracy measurement for HbA1c. Through deployment of this system, we hope to support workflow efficiency—from measurement through integration with electronic medical records—and thereby contribute to strengthening the role of primary care physicians in community healthcare and to delivering high-quality medical services. Going forward, we plan to expand into global markets and contribute to society by realizing testing that is "rapid, simple, and highly accurate." We also intend to pursue development of additional test items that are in high demand as POCT in clinical settings but have not yet been realized.

* Editorial note: This content is based on HORIBA's investigations in the year of publication, unless otherwise stated.

References

[1] 厚生労働省,「糖尿病」 https://www.mhlw.go.jp/www1/topics/kenko21_11/b7.html (2025/11/21参照) (in Japanese)

[2] 厚生労働省,「医療法改正等の経緯と検体検査の精度の確保に係る基準について」 https://www.mhlw.go.jp/content/10800000/000911173.pdf (2025/11/21参照) (in Japanese)

[3] 野村尚之：In Vitro Diagnostics 市場におけるHORIBA Medicalの歴史と今後の展望, *Readout*, 55 (2021) (in Japanese)

[4] Lenters-Westra E.; Slingerland, R. J.; Three of 7 Hemoglobin A1c Point-of-Care Instruments Do Not Meet Generally Accepted Analytical Performance Criteria. *Clinical Chemistry*, 60 (8), 1062-1072 (2014)

[5] 横川昭徳, 平田克樹：μTAS技術を用いた遠心方式血液分析装置 Yumizen M100 Banalystの開発, *Readout*, 54, (2020) (in Japanese)

[6] 作田尋路, 西森正志：HORIBA MEDISIDE LINKAGE next ～スマートメンテナンスで医療現場を革新～, *Readout*, 60, (2025) (in Japanese)

Takashi Nagai
Assistant Section Leader
Product Development Dept.
Bio & Healthcare Technology Division
HORIBA, Ltd.

High-Throughput Screening with Chemical Specificity in Biopharma with PoliSpectra Rapid Raman Plate Reader

Fiona Xi Xu

The PoliSpectra Rapid Raman Plate Reader addresses the critical trade-off in biopharma between high-throughput speed and chemical specificity by providing automated, label-free molecular fingerprinting. Designed for seamless integration into 96-well plate workflows which enables simultaneous measurement of multiple samples for condition optimization, the Rapid Raman Plate Reader utilizes multi-laser excitation and “walk-away” automation through automatic calibration and robotic-arm and liquid handler integration to deliver non-destructive analysis of complex samples. This Readout demonstrates the platform’s efficacy through three key applications: the precise quantification of nucleoside triphosphates (NTPs) in mixture, the determination of protein detection limits for BSA and lysozyme, and the monitoring of glucose levels in varied culture media. By delivering rapid, reproducible results across these diverse bioprocessing tasks, the Rapid Raman Plate Reader establishes itself as a high-speed complementary tool to traditional chromatography, enabling more efficient drug discovery and process development.

Introduction

High-throughput screening (HTS) is a central component of pharmaceutical research, enabling the rapid evaluation of thousands to millions of compounds during drug discovery and bioprocess development to find the next breakthrough. However, existing HTS approaches often involve a trade-off between speed and chemical specificity. Fluorescence and absorbance assays provide rapid readouts but typically require costly labels and lack the molecular-level information needed to avoid false positives. Conversely, chromatography techniques such as high-performance liquid chromatography (HPLC) and liquid chromatography–mass spectrometry (LC–MS) offer high selectivity and precision but are slow, labor-intensive, and consume vast amounts of reagents, making them difficult to scale for high-throughput workflows.

Raman spectroscopy provides a molecular fingerprint that enables label-free, chemically specific analysis with mini-

mal sample preparation. Despite these advantages, conventional Raman measurements are often limited by low throughput and complex workflows, restricting their adoption in screening environments. At HORIBA, we developed the patented PoliSpectra Rapid Raman Plate Reader (Figure 1) to address these limitations by transforming Raman spectroscopy into a high-speed, automated screening platform capable of non-destructive chemical analysis.

The Rapid Raman Plate Reader is designed to operate directly with standard 96-well plates commonly used in HTS workflows, with ongoing development toward compatibility with higher density formats such as 384-well plates to further increase throughput. Customization for different well-plate formats is also available.

The Rapid Raman Plate Reader incorporates a multi-laser system offering combinations of 532 nm and 785 nm excitation options. This flexibility allows researchers to tackle a diverse range of samples. The 532 nm laser provides strong signal strength for optically clear samples, while the 785 nm option is crucial for suppressing fluorescence interference in biological samples.

To ensure reliable operation in high-throughput and high-volume environments, the Rapid Raman Plate Reader is designed for "walk-away" automation. Every part, including the motorized door and self-calibration routines, is fully automated to ensure data reliability day-to-day. The system also supports server access for seamless integration with robotic arms and liquid handlers. Together, these features enable Rapid Raman Plate Reader to deliver rapid and reproducible Raman measurements suitable for routine screening and multivariate analysis model building.

In this work, we present three customer-inspired case studies to demonstrate the applicability of the Rapid Raman Plate Reader system across key biopharmaceutical workflows: nucleoside triphosphate (NTP) quantification in mixture, protein limit of detection evaluation, and glucose quantification in culture media. Collectively, these representative examples showcase how high-throughput Raman analysis can benefit a wide range of biopharma research interests and complement conventional analytical techniques.

Figure 1 PoliSpectra Rapid Raman Plate Reader.

Results and Discussion

Nucleoside Triphosphate Quantification

To demonstrate the system's transformative potential in reaction monitoring and optimization, we first focused on monitoring nucleoside triphosphates—ATP, CTP, GTP, and UTP—which are fundamental building blocks for nucleic acids and play essential roles in cellular energy transfer and biochemical signaling. Accurate and timely monitoring of NTP concentrations in mixtures is therefore important across a range of biochemical and analytical applications. However, conventional NTP quantification typically relies on chromatographic techniques such as HPLC coupled with UV absorbance, fluorescence detection, or LC-MS. While these methods provide high selectivity, they are poorly suited for rapid screening due to limited throughput, extensive sample preparation requirements, and high operating and maintenance costs. These constraints significantly limit the number of conditions, formulations, or reaction states that can be practically evaluated.

Raman spectroscopy is well-suited for addressing these limitations. As demonstrated in Figure 2A, each of the four NTPs exhibits distinct Raman features, enabling direct identification and quantification in mixture without any additional labeling or chromatographic separation. To evaluate quantification performance and detection limits with Raman, mixtures of ATP, CTP, GTP, and UTP were prepared in phosphate-buffered saline (PBS) solution across a concentration range of 0 to 2.5 mM in triplicate. Raman spectra were acquired with 532 nm excitation, with acquisition time of 40 seconds per well.

A Partial Least Squares (PLS) regression model was constructed to resolve the overlapping spectral contributions, with preprocessing using Savitzky-Golay 1st derivative and mean centering. Four latent variables were selected for the final model. To validate the model robustness, we prepared a separate batch of NTP mixtures and acquired their spectra on a different day.

Strong agreement was observed between predicted and reference concentrations, with regression slopes greater than 0.997 for all four NTPs, as shown in Figure 2B. The model achieved a mean squared error of cross-validation

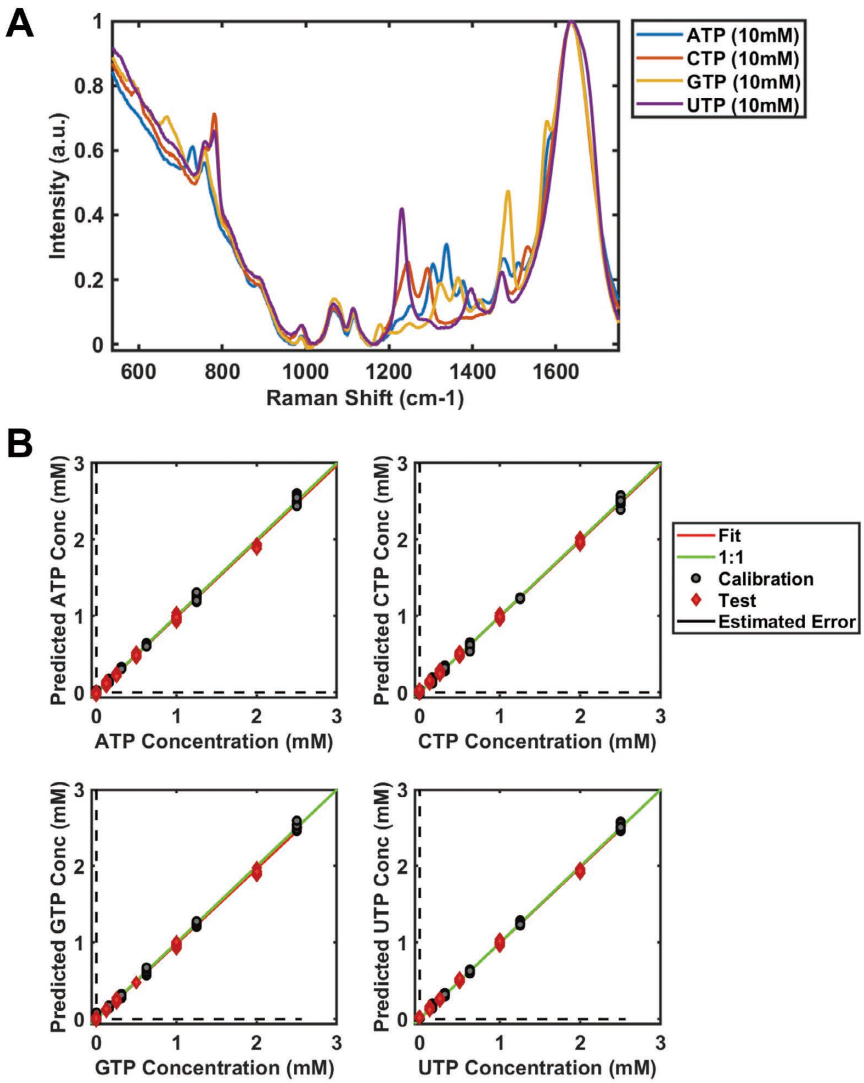

Figure 2 Nucleoside triphosphate (NTP) Raman spectra collected with Rapid Raman Plate Reader using 532 nm excitation.
(A) and PLS calibration model for concentration prediction (B).

(MSECV) value below 0.03 and enabled accurate prediction of NTP concentrations down to 0.1 mM. These results demonstrate the capability of the Rapid Raman Plate Reader to provide rapid, label-free quantification of NTPs in complex mixtures, supporting high-throughput screening and reaction analysis workflows in biopharmaceutical environments.

Protein Detection Limit Evaluation

Proteins are central targets in biopharmaceutical development; however, high-throughput protein detection and quantification are generally challenging. Common techniques such as UV absorbance, Bradford/BCA assays, and ELISA suffer from limited specificity, interference from formulation components, and dependence on calibration standards. HPLC and LC-MS offer higher accuracy but are slow, low-throughput, and require extensive sample preparation. Fluorescence or label-based assays improve sensitivity but introduce labeling artifacts and high reagent costs.

Raman-based protein analysis, despite its advantages in sample preparation simplicity, is challenging due to relatively weak Raman scattering and interference from fluorescence. To evaluate the detection capabilities of the Rapid Raman Plate Reader for protein analysis, two representative proteins were selected: bovine serum albumin (BSA, ~66 kDa) as a large protein and lysozyme (~14 kDa) as a smaller protein. A dilution series of each was prepared in PBS buffer in 96-well plates for Rapid Raman Plate Reader measurements.

Raman spectra, illustrated in Figure 3 left panel (A for BSA and B for lysozyme), were acquired using 785 nm excitation to minimize fluorescence interference. Two PLS regression models were constructed for each protein molecule with mean-centered spectra across a range of concentrations. As shown in Figure 3 right panel, good linearity was observed for both types of protein molecules. The Rapid Raman Plate Reader successfully

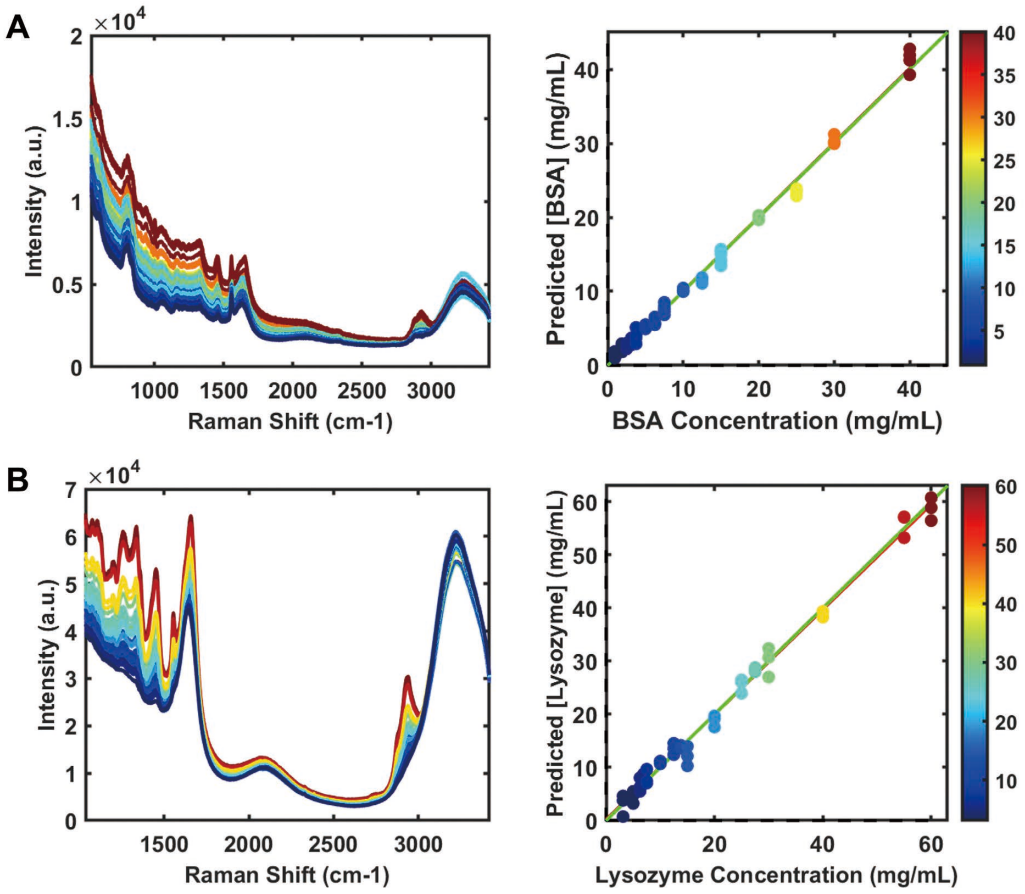

Figure 3 Limit of detection evaluation of protein molecules, BSA (A) and lysozyme (B) using Rapid Raman Plate Reader with 785 nm excitation. Raman spectra (left) and corresponding PLS calibration models (right).

detected protein concentrations down to approximately 3 mg/mL—specifically 2.6 mg/mL for BSA and ~5 mg/mL for lysozyme.

These results establish a baseline detection limit for Raman-based protein analysis using our high-throughput plate reader platform and demonstrate the feasibility of applying the Rapid Raman Plate Reader to protein formulation, stability studies, and drug-protein interaction screening without consuming or destroying samples.

Glucose Quantification in Culture Media

Glucose concentration is a key parameter in cell and yeast culture and fermentation processes, directly impacting cell viability and productivity. While HPLC is commonly used for glucose quantification, its limited throughput and operational cost and complexity restrict its use for rapid feedback during media optimization and process development. We evaluated the Rapid Raman Plate Reader's ability to quantify glucose directly in culture media formulations and spent culture supernatants using 785 nm excitation.

We analyzed five types of yeast spent media containing different glucose concentrations. As shown in Figure 4A, background fluorescence level varies significantly across media types. To explore the feasibility of predicting glucose concentration using one single model, we preprocessed the Raman spectra using 6th-order detrending followed by mean centering to isolate the glucose signal from the complex background. Predicted glucose concentrations were compared with HPLC-measured concentrations.

Glucose concentrations were accurately predicted in most media types, as shown in the right plot of Figure 4A. However, one medium type (Medium D, cyan) exhibited a different prediction slope, indicating complex matrix effects likely due to its significantly stronger fluorescent background. To address this, a separate PLS model could be constructed specifically for this medium during production or QC workflows. Alternatively, samples exhibiting strong background interference can be flagged for targeted HPLC analysis. This hybrid strategy enables efficient resource allocation while maintaining analytical rigor. This case study highlights the utility of the Rapid Raman Plate Reader as a rapid screening and down-selection tool prior to chromatographic analysis.

We also performed a separate study to evaluate the limit of detection of glucose in PBS buffer solution (Figure 4B). Using a simple PLS regression model with 1st-order

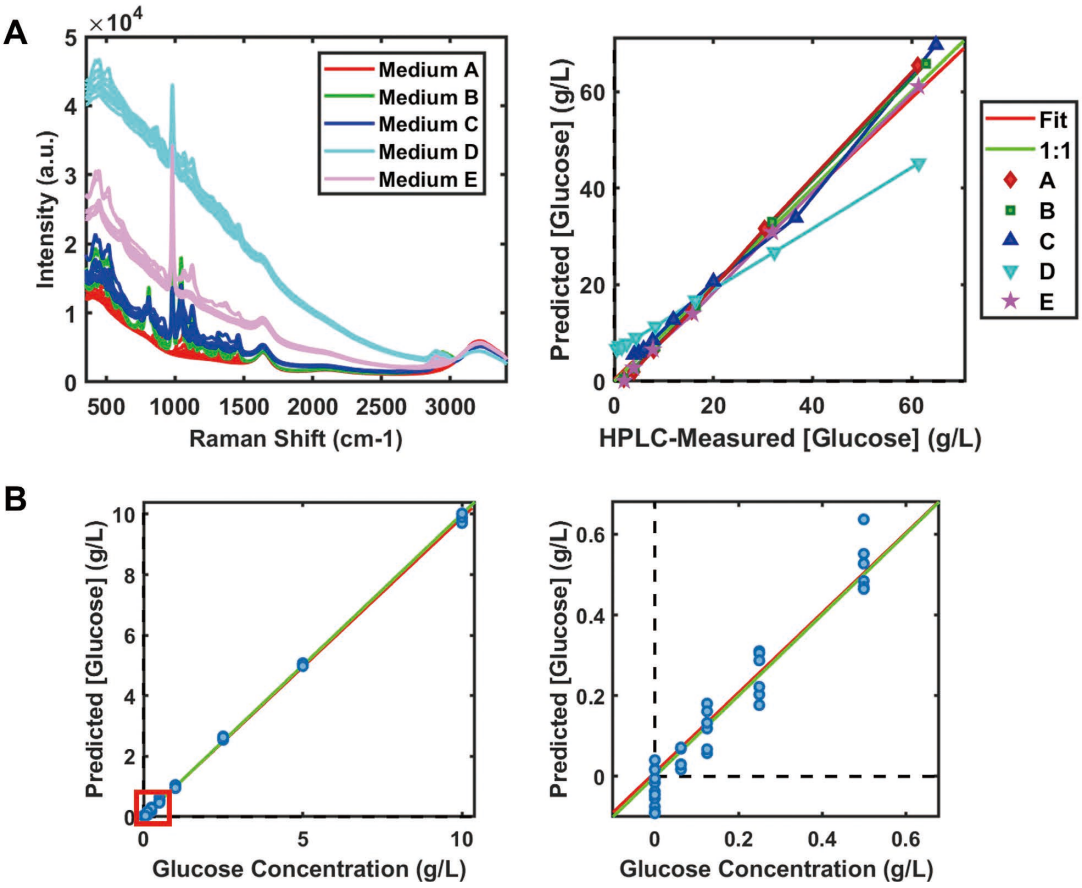

Figure 4 Glucose quantification using Rapid Raman Plate Reader with 785 nm excitation. (A) Raman spectra of five yeast spent media types containing different glucose level and corresponding PLS prediction compared with HPLC measurement. (B) Glucose limit of detection was evaluated in PBS buffer solution. Right plot shows the lower concentration region as marked by the red box in left plot.

detrending, mean centering, and 1 latent variable, the glucose detection limit was determined to be as low as 0.29 g/L.

Conclusions

Across three biopharmaceutical-relevant case studies, from NTP monitoring to protein detection and glucose quantification, the PoliSpectra Rapid Raman Plate Reader demonstrates its ability to deliver chemical specificity and label-free quantification at speed. By bridging the gap between research needs and industrial scale, HORIBA's team demonstrated that the Rapid Raman Plate Reader is not just an instrument—it is a practical high-throughput screening platform for accelerating drug discovery and bioprocess development.

* Editorial note: This content is based on HORIBA's investigations in the year of publication, unless otherwise stated.

Dr. Fiona Xi Xu
Life Science Applications Scientist
HORIBA Instruments Incorporated

FLIM – An Extra Dimension to Fluorescence Microscopy

Philip Yip

David McLoskey

Graham Hungerford

The use of imaging techniques is of fundamental importance in uncovering the structure and dynamics of biological substances. Fluorescence microscopy, in particular, is well suited to visualise cellular structures and interactions. This can use fluorescent labels or the measurement of endogenous fluorescence. Techniques, such as FRET (Förster resonance energy transfer) also enable the elucidation of interactions on the nanometre scale, below the diffraction limit. The use of the fluorescence lifetime is advantageous as it is an absolute measure and the best way to observe FRET and biomolecular interactions. Fluorescence lifetime imaging (FLIM) products such as the FLIMera and InverTau harness this power in the area of biological and life sciences.

Keywords
cell biology, macro imaging, metabolism, microplastics, TCSPC

Introduction

Fluorescence microscopy is an illuminating method to shed light on molecular interactions. It has the potential to work on the nanoscale up to the imaging of macroscale objects. It is a very sensitive technique, capable of detecting single molecules and makes use of either the intrinsic fluorescence properties of the sample or that of an introduced label or tag molecule. Simply put, molecules (fluorophores) take in energy in the form of light, raising their energy. This can be released a short time later in the form of light at a longer wavelength. This fluorescence signal is multiparameter; depending on the wavelengths of excitation and emission, excitation intensity, polarisation and the fluorescence lifetime[1]. The fluorescence lifetime is a measure of how long a molecule spends in the excited state (stores the excitation energy) and is typically on the picoseconds (ps) to nanoseconds (ns) timescale. The fact that a molecule loses some energy in the excited state means that its emission is lower in energy compared to the excitation light (i.e. shifted to longer wavelengths). Therefore, it is easy to wavelength exclude the excitation, by use of a filter or monochromator, to just record the fluorescence. This enables a high degree of specificity, along

with sensitivity, in the fluorescence measurement. The fluorescence signal is highly dependent on the local microenvironment and molecular interactions, which makes it well suited to the study of biomolecules. Thus, fluorescence microscopes are extensively used in the biological field[2],[3]; in the study of cell biology, medical diagnostics, drug discovery, cancer research and neuroscience, for example.

Fluorescence microscopy is optical microscopy based on the imaging of light, which means that it is diffraction limited in resolution (~250nm). This is illustrated in Figure 1, which also illustrates two major forms of microscopy set ups: widefield and confocal (Figure 1b and 1c). Widefield illumination covers the whole of the sample and this can be imaged using a camera. This technique is rapid, but because light can penetrate and be imaged from different depths in the sample the resulting images can suffer from out of focus blurring. The confocal set up typically scans a laser over the sample, building up an image line by line. The addition of a spatial filter (pinhole) suppresses out of focus light, enabling optical sectioning. The image clarity in relation to the widefield approach comes at the expense of measurement speed. The detector is typically a single pixel and building up the image line by line means that it is a longer measurement compared to the widefield approach.

Typically in fluorescence microscopy it is the intensity that is measured, but by making use of a high repetition rate laser, single-photon detector and suitable timing electronics, etc, it is possible to measure the fluorescence lifetime and give the microscope fluorescence lifetime imaging (FLIM)[4] capability. This allows more of the fluorescence parameters to be obtained in a single measurement. Figure 1d shows this schematically. Use of the fluorescence lifetime parameter is advantageous since it is considered an absolute measure, generally independent of concentration, and a more sensitive method to monitor some molecular interactions (e.g. protein binding). It is therefore less affected by photobleaching, that can occur in samples under the microscope.

As mentioned earlier, fluorescence is an optical technique and therefore limited to resolving objects around hundreds of nm in size. However, by using Förster resonance

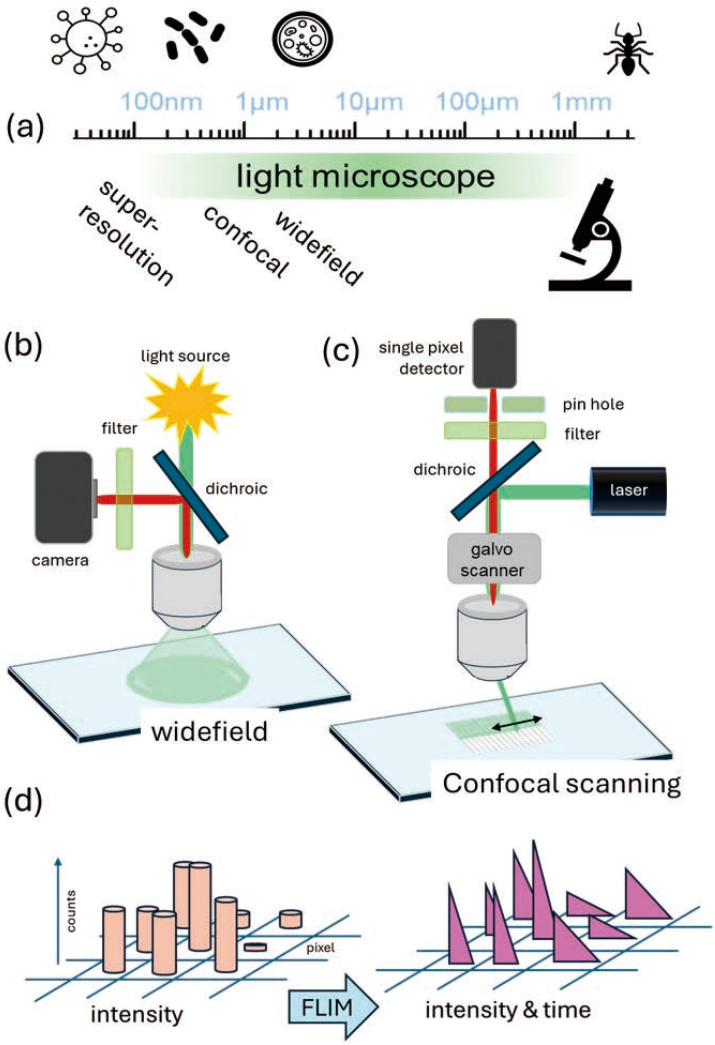

Figure 1 Schematic representations of (a) the distance scale for light microscopy techniques, (b) a widefield set up and (c) a confocal laser scanning set up. A representation of the pixel information between intensity and FLIM measurement is also shown (d).

energy transfer (FRET)[1], and interpretation of the fluorescence signal, interactions on the nanometre (~1-10nm) scale can be inferred. The use of the fluorescence lifetime parameter is particularly elucidating and greatly simplifies the measurement of FRET. Other fluorescence based methodologies do exist to image under the diffraction limit (termed super-resolution techniques) but will not be discussed here.

FLIM is therefore a powerful extension to fluorescence microscopy, enhancing the ability to provide image contrast and elucidate molecular and environmental interactions. HORIBA has recently introduced two products to address this market need. They are based on the time-correlated single-photon counting (TCSPC) technique, which is often considered the "gold standard" to measure the fluorescence lifetime[1]. Unlike time-gated and frequency domain techniques, TCSPC is digital and unaffected by fluctuations in excitation intensity. It is the best method to determine multiexponential decay kinetics. Large gate widths (several ns), rather than gate step size, is the limiting factor for time gating methods leading to less accurate determination of complex decay kinetics, whilst phase techniques are also typically not as sensitive.

The FLIMera widefield TCSPC camera is based on a SPAD (single-photon avalanche photodiode) array with in-pixel timing, whilst the InverTau – Fluorescence Lifetime Imaging platform is laser scanning making use of galvanometers. These two independent technologies are shown attached to an inverted microscope in Figure 2.

Figure 2 Top, an inverted microscope equipped with an InverTau (left) and a FLIMera (right). Bottom, left, a schematic of the optical path through the InverTau and, right, a FLIMera and its SPAD based sensor with in-pixel timing.

The InverTau is fully computer controlled and intended to simplify FLIM data acquisition, enabling high resolution images. It is designed to fit on the side port of an inverted microscope. The FLIMera, based on complementary metal-oxide semiconductor (CMOS) technology, can simultaneously measure over 24,000 fluorescence decays. Each of its pixels contains a SPAD detector and associated timing electronics, which can be read out over 12,000 times per second. This means that it is well suited to monitor moving samples and kinetic events, for example. In addition to microscope based imaging, it has application for macroscale imaging. Here the two complementary FLIM products will be described and examples of their use given.

Widefield and macro imaging using a SPAD array with in-pixel timing

In the case of widefield imaging, where the whole of the sample is illuminated, the measurement of the image data can be done relatively quickly (see Figure 1). Replacing an intensity camera with a FLIMera, and the light source with a pulsed laser, enables a simple transformation to a FLIM measurement system. Since it is a widefield approach no scanning is required. In fact, as well as usage on a widefield microscope the FLIMera can give lifetime functionality to light sheet microscopes[5] used in volume imaging and also enables the possibility of macroFLIM measurements. These are measurements not requiring the use of a microscope but used similarly to a normal camera. Out with fluorescence applications the FLIMera shows potential for time-domain near infrared imaging[6], an emerging area for imaging inside biological material.

The principal feature of the FLIMera is its 192 x 126 pixel array based on CMOS technology, where each pixel contains a detection element (SPAD) and its associated TCSPC timing electronics. Thus, it has the ability to record up to 24,192 fluorescence decays simultaneously. The FLIMera can measure fluorescence over wavelengths from ~400nm to 900nm and is optimised for measuring the lifetimes of common biological probes and endogenous fluorescence (range 200ps to 20ns). The in-pixel timing means that an average fluorescence lifetime can be visualised in real time (up to ~30fps), whilst post processed data can be temporally resolved down to the readout rate of the sensor (~80µs). This response speed means that moving samples or dynamic events can be imaged using the fluorescence lifetime. Thus, SPAD arrays based of CMOS technology exhibit a great deal of promise in bioimaging[7].

Recent concerns relating to the presence of microplastics in the general environment and their potential to cause

harm inside the body have led to methods to detect their presence. One approach to help visualise these particles, which range in size from 1μm to 5mm, is to stain them with Nile red[8].

This dye is highly sensitive to different environments. Thus different microplastic materials can affect its fluorescence emission, allowing their differentiation. As well as giving the usual histogram representation of the fluorescence lifetime data, HORIBA EzTime Image software that controls the FLIMera (and InverTau) and analyses FLIM data, can use a phasor representation[9]. This is a model free method to visualise and distinguish different lifetimes based on the use of Fourier analysis, with the decay data from each pixel plotted as a point on the phasor chart. Single exponential decays appear on the semicircle, increasing in lifetime from right to left, while more complex decays appear within the semicircle. This provides a quick visual method to distinguish between different fluorescence lifetimes. Its application is shown in Figure 3, where the phasor approach is used to select between different Nile red stained microplastics based on the fluorescence lifetime. Selecting different parts of the phasor chart (red box) selects the particles with similar fluorescence lifetimes.

The FLIMera, in addition to microscope based measurements, shows promise for macroscale FLIM and has been used for cancer margin identification in a model system[10]. An example of FLIM on different spatial scales is given in Figure 4. This shows a macroFLIM measurement of a whole variegated rubber tree leaf, using a custom lens and filter set up for the FLIMera and diffuse laser excitation. The green chlorophyll containing areas are clearly discerned in the lifetime image, but harder to make out in the intensity image. Further processing of the lifetime data could then give insight into the photosynthetic mechanism. These

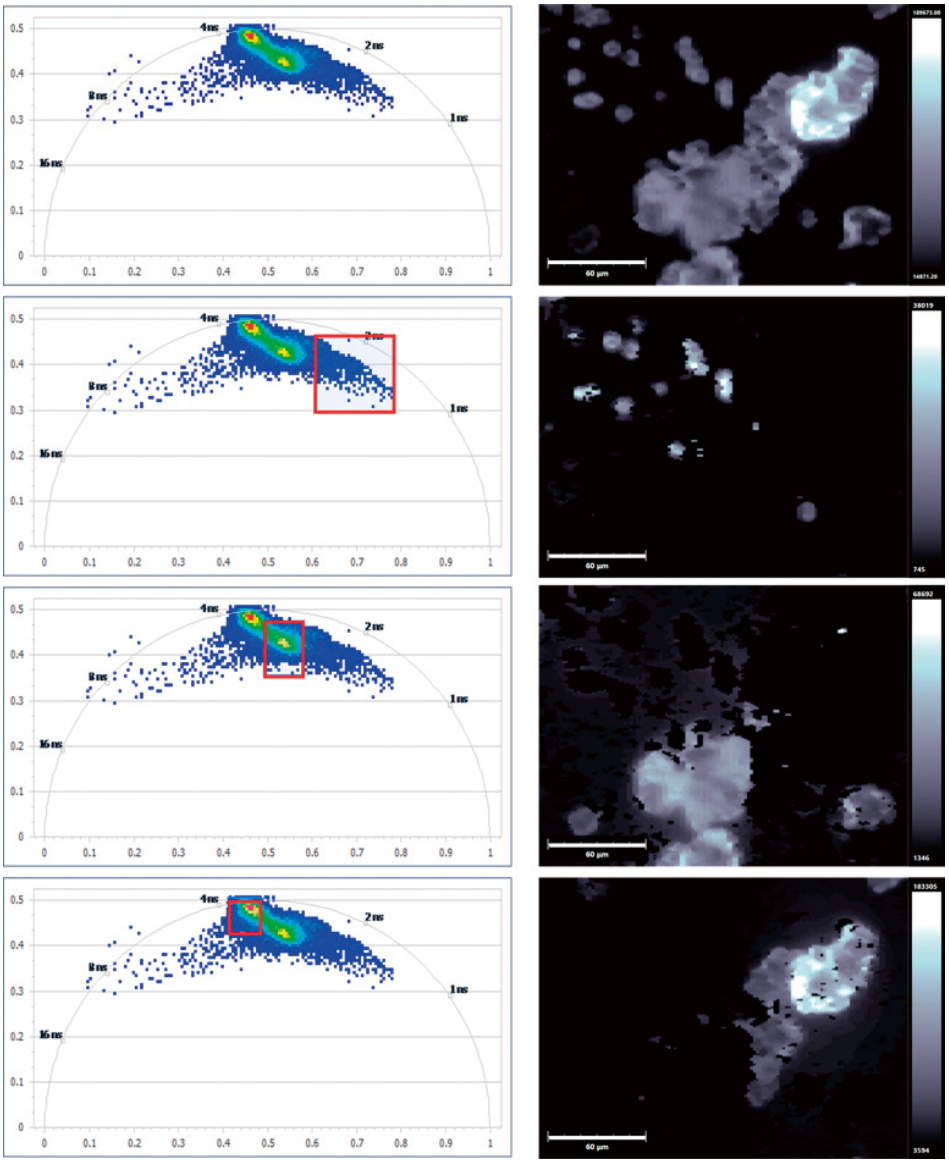

Figure 3 FLIM data from a mix of different Nile red stained polymers. The top data shows the whole image. Selecting different regions of the phasor plot (red box - left hand side) selects related Nile red lifetimes, differentiating the polymers in the image on the right hand side. These data were measured using a FLIMera and the scale bar is 60 μm.

macroscale measurements are complemented in that figure by an InverTau measurement showing the detail from the underside of a leaf (Figure 4b). In this case a two-photon excitation source was used which also enabled the second harmonic generated (SHG) signal to be monitored. Some biological substances exhibit this non linear effect and it can be used to determine structural information[11]. Figure 4c clearly shows the leaf stomata, which can be combined with the fluorescing structures in Figure 4b to provide a fuller picture. This methodology can also be applied to other biological tissue.

Although the FLIMera can provide simple non scanning FLIM, by replacing intensity based cameras on a microscope to enable real time determination of the average fluorescence lifetime, the widefield configuration does have some limitations. Common when using a widefield camera is out of focus blur. Also, the number of pixels in the FLIMera can mean that a trade off might be required between field of view (FoV) and resolution, although researchers have published work to enhance the resolution[12]. Where higher resolution FLIM is required the InverTau can be considered. It is capable of collecting images up to a 4K x 4K spatial resolution. The use of a pinhole enables optical sectioning by mitigating out of focus blur. However, galvanometer scanning of the laser beam over the sample is a slower approach compared to that of widefield. Thus, the FLIMera and InverTau may be considered complementary in imaging capability.

Laser scanning FLIM applied to cellular structure and processes

The InverTau has been optimised to make FLIM measurements as simple as possible by using EzTime Image software (also used with the FLIMera) and computer controlled optics. It is designed to attach a side port (C-mount) of an inverted microscope, as shown in Figure 1. To allow for future flexibility of use, the InverTau has two excitation ports and two emission ports. Typically a pulsed laser (eg DeltaDiode) is fibre coupled to one excitation port. The other port is optimised for use with two-photon excitation sources, as used for the data in Figure 4b and 4c. Typically, only one HPPD detector is employed, although it can be configured to collect from two detectors simultaneously.

A major use of FLIM is in the biological and life sciences, where many applications involve the study of cellular structure and the interaction between cellular components. Examples are in cellular biochemistry and cancer research. Fluorescent tags can be introduced to label specific components or endogenous fluorescence used. For example, NADH emission which is indicative of cell metabolism.

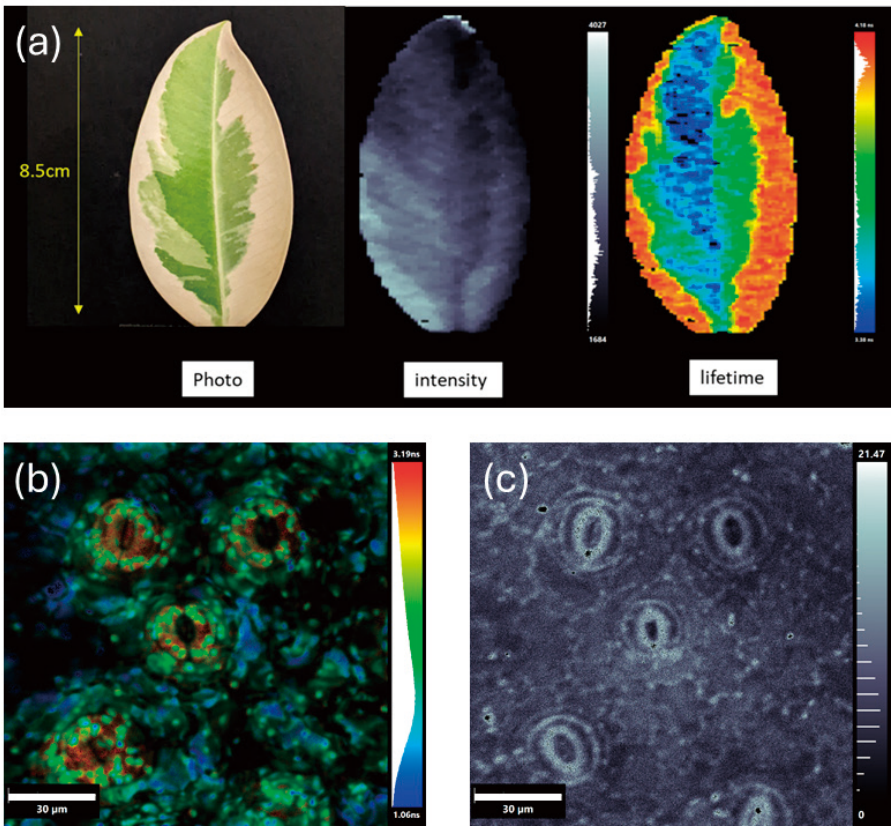

Figure 4 (a) Images of a whole leaf from *Ficus elastica tineke* taken with a phone camera (left) and a FLIMera (centre and right). (b) a two-photon excited fluorescence image showing the average lifetime from an abaxial leaf surface and the corresponding SHG image (c) made using an InverTau. The scale bar is 30µm.

An important aspect in the cell life cycle is that of division. The study of which is important in numerous fields of investigation. For example, drug / cancer research may focus on killing cells, thus monitoring their viability is paramount. Other drugs may need testing to ascertain that they do not harm a cell or cause mutations. Both cases involve monitoring the division process. Figure 5 gives some example measurements using the InverTau showing proteins or structures involved in mitosis. In each case (apart from Figure 5b) merged images are shown. These are the combined (using a software such as Fiji) images from separate measurements using different excitation and emission wavelengths. This is so tags or labels associated with different cell structures can be discerned. Figure 5a shows the position of a specific protein (red) within the cell nucleus (blue). Figure 5b shows the separation of the chromosomes, whilst the other images show both chromosomes (blue) and microtubules (green) at different points in cell division. Monitoring the fluorescence lifetime of the DAPI (DNA label) can show the DNA compaction[13], which varies during mitosis.

As well as using labels, endogenous fluorescence can be monitored. The coenzyme NADH involved in cell metabolism is a good example. It exists in a free and a bound form, each form has different lifetime. The ratio between the free and bound forms is indicative of the metabolic pathway. Typically in healthy animal cells oxidative phosphorylation occurring in the mitochondria is the pathway. In cancer cells (Warburg effect) the predominant pathway is glycolysis, which occurs in the cell cytoplasm. Figure 6 shows a study combining labels and endogenous fluorescence in the study of yeast cells. Yeast is often used in research as a model system and when grown under high glucose conditions these cells should use glycolysis as their metabolic pathway. First cell viability was checked via the presence of “red” fluorescence from the FUN-1 probe. A membrane label (CW – calcofluor white) was also used to help visualise the cell. FLIM data from living cells exciting and monitoring NADH fluorescence, which are at different wavelengths to the viability probe, were collected. Analysing the lifetimes and their relative proportions and comparing to NADH in solution confirms glycolysis as the principal pathway in this case. This involved fitting the data using the EzTime Image software to a three exponential decay model. In yeast a longer-lived decay, indicative of bound NADH, is present at a lower amount than the free form. This information is then used to confirm the glycolysis pathway.

The information that can be gained from FLIM is very dependent on the fluorophores (endogenous or labels). The fluorescence lifetimes are advantageous since they are an absolute measure, independent of concentration. They are

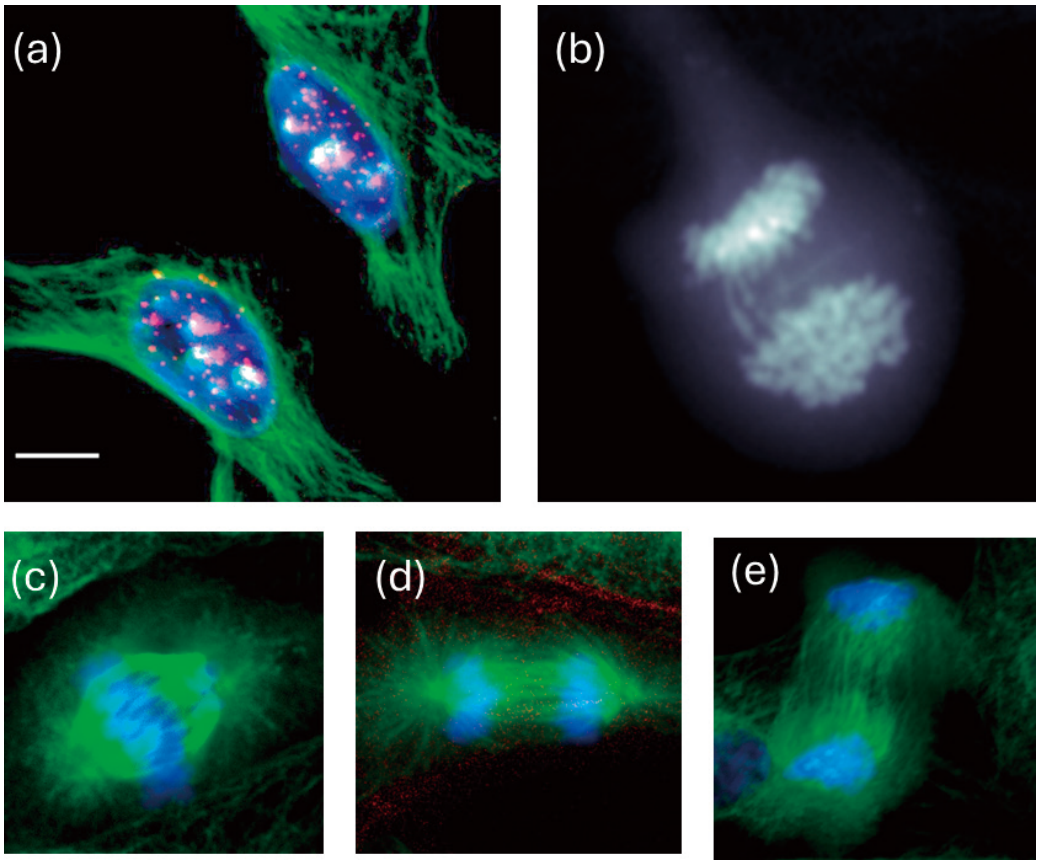

Figure 5 InverTau data showing the (a) localisation of a labelled protein (red) within the nucleus (blue) in multi-labelled HeLa cells. The microtubules are also seen (green). The scale bar is 10µm. (b) to (e) show BPAE cells undergoing mitosis with (c to e) genetic material shown blue and microtubules in green.

particularly advantageous when looking at FRET interactions, for example to investigate interactions between genetically encoded proteins, or using tension probes (eg Flipper T) for monitoring cell membrane rigidity for cancer research.

Conclusion

FLIM is a powerful tool for use in the biological and life science fields. The fluorescence lifetime parameter provides an additional means to add contrast to images and is fundamental in uncovering molecular processes at the cellular level. Both the InverTau and FLIMera use TCSPC, the "gold standard" in fluorescence lifetime determination, to add this measurement modality to fluorescence microscopes. Simple to use software (EzTime Image) moves FLIM from specialist centres to common research laboratories.

* Editorial note: This content is based on HORIBA's investigations in the year of publication, unless otherwise stated.

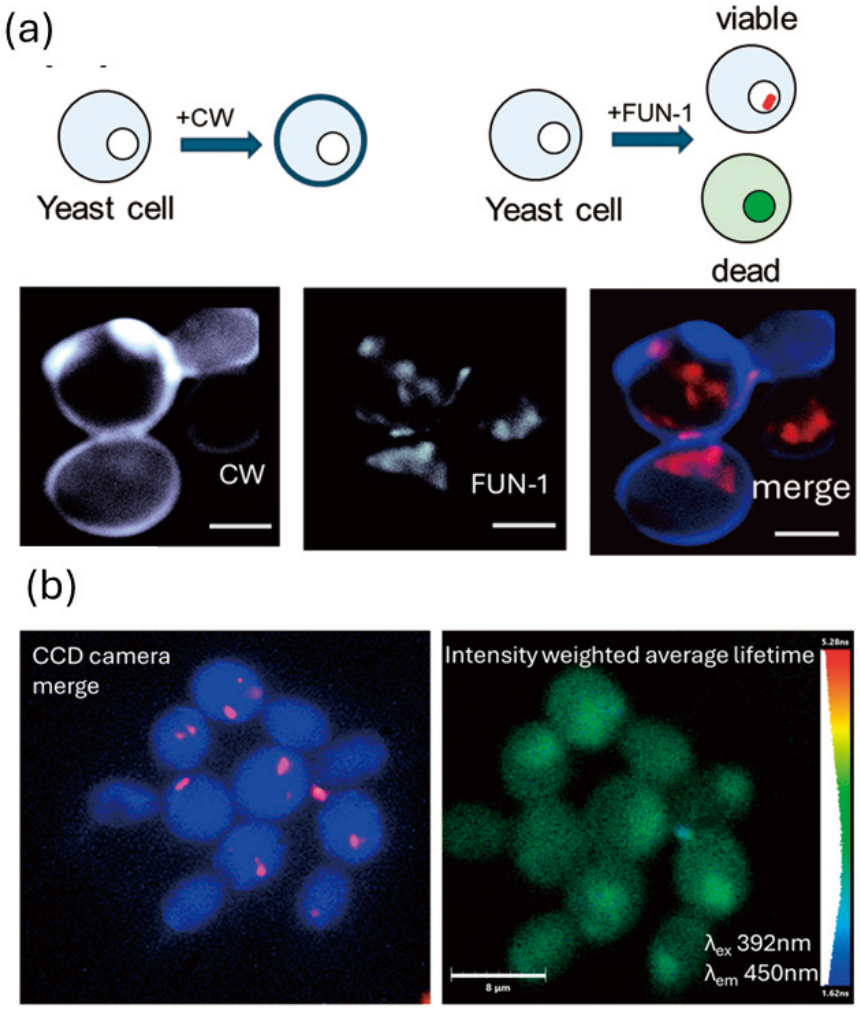

	τ_1 / ps	τ_2 / ps	τ_3 / ps	α_1	α_2	α_3	<τ> / ps
NADH	46	324	857	0.4	0.50	0.10	271
Yeast	205	960	3800	0.41	0.34	0.25	1365

Figure 6 InverTau data showing (a) a schematic for the use of a yeast viability stain (FUN-1) and a membrane label (CW), along with InverTau data showing labelled yeast cells. The scale bar is 4μm. (b) shows the viability stain used to select live cells for imaging and the resultant FLIM data monitoring NADH emission (scale bar 8μm). The lifetime parameters for NADH in PBS buffer and yeast autofluorescence are also given.

About FLIMera and InverTau

Both the FLIMera and InverTau can be sold individually or incorporated with an inverted microscope (Nikon Ti2-U), with the possibility of both being coupled on the same microscope. The InverTau comes with FiPho timing electronics and our DeltaDiode range of lasers provide the ideal excitation sources for both products.

Information can be obtained from the HORIBA website https://www.horiba.com/int/scientific/products/fluorescence-spectrometers/fluorescence-microscopy/

References

[1] Lakowicz JR *Principles of Fluorescence Spectroscopy: Third Edition*, 2006, Springer, New York.
[2] Hickey SM et al, *Cells*, 2022, 11, 35.
[3] Scheneckenburger H, Richter V, *Appl. Sci.*, 2021, 11, 733.
[4] Datta R et al, *J. Biomed. Opt.*, 2020, 25, 07203.
[5] Samini K et al, *J. Biomed. Opt.*, 2023, 28, 066502.
[6] Hungerford G et al, *Meas. Sci. Technol.*, 2023, 34, 085702.
[7] Bruschini C et al, Light: *Sci. Appl.*, 2019, 8, 87.
[8] Mason SA et al, *Front. Chem.*, 2018, 6, 407.
[9] Digman MA et al, *Biophys. J.*, 2008, 94, L14.
[10] Hopkinson C et al, *Biomed. Opt. Exp.*, 2024, 15, 212.
[11] Aghigh A et al, *Biophys. Rev.*, 2023, 15, 43.
[12] Kapitany V et al, *Sci. Adv.*, 2024, 10, eadn0139.
[13] Estandarte AK et al, *Sci. Rep.*, 2016, 6, 31417.

Dr. Philip Yip

Fluorescence Engineer
HJY-IBH Ltd.
Glasgow UK

Dr. David McLoskey

Managing Director
HJY-IBH Ltd.
Glasgow UK

Dr. Graham Hungerford

Principal Scientist
HJY-IBH Ltd.
Glasgow UK

The Essence of Open Innovation: From the Perspective of Value Creation

Yoshihiro Mori

1. Introduction

After gaining approximately 30 years of hands-on experience in technology development at private companies, I transitioned to academia in 2022 where I am now engaged in research and education in business administration, particularly in the field of innovation management. In this article, I will explore the concept of Open Innovation (OI), which has been attracting significant attention in recent years, from the perspective of both my professional and academic backgrounds.

The term "Open Innovation" itself is now widely recognized. However, in the actual business field concerns persist such as "it's difficult to produce results" and "how should we actually proceed?". I faced the same challenges during my time as a corporate manager of the R&D division, but after moving to academia, I discovered that a wealth of systematic knowledge has been accumulated regarding the determinants of success or failure of OI. In this article, drawing on this knowledge, I will outline the essential elements for guiding OI toward success.

Figure 1 JR West's Special Rapid Service train.

2. What Is Innovation?

Before discussing OI, it is important to note that innovation is not the same as "technological innovation." As an engineer myself, I have long valued technology. However, in the context of management studies, innovation refers not simply to new technologies or inventions themselves, but to outcomes that bring value to society by combining existing elements.

When explaining this, I often cite the example of JR West's Special Rapid Service "Shinkaisoku" (Figure 1). The Shinkaisoku combines existing train cars with existing tracks originally intended for freight and limited-express trains, yet it created significant value by connecting Kyoto and Osaka in under 30 minutes. It is a classic example of "not a technological innovation, but an innovation."

Figure 2 Segway personal transporter.
Image from PxHere / CC0 public domain.

On the other hand, in the same field of mobility, the Segway (Figure 2) achieved a technological innovation—a two-wheeled self-balancing mechanism using a six-axis accelerometer—but this technology was not accepted by society as having sufficient value and did not achieve widespread adoption. This contrast illustrates that innovation and technological innovation do not necessarily coincide.

So, what exactly is the "value" referred to here? In business administration "value" in principle is assumed to be economic in nature – that is, measurable in monetary terms (profit). No matter how much customers may praise a product, it cannot be considered to have economic value unless they pay an additional price for it. Some may find this way of thinking unsettling, but it is not a matter of right or wrong. We must understand that modern capitalism operates according to these rules. Therefore, innovation is the creation of economic value and its starting point does not necessarily have to be technology.

3. Open Innovation (OI)

3-1. Concept

OI is an approach that intentionally connects internal and external resources to generate innovations that would be difficult to achieve within a single company alone. Henry Chesbrough proposed this concept in 2003 and laid the groundwork for its systematization[1]. According to Chesbrough's analysis and observations, the spread of OI is attributed to a combination of social factors such as the decline in the cost of accessing information due to the proliferation of the internet, the increasing sophistication, complexity, and modularization of products, intensifying competition invovling emerging economies and rising labor mobility (Figure 3).

The fundamental concept of OI is to first define the value to be realized, achieve it quickly through OI, and secure first-mover advantage. The resulting profits are then shared with partners. OI is not about "jointly exploring the unknown," but rather the idea of "defining the value to be created and collaborating with external parties to realize it early." The majority of successful cases are based on this concept.

However, actually implementing OI presents numerous challenges. The most common obstacles are organizational culture and internal psychological resistance. It is often said that companies that have succeeded through their own efforts tend to have a culture that unconsciously shuns external technologies (the "NIH syndrome": Not Invented Here). Furthermore, we cannot overlook the

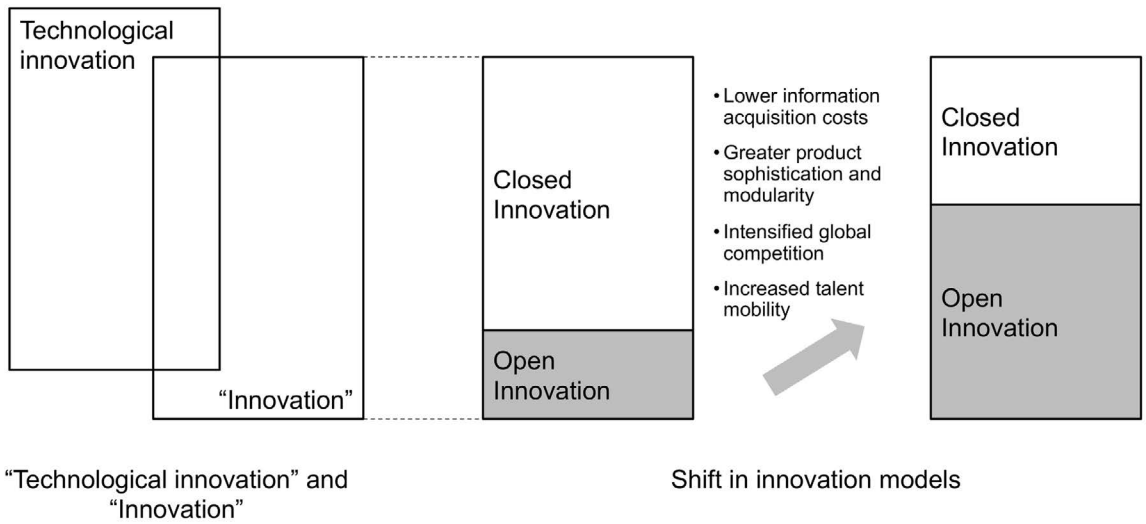

Figure 3 Technological advancement, innovation, and open innovation.

fact that employees are prone to harboring anxieties such as, “Will OI take away my job? ” or “Will relying on external parties undermine our company’s R&D capabilities?” Simply paying lip service to these issues is insufficient; it is considered essential to change the corporate culture itself under top-level leadership and intentionally establish mechanisms – ranging from product development processes to performance evaluation criteria – that align with this new culture[2].

3-2. Success Stories

P&G is frequently cited as a successful example of OI[3]. Driven by a sense of crisis that in-house development alone would not enable the necessary growth, the company made a major shift toward introducing a systematic framework for incorporating external knowledge. A famous example is the development of potato chips printed with characters. When this product idea emerged, rather than starting to develop the printing technology in-house as it had done previously, P&G searched its global network for existing similar technologies. As a result, they discovered that inkjet technology was already in practical use at a small bakery in Italy. By adopting this technology, they were able to bring the product to market in about half the time it would have taken to develop it in-house. P&G’ s approach was based on the idea that “While we have 7,500 engineers in-house, there are likely 200 engineers with similar expertise in each of their specialized fields worldwide. In other words, 1.5 million engineers could be potential partners. Let’s create a system that allows them to contribute.”

That said, this transition did not proceed smoothly from the outset. As mentioned earlier, organizational culture and psychological resistance were no exception at P&G and gaining internal buy-in was a major challenge. The key to success lay in designing the transformation including systems, evaluation criteria, and organizational structures from the top down, while acknowledging the existence of resistance. Specifically, the company introduced a performance evaluation system that treats innovations originating internally and externally equally, and deployed dozens of dedicated personnel whose mission was to connect with external partners. Furthermore, top management clearly set the goal of “50% of innovation coming from outside the company” and is said to have taken decisive action against managers who resisted this initiative.

In Japan, the example of Osaka Gas is well-known[4]. The company established a dedicated OI department and standardized the process from identifying internal needs to external exploration and collaboration. To seek out partners, they actively disclosed information about their needs to the outside world. Although there was reportedly some internal resistance to publicly sharing the company’s challenges, senior management made the decision and drove the initiative forward. As a result, Osaka Gas established itself as a hub where information converges from various sources and achieved significant value creation (social implementation) that would have been impossible on their own.

3-3. Success Factors

OI is merely a means to an end, the starting point is clarifying the objectives: “What do we want to achieve?” and “Why are we implementing this?” Based

on that, it is considered necessary to combine the four elements – "culture", "procedures", "skills", and "motivation" – in a way that suits the company's specific context[2]. Viewing the success stories of P&G and Osaka Gas from this perspective, it can be seen that in both cases, they first clarified their own challenges and the value they sought to realize. To address these through OI, they transformed their corporate culture and established systems under the leadership of top management.

4. Recent OI Research

A global OI boom began in the early 2000s and academic research advanced rapidly. Chesbrough, the proponent of OI, published a paper in 2024 summarizing OI research over the past 20 years[5]. In it he points out the following limitations and challenges of OI:

- Dependence on specific individuals: At P&G, performance stagnated after the management team and their subordinates who had strongly promoted and successfully implemented OI left the company. This suggests that the success of OI may depend on the specific individuals in charge.
- The commoditization of OI: Following P&G's success, many major consumer goods manufacturers shifted their focus to utilizing OI and as a result, OI ceased to be a source of competitive advantage in this industry. The strategy itself became commoditized.
- The Openness Paradox: A reverse U-shaped relationship has been observed between the degree of openness to the outside world and the outcomes of OI. Implementing OI requires costs associated with knowledge management and organizational operations. If openness is increased excessively, these costs can offset the benefits. It has been noted that this issue is particularly acute in small and medium-sized enterprises (SMEs).

These findings are highly instructive for practitioners involved in OI. By learning from the knowledge generalized by those who came before us, we should be able to reduce the likelihood of failure when embarking on new OI initiatives.

5. OI Pitfalls Commonly Encountered by Japanese Companies

Globally, there is a wealth of OI practice and academic research on success and failure factors is advancing. However, in the field at Japanese companies, it is not uncommon for OI initiatives to fail to deliver the expected results. So where do they stumble? NEDO's "White Paper on Open Innovation, 3rd Edition"[6] identifies the following as typical problems:

- Believing that simply engaging in OI will lead to innovation
- A lack of a clear objective regarding "what we want to achieve"

In other words, when initiatives are launched with an ambiguous understanding of "what value we want to create," external collaboration becomes an end in itself and fails to lead to business results. OI is a means, not an end. It is essential to keep this in mind at all times.

Furthermore, in practice, even while claiming to be "open", there is a tendency to be swayed by the mindset of "only our company should benefit." As mentioned above, the foundation of OI lies in "rapidly creating value through collaboration with partners to stay ahead of competitors and sharing the results in a mutually agreeable manner." Whether or not one can adopt this mindset is a critical factor that determines success or failure.

6. Conclusion

In this article, I redefined innovation not as "technological innovation" but as "value creation," and clarified the essence of OI. What this finding indicates is that rather than focusing on external collaboration itself, it is crucial to first clarify "what kind of value we want to realize" and then establish the culture and systems necessary to achieve it under top-level leadership.

Most companies in their startup phase rarely have the resources to handle everything on their own so they must have collaborated with external partners in some form to create value and seize opportunities for growth. This is nothing less than the practice of OI. However, as companies grow, they often lean toward self-reliance and before they know it, they are caught up with and even overtaken by later entrants who are actively practicing OI. Perhaps what is needed now is an effort to relearn the accumulated knowledge of OI research while recapturing the OI spirit of the company's early days when value creation moved at a rapid pace.

References

[1] H. Chesbrough, "Open innovation: The new imperative for creating and profiting from technology", Harvard Business Press (2003).
[2] University of Cambridge, "How to implement open innovation" (2006), Institute for Manufacturing, Cambridge, UK.
[3] L. Huston and N. Sakkab, "Connect and develop.", Harvard Business Review 84(3), p. 58 (2006).
[4] K. Kawaguchi, "Intrapreneurs and the Internalization of Technology Markets: A Case Study of Open Innovation at Osaka Gas", Hitotsubashi Business Review 2012. AUT., p. 56.
[5] H. Chesbrough, "Open Innovation: Accomplishments and Prospects for the Next 20 Years," California Management Review 67(1), p. 164 (2024).
[6] NEDO, "White Paper on Open Innovation, Third Edition," (2020) https://www.nedo.go.jp/library/open_innovation_hakusyo.html

Yoshihiro Mori

Former R&D Manager at HORIBA, Ltd. and
HORIBA Advanced Techno, Co., Ltd.
Professor,
Graduate School of Business, Doshisha University
PhD in Engineering, MBA

HORIBA World-Wide Network

Australia
- HORIBA Australia Pty Ltd

Austria
- HORIBA (Austria) GmbH - Tulln

Czech Republic
- HORIBA Czech
  Olomouc Factory / Prague Office

France
- HORIBA ABX SAS - Grabels
- HORIBA Advanced Techno France SAS
  - Montbonnot-Saint-Martin
- HORIBA Europe Research Center - Palaiseau
- HORIBA FRANCE SAS - Lyon
- HORIBA FRANCE SAS, Lille Office / Montpellier Office / Vénissieux Office

Germany
- BeXema GmbH
- HORIBA Europe GmbH - Darmstadt Office / Dresden Office / Flörsheim Brake Test Center / Hannover Office / Korschenbroich Office / Leichlingen Office / Munich Office / Oberursel Office / Potsdam Office / Stuttgart (Neuhausen) Office / Wolfsburg Office
- HORIBA FuelCon GmbH - Barleben
- HORIBA Jobin Yvon GmbH - Oberursel
- HORIBA Tocadero GmbH

Italy
- HORIBA ABX SAS - Italy Branch
- HORIBA ITALIA Srl - Roma
- HORIBA ITALIA SRL - Torino Office

Netherlands
- HORIBA Europe GmbH - Netherland Office

Poland
- HORIBA ABX Sp. z o.o. – Warszawa
- MLU Sp. z o.o.

Portugal
- HORIBA ABX SAS - Portugal Branch

Romania
- HORIBA (Austria) GmbH - Romania Branch

Russia
- HORIBA OOO - Moscow / Zelenograd Office

Spain
- HORIBA ABX SAS - Spain Branch

Sweden
- HORIBA Europe GmbH, Sweden Branch
  - (Gothenburg) / (Sodertalje)

Turkey
- HORIBA Europe GmbH - Istanbul Office

United Kingdom
- HORIBA Jobin Yvon IBH Ltd. - Glasgow
- HORIBA MIRA Limited - Nuneaton / Quatro Park
- HORIBA Test Automation Limited. - Worcester
- HORIBA UK Limited - Northampton

You can find detailed information on HORIBA Group locations here.

https://www.horiba.com/int/contact/worldwide-locations/

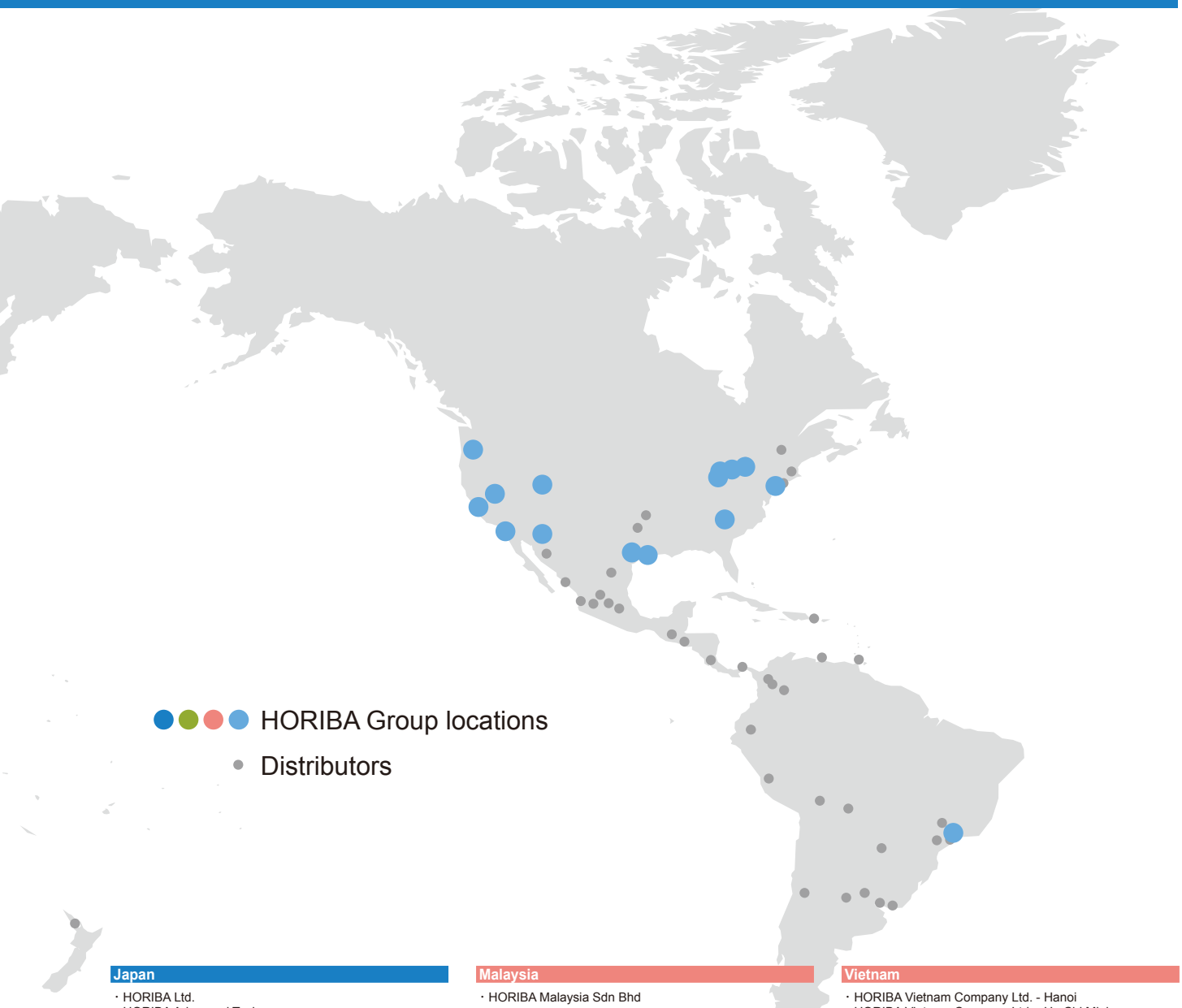

Japan

- HORIBA Ltd.
- HORIBA Advanced Techno
- HORIBA STEC
- HORIBA Techno Service

China

- HORIBA (China) Trading Co. Ltd. - Xi'an / Beijing / Beijing YiZhuang / Chengdu / Guangzhou Office / Shanghai / Shenzhen / Xiamen
- HORIBA INSTRUMENTS (SHANGHAI) CO., LTD - Shanghai
- HORIBA Precision Instruments (Beijing) Co., Ltd.
- HORIBA Technology (Suzhou) Co.,LTD.
- MIRA China Ltd. - Shanghai
- MIRA China Ltd. Xiangyang Workshop

India

- HORIBA India Private Limited - Bangalore Office / Chennai Office / Haridwar Factory / New Delhi / Technical Center / Kolkata Office / Nagpur Factory

Indonesia

- PT HORIBA Indonesia
- PT. HORIBA Indonesia - Tangerang

Malaysia

- HORIBA Malaysia Sdn Bhd

Philippines

- HORIBA Instruments (Singapore) Pte Ltd. - Manila Office

Singapore

- HORIBA Instruments (Singapore) Pte Ltd. –Singapore / West Office

South Korea

- HORIBA KOREA Ltd. - Anyang-Si / Dongtan Office / Ulsan Office
- HORIBA STEC KOREA, Ltd. - Gyeonggi-do

Taiwan

- HORIBA Taiwan, Inc. - Hsinchu
- HORIBA Taiwan, Inc. - Tainan Office

Thailand

- HORIBA (Thailand) Limited - Bangkok

Vietnam

- HORIBA Vietnam Company Ltd. - Hanoi
- HORIBA Vietnam Company Ltd. - Ho Chi Minh

Brazil

- HORIBA Instruments Brasil, Ltda. -São Paulo
- TCA/HORIBA Sistemas de Testes Automotivos Ltda. -São Paulo

Canada

- HORIBA Canada Inc. -Burlington / London Office

USA

- HORIBA Instruments Incorporated -Ann Arbor Office / Austin Office / Canton Office Fletcher Office / Houston Office / Irvine / Portland Office / Sunnyvale Office / Tempe Office / Troy Office / West Valley City Office
- HORIBA New Jersey Optical Spectroscopy Center
- HORIBA Reno Technology Center

Readout **HORIBA Technical Reports English Edition No.61**

Publication Date : June 30th, 2026
Publisher : HORIBA, Ltd.
Editor : Hiroshi Nakamura
Associate Editor : Susumu Hayashi
Publication Members : Chikako Urakami, Tetsuya Matsuda, Yoko Sugiyama,
Hiromi Satake, Akihiro Misumi, Akari Shirosaki, Naoko Okamoto
DTP, Printing : SHASHIN KAGAKU Co., Ltd.
Information : R&D Planning Center, R&D Division, HORIBA, Ltd.
2, Miyanohigashi-cho, Kisshoin, Minami-ku, Kyoto 601-8510, Japan
Phone : (81)75-313-8121
E-mail : readout@horiba.co.jp

HORIBA